The Role of Chromatin Modifying Enzymes in Fibroblast-to-Hepatocyte Direct Lineage Conversion

by

Eray Enustun

A Dissertation Submitted to the
Graduate School of Sciences and Engineering
in Partial Fulfillment of the Requirements for
the Degree of

Master of Science
in
Molecular Biology and Genetics

July 2018

The Role of Chromatin Modifying Enzymes in Fibroblast-to-Hepatocyte Direct Lineage Conversion

Koç University

Graduate School of Sciences and Engineering

This is to certify that I have examined this copy of a master's thesis by

Eray Enustun

and have found that it is complete and satisfactory in all respects,
and that all revisions required by the final
examining committee have been made.

Committee Members:

_____

Tamer Önder, Ph. D. (Advisor)

_____

Tuğba Bağcı-Önder, Ph. D.

_____

Şerife Esra Erdal, Ph. D.

Date: _____

ABSTRACT

Transdifferentiation is a reprogramming method to directly convert a differentiated cell into another differentiated cell type by overexpressing lineage-specific transcription factors. Compared to reprogramming of differentiated cells into induced pluripotent stem cells (iPSC), it is faster and potentially safer for clinical applications. However, the efficiency of lineage conversion remains low and needs to be improved for potential therapeutic applications. Reprogramming requires extensive remodeling of cellular epigenetic states, and chromatin modifiers have emerged as important regulators of iPSC generation. We hypothesized that such regulators may also play crucial roles in direct lineage conversion. To investigate the role of chromatin modifiers in transdifferentiation, we utilized an established protocol of direct conversion of human fibroblasts to induced hepatocytes (iHep) via overexpression of FOXA3, HNF1A and HNF4A. A lentiviral GFP-reporter for Albumin expression was generated to monitor conversion efficiency. Using this system, we observed that CRISPR/CAS mediated knockout and chemical inhibition of the H3K79 methyltransferase DOT1L increases direct conversion to hepatocytes at early time points. Dot1L inhibition accelerated the induction of hepatic markers and silencing of the fibroblast markers. In addition, we observed Albumin secretion is increased with the loss of DOT1L. Moreover, iHeps obtained through Dot1L inhibition displayed basic hepatic functions such as glycogen storage. Encouraged by these results, we performed a compound screen that targets a broad range of chromatin writers, erasers and readers. Using the albumin reporter, we identified compounds that increases transdifferentiation efficiency at day 6, day 9 and day 12 after the overexpression of required transcription factors. Among these Rocilinostat, SAHA, GSK8815, MS023, Valproic Acid, GSK8814, LP99 and IOX2 can increase transdifferentiation efficiency at early stages, while 3-DZNEP, Repsox and CHR-6494 have a role in later stages. These results provide important insights into how chromatin modifiers and epigenetic modifications affect transdifferentiation and may contribute to new strategies of obtaining iHeps with higher efficiencies for potential therapeutic applications.

ÖZETÇE

Transdiferensiyasyon, farklılaşmış bir hücrenin başka bir hücre türüne ait transkripsiyon faktörlerinin ifade edilmesini sağlayarak o hücre türüne dönüşmesini sağlama metodudur. Bu metot, farklılaşmış hücrelerin uyarılmış pluripotent kök hücrelere (UPKH) yeniden programlanmasıyla karşılaştırıldığında daha hızlı ve klinik uygulamalarda kullanmak için daha güvenlidir. Ancak, başka bir hücre tipine dönüşen hücrelerin yüzdesi azdır ve potansiyel terapi tedavilerinde kullanmak için bu metodun veriminin arttırılması gerekmektedir. Yeniden programlamada hücrelerin epigenetik durumlarının geniş çaplı bir değişime uğraması gerekir ve kromatin değiştiricileri UPKH oluşumunda önemli rol oynar. Bu çalışmadaki ana hipotezimiz, kromatin değiştiricilerinin transdiferensiyasyonda da önemli role sahip olduklarıdır. Kromatin modifikasyonlarını sağlayan enzimlerin insan deri hücrelerinden karaciğer hücrelerine transdiferensiyasyonundaki rolünü inceleyebilmek için FOXA3, HNF1A ve HNF4A transkripsiyon faktörleri kullanıldı. Hücrelerin dönüşüm yüzdelerini belirlemek için lentiviral bir Albumin – GFP habercisi oluşturuldu. Bu sistem ile CRISPR/CAS ile genomdan silinen veya kimyasal ile inhibe edilen H3K79 metiltransferazı DOT1L'in erken aşamalarda karaciğer hücrelerine direkt dönüşümü arttırdığı gözlemlendi. DOT1L'in inhibisyonu hepatosit genlerinin ifadelerini hızlandırdığını ve fibroblast hücrelerine ait genlerin ifadelerini azalttığını belirlendi. Ayrıca, DOT1L'in inhibasyonun Albumin'in hücre dışına salgılanmasını arttırdığı gözlemlendi. Oluşan hücrelerin hepatosit fonksiyonlarından biri olan glikojen depolayabildiğini gösterildi. Son olarak, oluşturduğumuz Albumin habercisi ile kromatin yazıcı, silici ve okuyucusunu hedefleyen küçük moleküllerin dönüşümün 6, 9 ve 12. günlerde Albumin ifade eden hücre oranlarına etkisini incelendi. Bu moleküllerden Rocilinostat, SAHA, GSK8815, MS023, Valproic Acid, GSK8814, LP99 ve IOX2'in erken aşamalarda transdiferensiyasyon verimini arttırdığını, ayrıca 3-DZNEP, Repsox ve CHR-6494 moleküllerinin ise sonraki aşamalarda bir rolünün olabileceğini gözlemlendi. Bu çalışmanın sonuçları kromatin modifikasyonunda görevli enzimlerin transdiferensiyasyonda nasıl rol aldıklarını ve terapi amaçla kullanılabilecek yapay hepatositlerin nasıl daha verimli elde edilebileceğini göstermektedir.

ACKNOWLEDGMENTS

First and foremost, I would like to thank my advisor Dr. Tamer Önder for giving me this opportunity. I believe his curiosity for science, advice, critics and scientific way of thinking made me a better scientist and I will always be grateful for that.

I would like to thank Dr. Tuğba Bağcı Önder and Dr. Esra Erdal for accepting to be in my thesis committee, for their time and effort to evaluate my work.

I am especially grateful to Burcu Özçimen for patiently showing me essential techniques and taking care of my cells as if they are hers when I could not come to the laboratory, Deniz Uğurlu for helping me whenever I needed and Ata Berk Demir for reminding me there is still life outside the laboratory.

I especially thank Fidan Şeker, Fatma Özgün and Ahmet Cingöz for creating a fun laboratory environment to work, supporting me when I was frustrated with my experimental results and many wonderful memories.

I would like to thank Filiz Şenbabaoğlu for helping me at my compound screen, sharing great tips about working in a laboratory and late-night snacks she left when everywhere was closed at the campus.

I would like to thank Gizem Nur Şahin and Dr. Serçin Karahüseyinoğlu for helping me at stainings and imaging of my samples.

I would also like to thank my undergraduate researchers Elif Koçak and Erkin Özel for their contribution to our project and teaching me how to teach in science.

I would like to thank the podcast I listened for keeping me sane at long cell culture sessions and late nights in laboratory, especially “O Tarz Mı” and “Hello Internet”.

I would like to thank my cat, Erik. He was a great companion for my graduate studies.

Special thanks to my best friends, Dila Kakırman Şalt, Yunus Can Erol, Hakan Yaraman and Burak Ural for their invaluable friendship, support, good times and fun memories outside the lab.

Finally, I am eternally grateful to my parents, Engin Enüstün and Tülay Enüstün for their continuous support, patience, unconditional love, always believing in me and helping me in any way they can.

Table of Contents

List of Tables

List of Figures

Nomenclature

BCA	Bicinchoninic acid assay
cDNA	Complementary DNA
DMEM	Dulbecco's Modified Eagle's Medium
DMSO	Dimethyl sulfoxide
DNA	Deoxyribonucleic acid
ESC	Embryonic stem cells
iHep	Induced hepatocytes
hiHep	Human Induced hepatocytes
iPSC	Induced pluripotent stem cells
MOI	Multiplicity of infection
mRNA	Messenger RNA
PAS	Periodic acid–Schiff
PEG	Polyethylene glycol
qPCR	quantitative (real-time) polymerase chain reaction
rpm	Revolutions per minute
min	Minutes
RT	Room temperature
s.d.	Standard deviation
s.err	Standard error
shRNA	Short hairpin RNA
FHH	FoxA3, HNF1A, HNF4A
FHHB	FoxA3, HNF1A, HNF4A, Blast

Chapter 1

INTRODUCTION

1.1 Direct Lineage Conversion

Somatic cell nuclear reprogramming has shown that development is not an irreversible process and cells can be de-differentiated. A major focus in regenerative medicine has been to find efficient and safe methods to create patient specific therapy strategies based on reprogramming. This would allow patient's own cells to be transformed into healthy cells that can participate in generation, maintenance and repair of the tissues. For this purpose, two methods have been intensely studied: Induced pluripotent stem cells (iPSC) and transdifferentiation (Kanherkar et al., 2014).

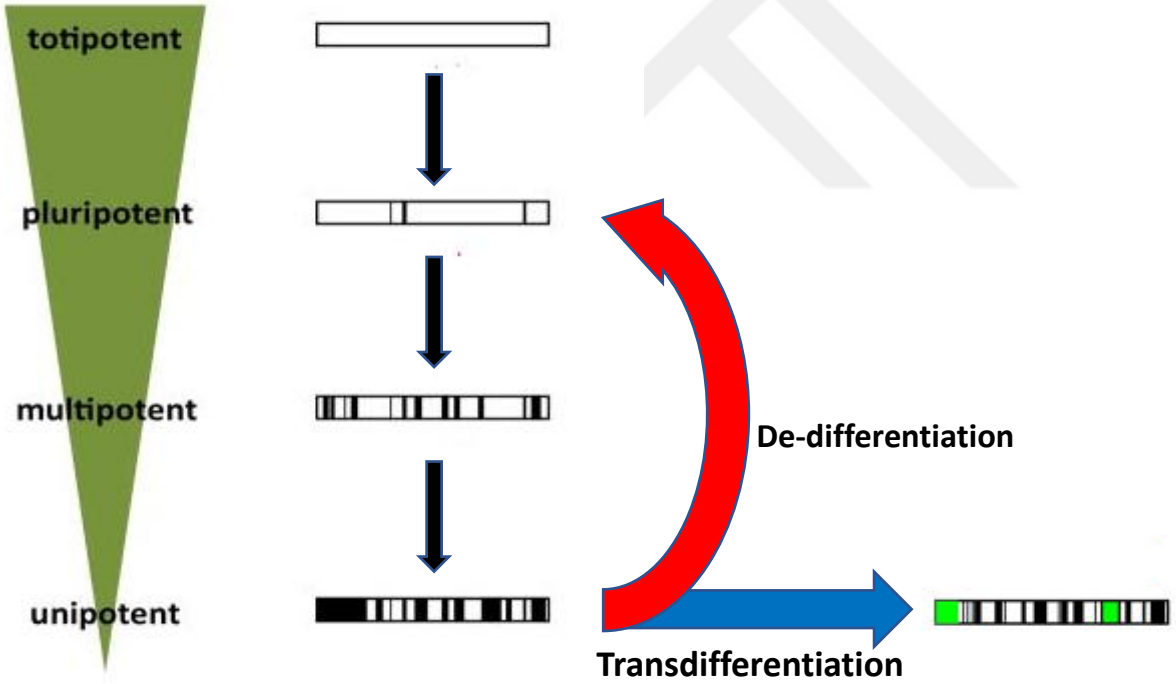

Figure1.1 Development and reprogramming methods
Development is the process by which cells differentiate (black arrows) from Totipotent stage to unipotent stage through epigenetic modifications (black bars). The cells can be reprogrammed to pluripotent stage with iPSC (red arrow) or transdifferentiated (blue arrow) into another cell-line by the overexpression of transcriptional factors (green bars). Figure is modified from reference (Vierbuchen et al., 2010).

The study of nuclear transfer with the nucleus of terminally differentiated cell and animal cloning experiments proved that development is a reversable process and that the epigenetic information acquired during differentiation can return to the "ground" state of pluripotency (Campbell et al., 1996). Pluripotent stage is important because the cells can differentiate into all three germ layers. With this idea, Yamanaka et al. screened transcription factors to reprogram the cells *in vitro* and discovered the combination of four transcription factors (*Oct4, Sox2, Klf4* and *c-Myc*) sufficient to convert the fully differentiated cells to iPSC (Takahashi and Yamanaka, 2006). This Nobel winning study was groundbreaking, but the efficiency of the reprogramming process was initially very low.

Transdifferentiation or direct lineage conversion is a reprogramming method which switches a mature somatic cell type into another functional somatic cell type with the overexpression of lineage specific transcription factors. These master transcription factors can impose upon the cell an open epigenetic state, override the key gene regulatory networks for the initial cell type, and cause the conversion to another specific cell type under approportionate culture and signaling conditions. Direct lineage conversion bypasses the pluripotent state (Xu et al., 2015). As a fully differentiated cell is generated, the potential for tumor formation from pluripotent cells is absent, which makes this method safer for future clinical applications. In addition, direct lineage conversion is generally faster and has a higher efficiency (Xu et al., 2015). Earlier studies reported protocols that can directly convert various cell lineages to somatic cells with high efficiency (Davis et al., 1987; Lassar et al., 1986; Taylor and Jones, 1979; Xie et al., 2004). Transdifferentiation requires only one step for target cell generation which can happen in several hours or days. In contrast, iPSC can take several weeks to generate and subsequent targeted differentiation is also required (Sancho-Martinez et al., 2012).

Early studies in Drosophila have shown that "master transcriptional regulators" can be used for reprogramming of leg or eye structures (Schneuwly et al., 1987)(Quiring et al., 1994). In 1979, Taylor et al. reported the first case of transdifferentiation when the mouse fibroblast cells were treated with 5-AZA-cytidine (AzaC), they were converted to muscle, adipocyte and chondrocyte cells (Taylor and Jones, 1979). It was subsequently reported that fibroblasts can be directly converted to myoblast like cells by AzaC treatment or the overexpressing the transcription factor *MyoD* (Lassar et al., 1986)(Davis et al., 1987). The potential of

transdifferentiating other cell types was later revealed as overexpressing C/EBPα was sufficient for the conversion of β-lymphocytes to functional macrophages (Xie et al., 2004). These findings were followed by the successful direct conversions reports to induced neuronal cells (Vierbuchen et al., 2010) , cardiomyocytes (Ieda et al., 2010), induced dopaminergic cells (Caiazzo et al., 2011), motor neurons (Son et al., 2011), hepatocytes (Sekiya and Suzuki, 2011), induced embryonic Sertoli-like cells (Buganim et al., 2012), induced endothelial and thymic epithelial cells (Xu et al., 2015). Most studies have focused on mouse fibroblasts as the starting cell type, but similar protocols have been established for human cells as well. To date, there are established protocols for directly converting human fibroblast cells into induced neurons (Vierbuchen et al., 2010)(Qiang et al., 2011)(Marro et al., 2011), cardiomyocytes (Efe et al., 2011; Ieda et al., 2010), macrophages(Feng et al., 2008) and hepatocytes(Huang et al., 2011; Sekiya and Suzuki, 2011).

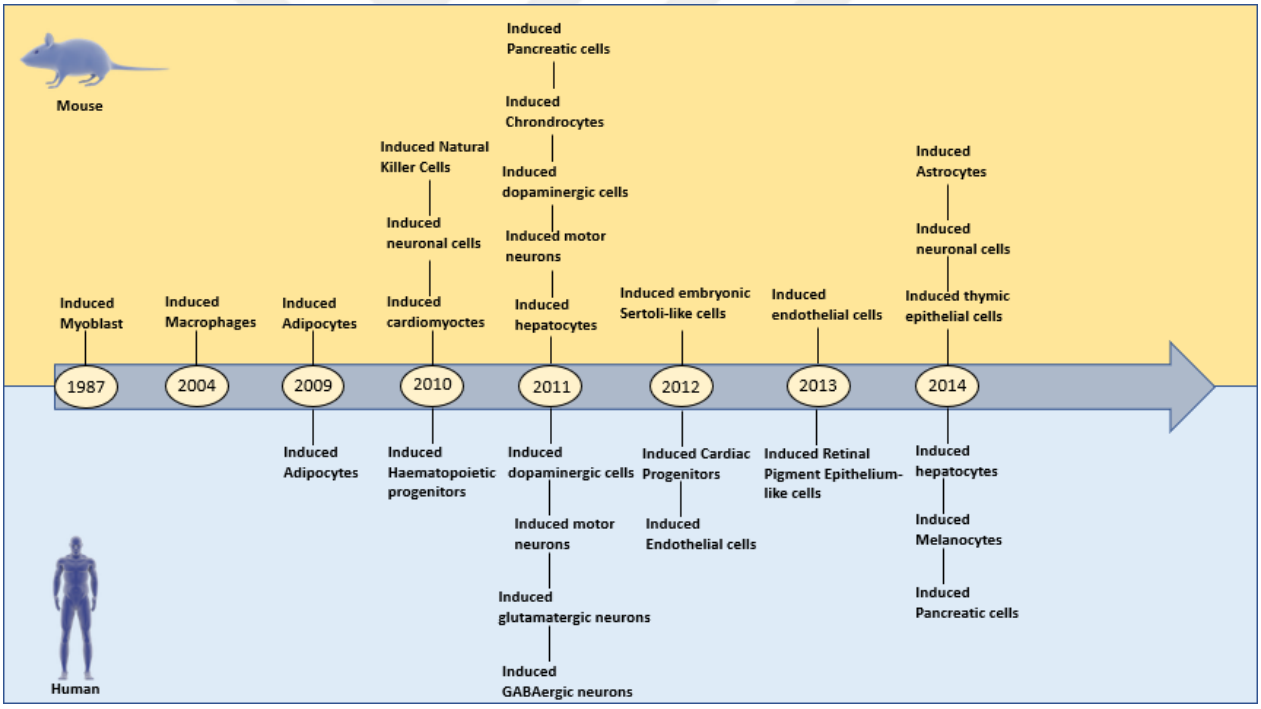

Figure1. 2 Timeline of lineage conversion studies
Selected advances in lineage conversion with mouse and human cells and the cells that are converted into. Figure is adapted from reference (Xu et al., 2015).

One of the challenges for these approaches is that the fidelity and efficiency of lineage conversions remain low. The first defined protocol had only 0.3% conversion efficiency from mouse embryonic fibroblast cells (MEFs) to induced hepatocyte like cells (iHeps) (Sekiya and Suzuki, 2011). Upon optimizations of transcriptional factors for humans, a protocol was reported in which 25% of the cells converted were Albumin (*Alb*) and Alpha-1 Antitrypsin (*Aat*) positive

(Huang et al., 2014). However, the conversion efficiency needs to increase for the therapeutic applications, since iHeps stop proliferating after lineage conversion. For this purpose, increasing the conversion rate remain an important field of study in direct lineage conversions.

1.2 Induced Hepatocytes

In early work, non-hepatic lineage cells could be programmed to a hepatic-like cells with particular stimuli or fusion with hepatocytes (Banas et al., 2007; Grompe, 2001; Lee et al., 2004; Reddy et al., 1984; Scarpelli and Rao, 1981; Vassilopoulos et al., 2003; Wang et al., 2003). Following these unexpected findings, a screen was performed with 12 candidate transcription factors to convert mouse embryonic and adult fibroblasts to induced hepatocyte-like cells (Sekiya and Suzuki, 2011). With this screen, authors identified transcription factors Hnf4a with Foxa1, Foxa2 or Foxa3 and formulated specific culture conditions crucial for the expression of hepatic lineage markers such as albumin and alpha-fetoprotein. Converted cells had multiple hepatocyte features and were able to rescue damaged hepatic tissues after transplantation into $Fah^{-/-}$ mouse livers (Sekiya and Suzuki, 2011). In this protocol, 0.3% of MEFs were converted to iHeps (Sekiya and Suzuki, 2011).

iHeps show functional similarities to mature hepatocytes such as glycogen storage, low-density lipoprotein uptake, secrete albumin and producing enzymes that metabolize drugs and other toxins (Sekiya and Suzuki, 2011). However, there are also differences between iHeps and mature hepatocytes such as aberrant expression of alpha-fetoprotein, which is an embryonic hepatocyte marker. Moreover, iHeps proliferate indefinitely in cell culture unless they are transplanted to $Fah^{-/-}$ mouse livers (Sekiya and Suzuki, 2011). Gene regulatory network analysis showed iHeps had little identity to hepatocytes when compared with mature hepatocytes (Morris et al., 2014). They found that iHeps express Cdx2 aberrantly, which is an intestinal marker. When Cdx2 expression was knocked down with shRNAs, there was an increase in hepatocyte marker genes such as *Alb*, *Afp* and *Aat* (Morris et al., 2014). Furthermore, iHeps were able to functionally engraft to mice colon, which indicated that the cells obtained from direct conversion were not in a terminally differentiated state, but rather remained as progenitors (Morris et al., 2014). Unlike iPSCs, iHeps also do not silence the exogenous transcription factors. However, the activated endogenous genes are not dependent on the exogenous genes after reprogramming (Sekiya and Suzuki, 2011).

As the efficiency of transdifferentiation from mouse fibroblast to iHeps is low, another screen performed to detect if there are any additional factors that can enhance the trans-differentiation (Lim et al., 2016). Authors showed that *c-Myc* and *Klf4* (CK) dramatically accelerated the conversion and remarkably improved iHep generation as Aat-positive colonies increased as high as 94.0-fold and Alb-positive colonies were enhanced to 48-fold with these two additional transcription factors. This study indicates that transdifferentiation has a very complex mechanism and there can be other regulators that can increase the efficiency even higher.

Along with the mouse models, several reports have provided the protocols for human fibroblast conversion to iHeps. Du et al. used *HNF1A*, *HNF4A* and *HNF6* in their work as fate conversion factors along with ATF5, PROX1 and CEBPA as maturation factors and p53-siRNA and C-MYC to promote cell proliferation (Du et al., 2014). On day 25 of the conversion, 90% of the induced cells were albumin positive and possessed drug metabolism capabilities. Authors also used these cells to functionally reconstitute livers of Tet-uPA/Rag2$^{-/-}$ mice. With this protocol, functional hi-Heps could be obtained starting from 1x10^{4} of fibroblasts. However, as this protocol requires maturation factors in addition to core transcriptional factors and the knockdown of p53, which is an important tumor suppressor, it is not suitable for therapeutic applications. Huang et al. reported another protocol that uses FOXA3, HNF1A, HNF4A to human fibroblasts and they used SV40 large T antigen to induce proliferation (Huang et al., 2014). After 12 days, 25.3% of the cells were positive for both albumin and alpha-1-antitrypsin, and the cells were expandable in culture because of SV40 large T antigen (LT). Generated cells generally displayed a gene expression profile that is similar to mature hepatocytes. The cells were also functional, as they extended the survival of mice with concanavalin-A-induced acute liver or fumarylacetoacetate dehydrolase deficiency. Not using any maturation factors and decreasing the time it requires to transdifferentiate with a high efficiency are great advantages. In addition, as this protocol utilize LT expression instead of previously used p19^{Arf} deletion by the same group, it is potentially a safer protocol as p19^{Arf} is an important tumor suppressor (Huang et al., 2014).

Along with the protocols that uses transduction of transcriptional factors, a new method has been studied, which is chemical reprogramming. A combination of small molecules that target signaling pathways and chromatin modifiers can activate or inhibit key gene regulatory networks, they induce the conversion of the cell into the cell type of interest (Xie et al., 2017).

Using chemical compounds have several advantages as they do not get integrated into DNA and can be applied transiently during the conversion process. Therefore, this method can be favored in clinical-related uses (Xie et al., 2017).

The first discovered compounds that can facilitate reprogramming were related with iPSC generation. Histone deacetylase inhibitors and DNA methyltransferase inhibitors were found to be inducers of iPSC generation (Huangfu et al., 2008). Researchers then discovered that a combination of chemical compounds and *Oct4* was sufficient to reprogram the cells into iPSC (Zhu et al., 2010). Finally, in 2013, Hou et al. discovered that Forskolin could replace *Oct4* and demonstrated fully chemical induction of iPSC (CiPSCs) (Hou et al., 2013). This study used the chemical cocktail of 7 compounds (VPA, CHIR99021, RepSox, Parnate, Forskolin, DZNep, TTNPB).

Recently, chemical-mediated transdifferentiation protocols have been reported both with mouse and human cell-lines. Cheng et al. published the first report of fully chemical-induced transdifferentiation (Cheng et al., 2014). They converted mouse fibroblasts and human urinary cells into neural stem/progenitor cells with Valproic acid (VPA, a histone deacetylase inhibitor), CHIR99021(a GSK3-beta inhibitor) and Repsox (a TGF-beta receptor inhibitor) under hypoxic condition (5% O_2). This study led others to perform chemical screens to either facilitate the reprogramming or enhance the efficiency. In 2015, several groups reported full-chemical reprogramming from mouse and human fibroblasts to Neurons and Cardiomyocytes (Xie et al., 2017). Even though Hepatocytes and Pancreatic β-cells were generated from other somatic cells by transcription factor overexpression, chemical mediated transdifferentiation has not been achieved yet for these cell types. However, Wang et al. showed that a small molecules cocktail of Bay-K-8644 (calcium channel agonist), Bix01294 (histone methyltransferase (HMTase) inhibitor), RG108(non-nucleoside DNMT inhibitor), and SB431542 (activin receptor-like kinase (ALK) receptors, ALK5, ALK4 and ALK7) was able to induced human gastric epithelial cells (hiEndoPCs) to multipotent endodermal progenitors which could then be differentiated into hepatocytes, pancreatic β cells and intestinal epithelial cells (Wang et al., 2016). Hepatocytes generated with this method were able to rescue liver failure in $Fah^{-/-}$ $Rag2^{-/-}$ mice after transplantation. Unlike hiEndoPCs, they did not give rise to teratomas. With this method, 3 billion hiEndoPCs could be generated in 4 weeks and then be differentiated to functional

hepatocytes in nearly 2 weeks. However, the resulting mature hepatocytes lose the ability to proliferate when they are converted from hiEndoPCs. Katsuda et al. proposed a strategy that converts rat and mouse mature hepatocytes to bipotent liver progenitors with Y-27632, A-83-01, and CHIR99021 (Katsuda et al., 2017). Since this chemically induced liver progenitors are proliferative for long time and can give rise to hepatocytes and biliary epithelial cells, they can be used in regenerative medicine *in vivo*. These cells were able to repopulate with a 75-90% efficiency at chronically injured liver tissue.

Li et al. reported another method similar to chemically-induced transdifferentiation which uses the extra-embryonic endoderm-like (XEN) cells generated by chemical induction of mouse fibroblast and directly reprogram them to functional neurons, hepatocytes and other cell. The group used seven-compound cocktail (VPA, TD114-2, 616452, Tranylcypromine, Forskolin, AM580, and EPZ004777; VC6TFAE) and XEN-like colonies were induced to neurons or hepatocytes in appropriate culture conditions types (Li et al., 2017). After a 20-day induction, cells co-expressed hepatic specific genes, efficiently secreted Albumin and Urea and the protocol had 20% efficiency, which was confirmed by co-immunostaining of AFP and ALB.

Recently it is reported that MEFs can be transdifferentiated into iHeps *in vitro* with overexpression of single transcription factor (*Foxa1*, *Foxa2*, or *Foxa3*) and chemical cocktail CRFVPTD (C, CHIR99021; R, RepSox; F, Forskolin; V, VPA; P, Parnate; T, TTNPB; and D, Dznep) under hepatic conditions (Guo et al., 2017). The same chemical cocktail was reported to result in both CiPSCs and chemically induced cardiomyocytes under different conditions (Guo et al., 2017). This study shows that some of the transcription factors can be replaced with chemicals; in this case the cocktail was able to replace *Hnf4a* but not *Foxa1*, *Foxa2* or *Foxa3* for mouse fibroblasts transdifferentiation. In addition, authors found that these iHeps were expendable *in vitro* and could reconstitute damaged hepatic tissues in $Fah^{-/-}$ mice (Guo et al., 2017).

Along with *in vitro* reprogramming, *in vivo* reprogramming studies also have been performed in recent years. Song et al. transduced the transcription factors (*FOXA3, GATA4, HNF1A, HNF4A*) required for transdifferentiation of hepatic myofibroblasts to iHeps *in vivo* with adenoviruses directly to mouse liver parenchyma (Song et al., 2016). These *in vivo* generated iHeps also showed similar functionality and overexpression of these four transcription factors can

ameliorate chemically induced liver fibrosis. Authors also showed that this method of reprogramming did not give rise to cells other than iHeps and that they were not a result of cell fusion but an actual case of reprogramming. In this study, percentage of in-vivo-generated iHeps was 0.2-1.2% of the total hepatocyte population and the reprogramming efficiency was less than 4% (Song et al., 2016).

Another study showed that human spermatogonial stem cells (SSCs) can transdifferentiate into hepatocytes *in vivo* (Chen et al., 2017). Instead of transfection or viral infection, they used transplantation of human SSC cells under the renal capsules of nude mice with liver injury. As the cells grafted, they expressed hepatocyte hallmarks such as ALB, AAT, CK18 and CYP1A2; however, VASA and GPR125 which are germ cell and SSC markers were undetected. Moreover, authors observed no obvious lesions or teratomas in several important organs and tissues of the recipient mice, which suggests the technique is safe and feasible. Katayama et al. developed another alternative method which uses piggyBac transposons to generate non-viral, transgene-free hepatocyte like cells by integrating *Hnf4a* and *Foxa3* and successfully obtained functional iHeps. Following this protocol, authors used immunofluorescent staining for E-cadherin and calculated the reprogramming efficiency to be 25.1% (Katayama et al., 2017).

As there are two working strategies (differentiation from iPSCs and transdifferentiation) to obtain Hepatocyte-like Cells (HLC), Gao et al. investigated how HLCs obtained by these two strategies compare with respect to gene expression and epigenetic signatures (Gao et al., 2017). Authors started from a single donor and observed that the two types of HLCs cluster distinctly from each other based on gene expression profiling (Gao et al., 2017). Gene expression differences were most pronounce in genes related to phase II drug metabolism and lipid accumulation, which the authors suggested could be due to differential H3K27 acetylation at the relevant loci (Gao et al., 2017). However, both HLC types had similar functions upon transplantation into Fah-deficient mice suggesting that both strategies could be used. Importantly, HLCs from both strategies did not engraft as well as primary hepatocytes, which indicates better differentiation protocols are needed as well as new combinations of transcription factors and growth factors for transdifferentiation (Gao et al., 2017). Another important result from this study was that both types of HLCs had stable epigenetic modifications which the authors argue are required for HLC functionality (Gao et al., 2017).

1.3 FOXA, HNF4 and HNF1 Transcription Factors

Both in fetal and adult liver cells, FOXA (forkhead box A) transcription factors are crucial for the regulation of almost all liver specific genes and other endoderm- originated tissues (Lai et al., 1990, 1991). *Foxa2* expression starts at E6.5 in the primitive streak and in Hensen's node. The loss of *Foxa2* leads to severe irregularities in neural tube and in foregut morphogenesis and eventually lethality after gastrulation (Ang and Rossant, 1994; Weinstein et al., 1994). *Foxa1* begin to be expressed before organogenesis at the day E7-E8. Homozygous loss of *Foxa1* causes glucagon expression defects in pancreases and death after birth (Kaestner et al., 1999). Finally, *Foxa3* starts to be expressed at E8-E9 at midgut and hindgut. Homozygous *Foxa3* mutations do not cause a dramatic phenotype but lead to significant decreases in the expression of liver specific genes (Kaestner et al., 1998).

HNF4 (hepatocyte nuclear factor 4) transcription factor belongs to nuclear receptor superfamily and it has two isoforms: *HNF4α* and *HNF4γ*. The known targets for HNF4α are alpha-1 antitrypsin, transthyretin genes, and *Hnf1α.* The loss of *Hnf4* causes defects of the visceral endoderm(VE) (Duncan et al., 1997) and results in embryonic lethality before gastrulation (Chen et al., 1994). However, this can be overcome by tetraploid chimera as $Hnf4^{+/+}$ VE complements $Hnf4^{-/-}$ ES cell-derived embryos and allows complete gastrulation (Duncan et al., 1997), although crucial hepatocyte specific gene activation is impaired (Li et al., 2000).

HNF1 (hepatocyte nuclear factor 1 homeobox A) regulates genes related to gluconeogenesis, lipid and carbohydrate metabolism in hepatocytes (Odom, 2004), in addition to those involved in glucose, amino acid, and tricarboxylic acid metabolism in pancreatic island cells (Servitja et al., 2009) and several genes that regulate kidney function (Pontoglio et al., 1996). The mutations of HNF1A cause progressive hepatic failure, phenyl-ketonuria, renal Fanconi syndrome (Pontoglio et al., 1996), diabetes mellitus and growth hormone insensitivity (Lee et al., 1998) in mice. They have been extensively investigated early-in-age manifestation of diabetes mellitus in humans (Mcdonald et al., 2011; Stride and Hattersley, 2002).

1.4 Epigenetics

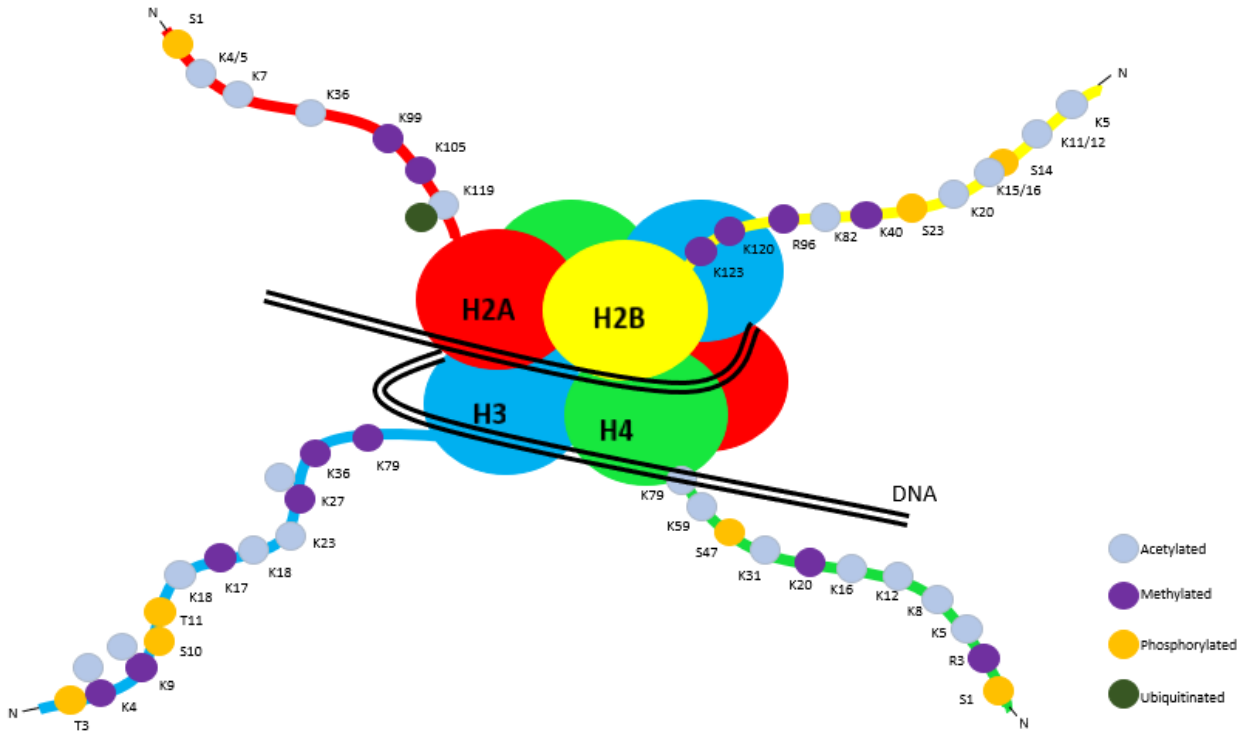

Figure1. 3 Schematic of highly studied post-modifications of the histone tails

The location of some highly studied histone post-translational modifications (Acetylation = Light blue, Methylation = Purple, Phosphorylation = Orange, Ubiquitination = Dark Green) of the histone tail residues (K = lysine, R = arginine, S = serine, T = threonine). Figure is adapted from Lawrence et al. (Lawrence et al., 2016)

Epigenetics is the study of chromatin-related modifications that dynamically changes DNA's accessibility to the transcriptional machinery. Developmental and environmental cues can affect gene transcription through modulation of these chromatin modifications. Chromatin is composed of DNA wrapped around octamer histone proteins that has four core histones: H2A, H2B, H3 and H4. These complexes are connected with H1 histone proteins that bind to linker DNA. There are two main types of chromatin-associated modifications: DNA methylation and histone modifications. In the first case, C5 position of cytosines at DNA can get methylated and the methylation in CpG dinucleotide (CpG islands) are associated with transcriptionally repression (Kass et al., 1997). In the second case, histone proteins can undergo post-translational modifications. Most common histone modifications are methylation, phosphorylation, acetylation. However, ubiquitylation, and sumoylation, ADP ribosylation, deimination and

Proline Isomerization also occur (Kouzarides, 2007). Lysine residues can get acetylated which regulates the functions of transcription, repair, replication and condensation. Methylation, which can occur on Lysines and Arginines, is associated with transcriptional regulation and repair. Serine and Threonine residues can be modified by phosphorylation and are associated with transcription, repair and condensation. Generally, the modifications regulate the functions by causing chromatin contact disruption or allowing docking site for other regulatory proteins (Kouzarides, 2007). The focus of this study is how certain chromatin modifying enzymes affect direct lineage conversion.

Histone modifying enzymes direct the chromatin modifications. Most of these enzymes are identified and has been extensively studied for the last 20 years (Kouzarides, 2007). Lysine 27 of histone H3 histone (H3K27) is one of the most studied residues in the field of epigenetics which methylation of it is recognized as a repressive mark. PRC2 (Polycomb repressive complex 2) complex catalyzes the tri-methylation of H3K27 (Campos and Reinberg, 2009). PRC2 has 3 main components (Cao et al., 2002): EZH2 (enhancer of zeste homologue 2) which catalyzes the addition of methyl groups to H3K27 (Margueron and Reinberg, 2011), EED (embryonic ectoderm development) which interacts with H3K27 that allows mark to spread (Kuzmichev et al., 2002) and SUZ12 (suppressor of zeste). All of these components are required for PRC2's activity both *in vitro* and *in vivo* (Kuzmichev et al., 2002).

Histone methylations was considered as stable modifications; however, later studies proved that demethylase enzymes can reverse the methylation. For example, the first identified demethylase uses amine oxidase reaction to remove methylation at H3K4 and H3K9 methylation sites (Iwase et al., 2007; Metzger et al., 2005). In addition, JmjC domains are demethylase signature domains. By selecting JmjC containing proteins (Tsukada et al., 2005), novel histone demethylases have been identified such as KDM6 family. KDM6 family demethylases shown to play important roles in differentiation, senescence, inflammatory response and cancer (De Santa et al., 2007). JMJD3 has been found to remove the trimethyl group from the H3K27 residue, but has no effect on di or monomethyl H3K27 (Xiang et al., 2007). With De Santa et al.'s work, JMJD3 is important to regulate H3K27me3 levels and transcriptional activity which allows lymphoendothelial transdifferentiation of macrophages in response to bacterial products and inflammatory cytokines (De Santa et al., 2007). UTX is another demethylase from KDM6 family

that removes the repressive trimethylation of H3K27 and allows for chromatin to be transcriptionally permissive. Unlike JMJD3, which is coded by an autosomal gene, UTX is coded on a gene at X chromosome and escapes X chromosome inactivation (Faralli et al., 2016). Faralli et al. demonstrated that UTX demethylase activity is required muscle regeneration, and if the activity of the demethylase is blocked by an inhibitor or knock-in of a demethylase-dead mutant, muscle-specific genes cannot be expressed (Faralli et al., 2016).

H3K79 is another residue that has been linked pluripotency, differentiation and reprogramming. H3K79me2 mark is commonly found with H3K4me3 mark which is an activating mark near the transcription start site of actively transcribed genes. DOT1L (disruptor of telomeric silencing like protein) is the only known methyltransferase for H3K79, and it is unique because it does not have a SET domain unlike other methyltransferases (Feng et al., 2012; Onder et al., 2012; Pereira et al., 2010). Upon loss of *DOT1L*, embryonic lethality occurs at E9.5-E10.5 due to defects in growth and angiogenesis (Jones et al., 2008). To this date, there is no identified protein for H3K79 demethylation.

1.5 PRC2 and DOT1L is Related with Pluripotency

Several reports indicate that PRC2 complex and DOT1L is related with pluripotency, differentiation and reprogramming. PCR2 targets at least 10% of genes in embryonic stem cells (Mohn et al., 2008) such as *Hox* and other developmental regulators (Boyer et al., 2006; Bracken et al., 2006; Lee et al., 2006). There are two models to explain the effect of PRC2 complex at pluripotency. First model claims that PRC2 is important for the repression of genes that are responsible for differentiation. The second method states the pluripotency is lost when the genes are silenced to maintain pluripotency (Margueron and Reinberg, 2011). It was shown that the loss of SUZ12, which is a PRC2 complex component, causes inefficient silencing of *Nanog* and *Oct4* which are two pluripotency factors (Walker et al., 2010).

During fertilization, mouse oocytes have H3K79me2 and me3 marks, however they disappear following fertilization (Ooga et al., 2008). This indicates that this mark has some role in totipotency. In reprogramming studies, the efficiency of conversion of mouse fibroblasts to induced pluripotent stem cells get increased by 3-4-fold when DOT1L is inhibited by small molecules or the gene is knocked down (Onder et al., 2012). The inhibition of Dot1L allows for the transition from mesenchymal to epithelial state by the loss of H3K79me2 mark from

fibroblast specific genes that are silenced at reprogramming. In 2015, Zhao et al. establish a chemical reprogramming protocol with a yield greater than 1,000-fold from the previously reported protocol (Zhao et al., 2015). In this protocol, authors used a cocktail of small molecules which included DZNep and EPZ004777. DZNep is an EZH2 inhibitor and EPZ004777 is a DOT1L inhibitor. The most notable increase was obtained with SGC0946 molecule which is a slightly modified EPZ004777 by its structure. This study showed that chemical reprogramming and epigenetic modifications are promising strategies to increase reprogramming efficiencies.

1.6 Epigenetics' Influence on Transdifferentiation

There have been reports that conversion rate of transdifferentiation of fibroblasts to functional induced hepatocyte-like (iHep) cells can be increased by additional factors such as histone demethylases. In 2016, Zakikhan et al. published that Kdm2b, which is a histone demethylase for H3K36 mark can promote a higher conversion rate with previously reported hepatic lineage conversion transcription factors *Hnf4a* and *Foxa3* (Zakikhan et al., 2016). They showed the resulting cells were functional by Periodic acid-Schiff (PAS) staining, CYP450 activity, low density lipoprotein, indocyanine green uptake and Albumin secretion. When the limb fibroblasts were infected with the combination of Hfn4a, Foxa3 and Kdm2b lentivirus vectors, it yielded nearly 4-fold increased colony number of iHeps than the combination Hfn4a and Foxa3 lentiviruses alone (Zakikhan et al., 2016).

There have been many studies that investigate if epigenetic marks are a barrier against cell differentiation. According to Vanhove et al.'s findings, H3K27me3 does not control regions related to the expression of lineage-specific markers in hESC derived hepatocytes *in vitro*, and reduced level of H3K27me3 did not improve the hepatocyte maturation (Vanhove et al., 2016). On the contrary, Akiyama et al. reported that ectopic expression of JMJD3 can accelerate the differentiation of human pluripotent stem cells to hepatic cells by removing H3K27me3 mark (Akiyama et al., 2016). This finding was supported by the work of Dal-Pra et al. which they showed that demethylation of H3K27 is essential for the direct reprogramming of cardiac fibroblasts to cardiomyocytes with four microRNA combination, both *in vitro* and *in vivo*; which is suggesting that removal of this methyl mark can be used to improve transdifferentiation (Dal-Pra et al., 2017).

In addition to genetic modifications of chromatin modifier genes, non-viral and non-integrating approaches with chemicals is also used to increase the efficiency of reprogramming. In the last decade, there are many reports using chemical approach to increase the efficiency of induced pluripotent stem cells, neurons, cardiomyocytes, pancreatic β cells and hepatocytes (Ma et al., 2017). Inhibitors of DNA methyltransferases (5-aza, 5-aza-dc, RG108), histone methyltransferases (DZNep, EPZ004777, SGC0946), histone deacetylases (Valproic Acid (VPA), Sodium Butyrate (NaB), Lysine-specific demethylases (Tranylcypromine (Parnate)) and Protein arginine methyltransferases (AMI-5) have been shown to increase iPSC generation (Ma et al., 2017).

From these chemicals, RG108, Parnate, VPA and NaB also increases the efficiency of induced Neuronal Stem Cells (iNSC) reprogramming (Ma et al., 2017). AS8351 (KDM5B inhibitor), Parnate (LSD1 inhibitor) and VPA also increases the transdifferentiation efficiency to induced Cardiomyocytes (iCM) (Ma et al., 2017). Vitamin C, which is a cofactor of histone demethylases is known to increase reprogramming efficiency (Ma et al., 2017). For the generation of iHep cells, the chemicals inhibitors of chromatin modifiers that can increase the efficiency has not been reported in the literature (Ma et al., 2017). However, there are studies that show signaling inhibitors such as CHIR99021 (GSK3β inhibitor), A83-01 (TGFβ signaling pathway inhibitor), Compound E (Notch signaling inhibitor) can increase the efficiency of direct lineage conversion to induced hepatocytes (Ma et al., 2017).

The exact mechanisms of these chemical conversions and the role of epigenetic modifiers remain largely unknown. However, one possible mechanism is that inhibition of these modifiers removes the epigenetic barriers between two cell types. This can explain the effects of HDAC inhibitors or DNA/Histone methyltransferase inhibitors since they directly affect the epigenetic barriers (Xie et al., 2017). The second mechanism is that these modulators may suppress the characteristics of the starting cell line. This can be deduced from the TGF pathway inhibitors and Wnt pathway activators (Xie et al., 2017). The third mechanism can be that these compounds and enzymes induce the characteristics of the cell type of interest or enhance the survival and function of the desired cell type such as ISX9 and Dorsomorphin for neurons (Hu et al., 2015; Li et al., 2015).

Considering these previous studies, one can postulate that chromatin marks such as H3K79 methylation can have an effect on transdifferentiation efficiency. In this thesis, I addressed the hypothesis that removal of these marks though genetic or chemical inhibition of the responsible enzymes can increase the efficiency of direct conversion to obtain iHep cells.

Chapter 2

MATERIALS AND METHODS

2.1 Cell Culture

HEK 293T cells, dH1f cells (Park et al., 2008) and HepG2 cells were cultured in DMEM (Gibco) supplemented with 10% Fetal Bovine Serum (Gibco) and 1% Penicillin-Streptomycin (Gibco) (referred to as D10 Medium), at 37°C with 5% CO_2. Puromycin selection was done with 2ug/ml and Blasticidin S selection was done with 10 µg/ml. Two days after the transduction with FHHB viruses, fibroblast cells were cultured in Hepatocyte maintenance medium (HMM) which is DMEM/F12 (STEMCELL Technologies) supplemented with 0.544mg/L ZnCl2 (Sigma-Aldrich), 0.75mg/L ZnSO4·7H2O (Sigma-Aldrich), 0.2 mg/L CuSO4·5H2O (Sigma-Aldrich), 0.025mg/L MnSO4 (Sigma-Aldrich), 2g/L Bovine serum albumin (Sigma-Aldrich), 2g/L Galactose (Sigma-Aldrich), 0.1g/L Ornithine(Sigma-Aldrich), 0.03g/L Proline(Sigma-Aldrich), 0.61g/L Nicotinamide, 1X Insulin-transferrin-sodium selenite media supplement (Sigma-Aldrich), 40 ng/ml TGFα (Peprotech), 40 ng/ml EGF (Peprotech),10µM dexamethasone (Sigma-Aldrich), 1% Penicillin-Streptomycin (Gibco) and 1% Fetal Bovine Serum (Gibco). For imaging of cell cultures, Nikon Eclipse TS100 inverted microscope was used. For fluorescent imaging of cell cultures Nikon C- Hg Mercury lamp was used with its GFP and RFP cubes.

2.2 LentiCRISPRv2 Plasmids Cloning

Exonic sequences to be targeted were obtained from the UCSC Genome Browser (https://genome.ucsc.edu/). CRISPR DESIGN (http://crispr.mit.edu/) tool was used to design the required guide RNAs (Table2.1). CACCG sequence was added to the 5' of the forward oligonucleotides, Reverse complement of the designed primer was generated and AAAC sequence was added to 5' and C was added to 3' of the reverse primer. LentiCRISPR v2 plasmid (Addgene, #52961) was used as the backbone plasmid. Plasmid was digested with BsmBI (NEB) restriction enzyme and gel purified with NucleoSpin Gel and PCR Clean-up kit (MN) according to manufacturer's protocol. Each pair of oligos was phosphorylated (1µl of 100µM) and annealed with T4 PNK (NEB) and T4 Ligation Buffer (NEB) (37ºC for 30 min, 95ºC for 4 min and then ramp down to 25ºC at 5ºC/min). Annealed and phosphorylated oligos were ligated with 50ng BsmBI digested plasmid by using Quick Ligase (NEB) and 2X Quick Ligase Buffer (NEB) (30 min incubation at RT). Stbl3 bacteria were used for the transformation.

Table2. 1 guideRNAs for CRISPR-Cas9 Mediated DOT1L Knockout

DOT1L-gRNA-1 (HD1)	Top	CACCGGTCCACAAACAGGTCGTCGT
	Bottom	AAACACGACGACCTGTTTGTGGACC
DOT1L-gRNA-2 (HD2)	Top	CACCGGGTCTCCCCGTACACCTCGG
	Bottom	AAACCCGAGGTGTACGGGGAGACCC

2.3 Transdifferentiation Plasmids (FHHB and FHHR) Cloning

For FHHB and FHHR plasmids, sequences of FOXA3(NM_004497), HNF1A(NM_000545), HNF4A(NM_000457.4) and RFP were obtained from EX-A1385-Lv165, EX-Q0535-Lv156 and EX-Z2593-Lv166 plasmids (GeneCopoeia). Blasticidin-resistance sequence (Blast) was obtained from pWZL Blast GFP plasmid (Addgene, #12269). cDNA sequences were amplified with primers (Table 2.2 and Table 2.3). FOXA3 forward primer incorporated Kozak and Start sequences, while Blast or RFP reverse primers contained the Stop sequence. HNF1A (P2A), HNF4A (T2A) and Blast or RFP (E2A) forward primers contained 2A self-cleaving peptides(Liu et al., 2017) to individually overexpress transcription factors and selection markers. After PCR amplification with relevant oligos, products (FoxA3 - 1145bp, HNF1A - 2018bp, HNF4A - 1551 bp, Blast - 519bp and RFP - 807bp) were gel purified with NucleoSpin Gel and PCR Clean-up (MN) according to manufacturer's protocol. First, pENTR1A no ccDB (w48-1) (Addgene, #17398) and FOXA3 oligos were digested with BamHI (NEB) and KpnI (NEB) and ligated with Quick Ligase (30 min incubation at RT, 3:1 insert to backbone molar ratio). After colony picking, plasmids were isolated using NucleoSpin Plasmid (MN) kit. Same procedure was sequentially applied to plasmids from previous steps with oligos P2A-HNF1A (KpnI and EcorI), T2A-HNF4A (EcorI and NotI) and E2A-Blast/E2a-RFP (NotI and XbaI). Finally, pENTR1A-FOXA3-HNF1A-HNF4A-Blast and pENTR1A-FOXA3-HNF1A-HNF4A-RFP plasmids were cloned to pLOVE empty vector (Addgene, #15948) backbone using Gateway Cloning in which Gateway LR Clonase II Enzyme mix (Thermo Fisher) was used. Individual colonies were confirmed by restriction digestion with NcoI (NEB), KpnI (NEB) combined with EcorI (NEB) and Sanger sequencing.

Table2. 2 Primers for FHHB and FHHR Cloning

pENTR1A FHHB Plasmid	**BamH1-Kozak-Start-FoxA3 Forward**	AGCAGGATCCACCATGCTGGGCTCAGTGAAGATG
	KpnI-Foxa3 Reverse	AGCAGGTACCGGATGCATTAAGCAAAGAGCGG
	KpnI-P2A-HNF1A Forward	AGCAGGTACCGGAAGCGGAGCTACTAACTTCAGCCTGCTGAAGCAGGCTGGAGACGTGGAGGAG AACCCTGGACCTGTTTCTAAACTGAGCCAGCTGCAG
	EcorI-HNF1A Reverse	AAGCAGAATTCCTGGGAGGAAGAGGCCATCTG
	EcorI-T2A-HNF4A Forward	AAGCAGAATTCGGAAGCGGAGAGGGCAGAGGAAGTCTGCTAACATGCGGTGACGTCGAGGAGAA TCCTGGACCTCGACTCTCCAAAACCCTCGTC
	Not1-HNF4A Reverse	AGCAGCGGCCGCGATAACTTCCTGCTTGGTGATG
	Not1-E2A-Blast Forward	AGCAGCGGCCGCAGGAAGCGGACAGTGTACTAATTATGCTCTCTTGAAATTGGCTGGAGATGTTG AGAGCAACCCTGGACCTAAAACATTTAACATTTCTCAAC
	Xba1-Stop-Blast Reverse	AGCATCTAGATTAATTTCGGGTATATTTGAG
pENTR1A FHHR Plasmid	**BamH1-Kozak-Start-FoxA3 Forward**	AGCAGGATCCACCATGCTGGGCTCAGTGAAGATG
	KpnI-Foxa3 Reverse	AGCAGGTACCGGATGCATTAAGCAAAGAGCGG
	KpnI-P2A-HNF1A Forward	AGCAGGTACCGGAAGCGGAGCTACTAACTTCAGCCTGCTGAAGCAGGCTGGAGACGTGGAGGAG AACCCTGGACCTGTTTCTAAACTGAGCCAGCTGCAG
	EcorI-HNF1A Reverse	AAGCAGAATTCCTGGGAGGAAGAGGCCATCTG
	EcorI-T2A-HNF4A Forward	AAGCAGAATTCGGAAGCGGAGAGGGCAGAGGAAGTCTGCTAACATGCGGTGACGTCGAGGAGAA TCCTGGACCTCGACTCTCCAAAACCCTCGTC
	Not1-HNF4A Reverse	AGCAGCGGCCGCGATAACTTCCTGCTTGGTGATG
	Not1-E2A-RFP Forward FHHR	AGCAGCGGCCGCAGGAAGCGGACAGTGTACTAATTATGCTCTCTTGAAATTGGCTGGAGATGTTG AGAGCAACCCTGGACCTGTGAGCAAGGGCGAGGAGGATAAC
	Xba1-Stop-RFP Reverse FHHR	AGCATCTAGACTACTTGTACAGCTCGTCCATGCCG

Table2. 3 Primers for cloning RFP control

pENTR1A RFP	Not1-RFP with start	AGCAGCGGCCGCAATGGTGAGCAAGGGCGAGGAG
	Xba1-RFP with stop	AGCATCTAGACTACTTGTACAGCTCGTCCATGCCG

2.4 pALB-GFP-PURO (PGP) Reporter Cloning

For the cloning of pALB-GFP-PURO reporter, Albumin promoter sequences were amplified from pALB-GFP plasmid (Addgene, #55759) with primers (Table2.4) that would allow for KpnI and PacI cut sites. For the backbone of plasmid, pENTR1A-UBE2C-eGFP plasmid (Gift of Nathan Lack, Koc University) was used. Plasmid and oligos were digested with KpnI (NEB) and PacI (NEB) restriction enzymes and gel purified with NucleoSpin Gel and PCR Clean-up (MN).

Products were ligated with Quick Ligase (NEB) (30 min incubation at RT, 3:1 insert to backbone mol ratio) and transformed Stbl3 bacteria. Plasmids were isolated with NucleoSpin Plasmid (MN) kit. Gateway Cloning with Gateway LR Clonase II Enzyme mix (Thermo Fisher) used to clone the reporter with pLENTI X1 Puro DEST (694-6) (Addgene, #17297) backbone.

Table2. 4 Primers for cloning pALB GFP Puro

pALB GFP Puro	Forward	AGCAGGTACCCACCGCGGTGGCGGCCGCTC
	Reverse	AGCATTAATTAAGGGCCCCCCCTCGAGGTCGAC

2.5 Preparation of Competent Bacteria

A single colony was picked from plated Stbl3 (Invitrogen, C737303) or DH5α (Invitrogen, 12297016) and grown at 2 ml LB broth for overnight culture without antibiotics. 16 hours later, 0.5 ml from the culture was diluted to 100 ml LB broth without antibiotics and cultured again for 3 hours. When OD600 value was between 0.4-0.6 (OD of culture-OD of LB broth), culture was incubated on ice for 15 minutes. Then, culture was distributed to 50ml conical tubes and centrifuged 3000 rpm for 15 minutes with a table-top centrifuge. Supernatant was removed, and cell pellets was resuspended in total of 33 ml RF1 (100mM RbCl, MnCl2.4H2O, 30mM K Acetate, 10mM CaCl2, 15% glycerol). The samples were incubated on ice for 15 minutes, then centrifuged as before. Supernatant was removed, and pellets were resuspended in total of 8 ml RF2 (10mM MOPS, 10mM RbCl, 75mM CaCl2, 15% glycerol). Competent cells were aliquoted on ice and snap freezed in liquid nitrogen. Competent bacteria were stored at -80 ºC.

2.6 Transient Transfection

2.5 x 10^6 of HEK293T cells were seeded to 10 cm tissue culture plates. Next day, 2500 ng plasmid of interest was mixed with 20 µl FuGENE 6 Transfection Reagent in total volume of 400 µl DMEM. After 16 hours, medium was refreshed with D10. 48 hours later the transfection, selection markers of plasmids were able to be detected.

2.7 Production of Viral Particles

2.5 x 10^6 of HEK293T cells were seeded to 10 cm tissue culture plates. Next day, cells were transfected with 250 ng envelope protein (VSVG (Addgene, #8454)), 2250 ng Gag Pol (pUMVC (Addgene, #8449) for retroviruses and 8.2DeltaVPR (Addgene, #8455)) or PSPAX2 (Addgene, #12260) for lentiviruses) and 2500 ng viral vector of interest using 20 µl FuGENE 6 Transfection Reagent (Promega) in a total volume of 400 µl DMEM. 16 hours later, medium was changed with fresh 8 ml D10 media. 48 hours after the transfection, medium was collected and stored at

4°C and fresh 8 ml of D10 media were added. Second virus collection was performed at 72 hours after transfection. Collected media containing viruses were centrifuged at 1500 rpm for 5 minutes and supernatant was filtered with a 45 µm low protein binding syringe filter.

2.8 Production of Concentrated Viral Particles

The initial part of this procedure is same with the production of viral particles. Later, PEG-8000 (Sigma) 50% was dissolved in PBS as 5X and added to collected viral supernatant in 1:5 ratio. The mixture was incubated for two days at 4°C. The mixture was centrifuged at 2500 rpm for 20 minutes at 4°C. The supernatant was discarded, and pellet was resuspended in cold PBS with concentrating the virus 100-fold. The resuspended viruses were stored in aliquots at -80°C.

2.9 hiHEP Induction

For hiHep induction, dH1f cells were used between the passages 12 and 15. To generate hiHep cells, $4x10^5$ (for 6-well plates) or 2000 (for 96 well plates) dH1f cells were seeded on collagen I (Gibco, A1048301) coated plates. One day later, cells were infected with the viruses (each MOI=5 or 10, titer of the viruses was calculated with number of cells surviving after blast selection) with 8 µg/ml protamine sulfate (Sigma-Aldrich) for 16 hours and then changed to D10 media for another 24 hours. Next day, the media were changed to HMM. At every 2 days until the end of experiment, the media were refreshed with HMM.

2.10 Histone Extraction

Cell pellets were resuspended with Triton Extraction Buffer (PBS with containing 0.5% Triton X 100, 2 mM phenylmethylsulfonyl fluoride (PMSF) added fresh, 0.02% NaN_3) with 10^7 cells per ml and incubated 10 minutes on ice with gentle stirring. Cells were centrifuged at 6500 x g for 10 minutes at 4°C. The pellet was resuspended in half volume of TEB and centrifuged again. The remaining nuclei was resuspended in 0.2 N HCl at a density of $4x10^7$ nuclei per ml and incubated overnight at 4°C. 16 hour later, samples were centrifuged at 6500 x g for 10 minutes at 4°C to pellet debris. The supernatant was collected and mixed with 1:5 volume of 0.1M NaOH to neutralize the pH. The protein concentration was measured using Pierce BCA Protein Assay Kit (Life Technologies) according to the manufacturer's instructions.

2.11 Whole Cell Lysis

Cell pellets were resuspended in Whole Cell Lysis Buffer (50mM Tris pH 8.0, 250mM NaCl, 5mM EDTA, 50mM NaF, 1% NP-40, 1mM PMSF, 1x cOmplete EDTA-free protease inhibitor tablets (Roche) and dH_2O) and incubated on ice for 40 minutes with gentle stirring. Samples were centrifuged for 10 minutes at 14000 rpm at 4°C.

2.12 Cytosolic and Nuclear Lysis

For cytosolic lysis, cell pellets are resuspended with cytosolic lysis buffer (10mM HEPES pH 7.9, 10mM KCl, 0.1M EDTA, 1% NP-40, 1x cOmplete EDTA-free protease inhibitor tablets (Roche) and dH_2O) and incubated on ice for 15 minutes with gentle stirring. Samples were centrifuged for 3 minutes at 3000 x g at 4°C. Supernatants were collected and centrifuged at 3000 x g for 5 minutes at 4°C. These supernatants were collected as cytosolic fractions.

For nuclear fractions, pellets were washed 2 times with cytosolic buffer, then resuspended in nuclear lysis buffer (20mM HEPES pH 7.9, 0.4M NaCl, 1 mM EDTA, 10% Glycerol 1x cOmplete EDTA-free protease inhibitor tablets (Roche) and dH_2O). Later, samples were sonicated (2 times with amplitude 40 for 10 seconds). After centrifuge at 15000 x g for 5 minutes at 4°C, supernatants were collected as nuclear fractions.

2.13 Western Blotting

Proteins and 4X Loading Dye (9:1 mixed 4X Laemmli Sample Buffer (Bio-Rad), and β-mercaptoethanol (Bio-Rad)) to a final concentration of 1X and boiled at 95°C for 10 minutes. Boiled samples were run on a 4-15% gradient Mini-PROTEAN® TGX™ Precast Protein Gels (Bio-Rad) using 1x Tris/Glycine/SDS running buffer (TGS) (Bio-Rad) in a Mini-PROTEAN Tetra cell electrophoresis chamber (Bio-Rad) at 25mA for 40 min. The proteins were transferred from gel to PVDF membrane (Bio-Rad) by semi-dry transfer using the Trans-Blot® Turbo™ Transfer System (Bio-Rad) using default settings for mini gels. For transfer buffer, 1x TGS is mixed with 1:5 volume Methanol. After the transfer, Ponceau S Red (Bio-Rad) solution was applied for 10 minutes. Staining was washed with TBS containing 0.1% Tween 20 (TBS-T) for 3 times of 15 minutes. Membrane was blocked with 5% non-fat dry milk (Bio-Rad) dissolved in TBS-T for an hour at room temperature. After blocking, membrane was incubated overnight at 4°C with gentle shaking with the related primary antibody (Table2.5), which was diluted in primary antibody solution (2% bovine serum albumin (BSA), 0.02% NaN3 in TBS-T). Next day, membrane was washed with TBS-T for three times of 15 minutes and incubated with related HRP-conjugated secondary antibody diluted in 5% milk in TBS-T or infrared secondary antibody in TBS (Table2.5). Following the incubation, membrane was washed three times with TBS-T for 15 minutes and ECL Western Blot (Thermo Fisher) was applied if the antibody was HRP-conjugated or directly imaged with LI-COR Fc Imager.

Table2. 5 List of all antibodies used for Western Blotting

Antibody	Host	Brand	Catalog No	Secondary Antibody
H3K79me2	Rabbit	Abcam	ab3594	ab97051
H3 Total	Rabbit	Abcam	ab1791	ab97051
FOXA3/HNF-3γ	Mouse	Santa Cruz	sc-74424	ab97023
HNF1A	Rabbit	Abcam	ab96777	925-68071 (IR680)
HNF4A	Mouse	Santa Cruz	sc-374229	ab97023
HDAC1	Rabbit	Santa Cruz	sc-7872	ab97051

2.14 Gene Expression Analysis by Quantitative PCR (qPCR)

RNA was isolated from harvested cells by using Direct-zol RNA miniprep kit (Zymo Research). To synthesize cDNA, 1ug RNA was mixed with 2.5µl 2 mM dNTP (Life Technologies) and 2 µl 50 µM hexanucleotide mix (Invitrogen) in a PCR tube and dH_2O was added up to 16.5 ul total reaction volume. The mixture was incubated in a BIO RAD T100 Thermal Cycler at 65°C for 5 min, and quickly incubated on ice for 5 minutes. Reverse Transcription master mix was prepared with 5 µl 5X First Strand Buffer (Invitrogen), 2 µl 0.1M DTT (Invitrogen) and 0.5 µl RNasin (Promega). The mixture is added to the samples and incubated for 10 minutes at room temperature. 1 µl of MMLV-RT enzyme (Invitrogen) was added to each sample and samples are incubated at 37°C for 1 hour for the synthesis and 70°C for 15 minutes for inactivation of the enzyme. The samples were diluted to 100 µl with dH_2O.

In 96 well opaque plates (Roche), 20 µl PCR reaction was set up with using 10 µl of LightCycler 480 SYBR Green I Master Mix (Roche), 2 µl of cDNA, 2 µl of 2.5 mM forward and reverse primer mix (Table 2.6), and 6 µl of dH_2O. Threshold cycles are measured with LightCycler 480 Instrument II (Roche) with "Abs Quant/2nd Derivative Max" analysis. Every threshold cycle of interest (TC) was subtracted from that samples actin threshold of Actin (TG) and mean of it was calculated. Then, $2^{|TG-TC|}$ values were used to calculate fold changes according to control samples.

Table2. 6 List of all primers used for qPCR

Gene	Forward Sequence	Reverse Sequence
ACTB	TGAAGTGTGACGTGGACATC	GGAGGAGCAATGATCTTGAT
FOXA3	GGCGGGCGAGGTCTACT	CAGGGTCATGTAGGAGTTGAGG
HNF1A	AACACCTCAACAAGGGCACTC	CCCCACTTGAAACGGTTCCT
HNF4A	CGAAGGTCAAGCTATGAGGACA	ATCTGCGATGCTGGCAATCT
ALB	TGCAACTCTTCGTGAAACCTATG	ACATCAACCTCTGGTCTCACC
AFP	AGTGAGGACAAACTATTGGCCT	ACACCAGGGTTTACTGGAGTC
CK8	CAGAAGTCCTACAAGGTGTCCA	CTCTGGTTGACCGTAACTGCG
CK18	TCGCAAATACTGTGGACAATGC	GCAGTCGTGTGATATTGGTGT
ASGPR1	ATGACCAAGGAGTATCAAGACCT	TGAAGTTGCTGAACGTCTCTCT
APOB	CAGCTGATTGAGGTGTCCAG	CACTGGAGGATGTGAGTGGA
ITIH2	ACCAGGTCTCCACTCCATTG	ATCCTGCAAGTCGTCCATCT
COL1A2	GGCCCTCAAGGTTTCCAAGG	CACCCTGTGGTCCAACAACTC
MMP14	CGAGGTGCCCTATGCCTAC	CTCGGCAGAGTCAAAGTGG
SNAI2	CTGGGCTGGCCAAACATAAG	CTTCTCCCCCGTGTGAGTT
TWIST2	CAGAGCGACGAGATGGACAA	CGGAGAAGGCGTAGCTGAG
EPCAM	GCCAGTGTACTTCAGTTGGTGC	CCCTTCAGGTTTTGCTCTTCTCC
CDH1	TGCCCAGAAAATGAAAAAGG	GTGTATGTGGCAATGCGTTC

2. 15 Cytation5 Image Reader Analysis

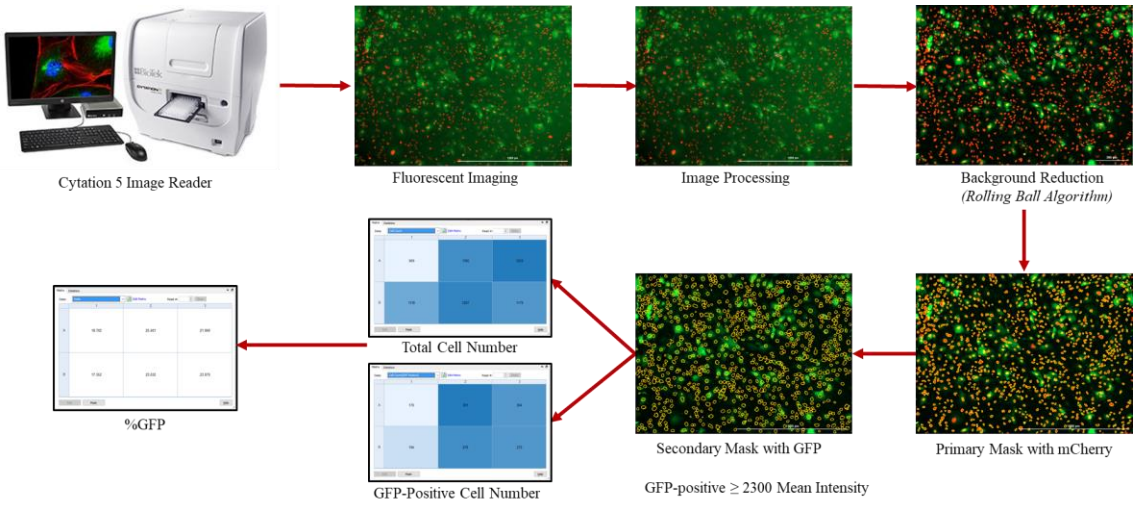

Figure 2.1 %GFP Analysis Steps

For % GFP analysis, total cell number was obtained from Texas Red signal using the PGK-H2BmCherry (Addgene, #21217) transduced cells. To quantify the transdifferentiated cells, GFP signal was measured with pALB-GFP-Puro (PGP) reporter construct. Gen5 Image Prime 3.03 software was used for all CYTATION 5 analyses. From the Task Manager, a new protocol was created with Standard Protocol. First, a new plate type was defined to adjust the bottom elevation for fluorescent imaging. Bottom elevation was decided according to cell type with optimal focus. Next, a new procedure was defined with: Read method's Image detection. Other settings were left as default at this step. GFP (469,525 nm) was selected as the first and Texas Red (586,647 nm) was selected as the second channel. Exposure and Focus was selected as auto for each well to be imaged. Horizontal and vertical offsets were selected according to plate type. 2 independent (top and middle) imaging areas were selected for 96 well plates and 5 imaging areas were selected for 6 well plates (top left, top right, bottom left, bottom right and middle). From the command "actions", temperature of equipment was selected to be 37°C. After imaging was completed, a new Image Processing step was defined with "Image Preprocessing" step. To reduce the background, "Rolling ball diameter" option was used and set with 3x of the length of an average cell. For GFP, same options were used from channel 1. The software generates new Images as "Tsf" by subtracting the background. To analyze the background-subtracted images, "Analyze" option was used by setting a new "Image Analysis". From edit options, Primary mask was created with options that cover every cell signal from H2B mCherry. For GFP, "Measure within a Primary mask" option is used as primary mask. From calculated metrics, "Cell Count", "Object Mean[TSF[Texas Red]]" and "Object Mean[TSF[GFP]]" were selected. To count the GFP cells, a new analysis is set from "Subpopulation Analysis" by adding a condition that GFP Mean is larger or equal to a certain mean. This mean was decided according to a scatter plot where X axis was "Cell Index" and Y axis was "GFP Mean". For this mean, usually 2300 was used from the optimization experiments, however it was changed according to background of different cell types or plates. After applying the changes to all wells, a cell count for GFP positive cells and cell number was calculated from Texas Red masks. To obtain the GFP ratio, "Ratio Transformation" from "Data Reduction" menu was used. For DS1, "Cell Count[GFP Positive]" and for DS2, "Cell Count" were selected and factor was selected as 100; which gave us the formula of "%GFP Ratio= DS1/DS2*100". After "Ratio" was calculated, the data was exported to excel files for analysis.

2.16 PAS Staining

Cells were fixed with 4% PFA (Electron Microscopy Sciences, 15735-60S) for 20 minutes. PFA was washed away with PBS and dH_2O. Cells were incubated in periodic acid solution for 5 min at Room Temperature. Samples were rinsed with distilled water and were incubated in Schiff's reagent for 15 minutes at Room Temperature. The solution was washed away with water for 5 min. After Ethanol and Xylene dehydration, the slides are closed with Entellan (Sigma-Aldrich).

2.17 Oil Red O Staining

Cells were fixed with 4% PFA (Electron Microscopy Sciences, 15735-60S) for 20 minutes. PFA was washed away with PBS and dH_2O. Cells were incubated 60% 2-propanol briefly. Then, samples treated with Oil Red O solution (0.5 g Certistain Oil Red O in 100 ml 2-propanol 60%, filtered with filter paper) for 20 minutes. Later, the cells were first rinsed with 2-propanol, then distilled water. Finally, samples were treated with Hematoxylin (Sigma-Aldrich) for 5 minutes and slides were closed with Aquatex (Sigma-Aldrich).

2.18 Compound Screen for Chromatin Modifiers

Compounds (Table2.7) were a gift from Udo Oppermann (Oxford University) and stored at -80°C. Compounds were diluted first 1:10 in DMSO and then 1:10 in HMM and placed in 96 well plates in 3 adjacent wells to serve as technical replicates. DMSO was used a control and occupied 6 wells on each plate. These plates had 10X working concentration and they were stored at -80°C after each step. Before the start of experiment, 96-well plates were coated with Collagen Type I and $2x10^4$ PGP-H2BmCherry dH1f cells were seeded at day -1. At day 0, cells were infected with pLOVE FHHB, and medium was refreshed 16 hours later. From the start of day 2, culturing medium was changed to HMM (90ul per well). 10ul of assay compounds diluted in HMM were then added onto each well. The medium was changed with fresh media containing related compound every 2 days until day 12. GFP percentage analysis with Cytation5 Image Reader was performed at day 6, day 9 and day 12.

Table2. 7 List of all compounds used for screen

Compound	Target	Working Concentration (M)
GSK2801	Bromodomains - BAZ2A, BAZ2B	0.5
K00135	Kinase inhibitor - ATP competitive - PIM	0.5
CHR-6494	Kinase inhibitor - Haspin	0.5
Tubastatin A HCl	HDAC - HDAC6	5

CPI-169	Histone methyltransferase - EZH2, EZH1	5
ML324	Histone demethylase - JMJD2E	2.5
PFI-3	Bromodomains - SMARCA2/4, PB1(5)	0.5
Rocilinostat	HDAC - HDAC6	5
KDOAM-25a	Lysine demethylases - JARID	0.5
Chaetocin	Histone methyltransferase - SUV39H1	0.025
A-366	Histone methyltransferase - G9a, GLP	1
GSK-LSD1 (irreversible)	Lysine demethylases - LSD1	0.25
OF-1	Bromodomains - pan-BRPF	2.5
KDOBA67	Histone demethylase	5
MS023	Arginine methyltransferase - Type I PRMTs	0.5
GSK8815	Bromodomains - ATAD2	5
GSK J4	Lysine demethylases - JMJD3, UTX, JARID1B	5
PFI-4	Bromodomains - BRPF1B	0.5
UNC1999	Histone methyltransferase - EZH2	0.5
LP99	Bromodomains - BRD9, BRD7	0.5
GSK8814	Bromodomains - ATAD2	5
BAZ2-ICR	Bromodomains - BAZ2A, BAZ2B	0.5
SMARCA	Bromodomains - SMARCA, PB1	1.25
CBP/BRD4 (0383)	Bromodomains - CBP, BRD4	2.5
Rucaparib	Poly ADP ribose polymerase (PARP)	5
PFI-2	Histone methyltransferase - SETD7	1
SRT1720	HDAC - SIRT1 activator	0.5
RGFP966	HDAC - HDAC3	5
CPI-360	Histone methyltransferase - EZH2 and EZH1	5
OICR-9429	Methyl Lysine Binder - WDR5	0.5
GSK864	Dehydrogenase	2.5
MAZ1805	tRNA loading inhibitor	0.5
GSK343	Histone methyltransferase - EZH2	1.5
IOX2	Prolyl-Hydroxylases - PHD2 (EGLN1)	5
5-Azadeoxycitidine	DNA methyltransferase (DNMT) - DNMT1/3	2.5
CI-994	HDAC - 1,2,3,8	0.5
Trichostatin A	HDAC - hydroxamic acids - Class I & II	0.25
C646	Histone acetyltransferase (HAT) p300/CBP	0.5
BAY-598	Histone methyltransferase - SMYD2	0.5
I-CBP112	Bromodomains - CREBBP, EP300	0.5
BI-9564	Bromodomains - BRD9, BRD7	0.5
Valproic acid	HDAC - aliphatic acid compounds	500
MAZ1392	tRNA loading inhibitor	0.5
SGC707	Arginine methyltransferase - PRMT3	0.5
LLY-507	Histone methyltransferase - SMYD2	0.5

Methylstat (Ester)	Histone demethylase	1.25
GSK J5 (inactive)	Lysine demethylases - Negative control	5
Repsox	TGF-βR	5
CHIR99021	GSK3	2.5
Forskolin	Hedgehog Signalling	10
3-Dznep	EZH2	0.25
OAC1	38261	5
SRT1724	SIRT1	0.25
L.asc (Vit C)	Cofactor of epigenetic modulators	25
D4476	Casein Kinase I	2.5
MI-2	MALT1	1.5
EPZ004777	DOT1L	1.5
AM580	RARα agonist	0.025
5-Iodotubercidin	Kinase inhibitor - ATP mimetic - Haspin	0.5
EX 527	HDAC - SIRT1	0.5
GSK484	Peptidyl arginine deiminase (PAD4)	0.5
Tranylcypromine	Lysine demethylases - LSD1	10
NVS-CECR2-1	Bromodomains - CECR2	0.5
SAHA	HDAC - hydroxamic acids	1.25
Bromosporine	Bromodomains - pan-Bromodomain	0.5
(+)-JQ1	Bromodomains - BRD2, BRD3, BRD4, BRDT (BET)	0.5
A-196	Histone methyltransferase - SUV420H1/H2	0.5
SGC0946	Histone methyltransferase - DOT1L	3.75
SGI-1776	Kinase inhibitor - Haspin	5
PCI-34051	HDAC - HDAC8	2.5
UNC1215	Methyl Lysine Binder - L3MBTL3	2.5
PFI-1	Bromodomains - BRD2, BRD3, BRD4, BRDT (BET)	2.5
IOX1 (5-carboxy-8HQ)	Lysine demethylases - pan-2-OG	20
UNC0642	Histone methyltransferase - G9a, GLP	0.5
NI-57	Bromodomains - pan-BRPF	0.5
Belinostat	HDAC - hydroxamic acids	2.5
SGC-CBP30	Bromodomains - CREBBP, EP300	0.5
(E)-JIB-04	Histone demethylase - Pan JmjC	0.025
UNC2400	Histone methyltransferase - EZH2	0.5
KDM5-C70	Histone demethylase - JARID1	5
I-BET	Bromodomains - BRD2/3/4	0.5
GSK106	Peptidyl arginine deiminase (PAD4)	0.5
MS049	Arginine methyltransferase - PRMT4, PRMT6	0.5
RVX-208	Bromodomains - BRD2, BRD3, BRD4, BRDT (BET, BD2)	2.5
UNC0638	Histone methyltransferase - G9a, GLP	0.5
(-)-JQ1 (inactive)	Bromodomains - Negative control	0.5

Entinostat	HDAC - ortho-amino anilides	0.25
Olaparib	Poly ADP ribose polymerase (PARP)	0.5
5-Azacitidine	DNA methyltransferase (DNMT)	5
BAY-299	Bromodomains - BRD1, TAF1	0.5
PCI-24781	HDAC	5
Romidepsin	HDAC	0.5
Santacruzamate	HDAC 2	25
KDOAM32	Lysine demethylases - JARID	0.5
TP-472	Bromodomains - BRD9	0.5
TP-472N	Bromodomains - BRD9	0.5
AMI-1	Arginine methyltransferase - PRMT	25
TMP269	HDAC - 4, 5, 7 &9	5
AGK2	HDAC - SIRT2	5
Mocetinostat	HDAC	5
A-395	Methyl Lysine Binder - EED	0.5
MS409N	Arginine methyltransferase - PRMT4, PRMT6	0.5
A-395N	Methyl Lysine Binder - EED	0.5
I-BRD9	Bromodomains - BRD9	5
TP-064	Arginine methyltransferase - PRMT4	0.5
TP-064N	Arginine methyltransferase - PRMT4	0.5

Chapter 3

RESULTS

3.1 Cloning of the plasmids required for overexpression of FOXA3, HNF1A, HNF4A

To understand the role of chromatin modifiers' in direct conversion of human fibroblast cells to hepatocytes, we chose to use a modified version of the Huang et al. protocol (Huang et al., 2014). For this purpose, we sought to overexpress FoxA3, HNF1A and HNF4A transcription factors. Previous work in reprogramming to pluripotency indicated that transcription factor stoichiometry and delivery is an important determinant of reprogramming efficiency (Sommer et al., 2016). Therefore, to ensure that cells receive all the factors at equal amounts, we generated a single expression cassette that can express FOXA3, HNF1A and HNF4A from a lentiviral backbone pLOVE. Individual cDNAs linked by self-cleaving 2A peptide sequences were cloned into the Gateway compatible pENTR1A vector. 2A "Self-cleaving" peptides are oligopeptides derived from viruses and cause ribosome skipping during translation in eukaryotic cells which then generates individual polypeptides from a single mRNA (Liu et al., 2017).

We added two different selection markers to create two overexpression cassettes, one of them containing blasticidin resistance gene (FHHB) and the other Red Fluorescent Protein RFP (FHHR). We then used gateway cloning to transfer these casettes to lentiviral (pLOVE) and episomal (pCXLE) backbones. As episomal plasmids allow overexpression without integration to genome, they avoid unwanted effects such as insertional mutagenesis. Since we inserted 2A self-cleaving peptides in between the transcription factors, we were able to individually overexpress them from a single vector (Figure 3.1A). Under fluorescent microscopy, we were able to observe RFP signal from pLOVE FHHR and pCXLE FHHR (Figure 3.1B). GFP or RFP signal was not detected from pLOVE FHHB or pLOVE FHHB transfected cells, but they were resistant to 10 µg/ml Blasticidin S selection (data not shown).

We confirmed overexpression of the three factors by qPCR (Figure 3.2A) and Western Blot (Figure 3.2B). For these experiments, we used uninfected HEK293T cells as negative controls in which we did not detect expression of any of these transcription factors. As a positive control, we used the HepG2 cell line which is derived from a human hepatocellular carcinoma and we observed similar or higher expression with infection or transfection of these plasmids.

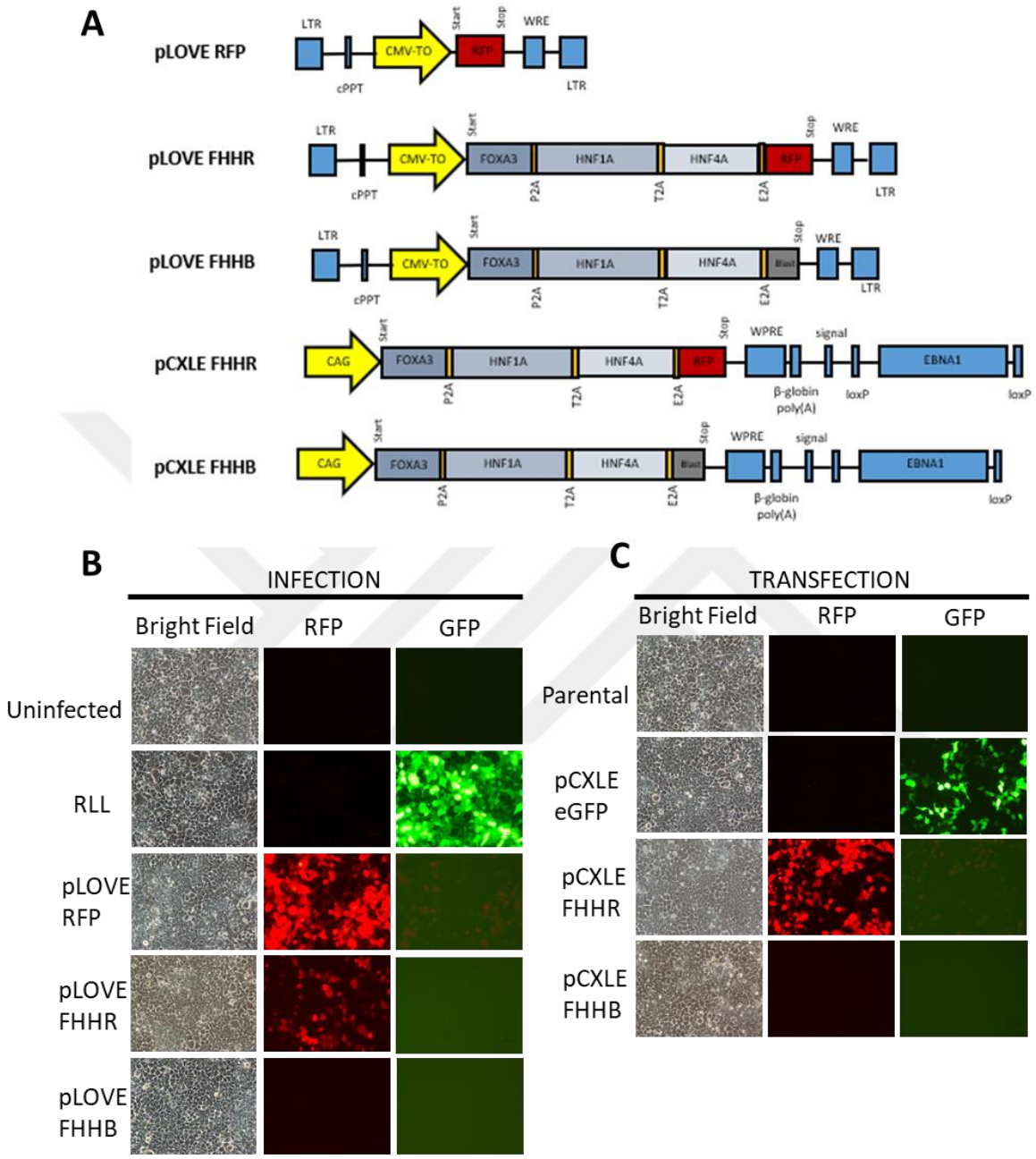

Figure 3.1 FOXA3, HNF1A and HNF4A overexpression plasmids

(A) Plasmid map schematics of overexpression plasmids (pLOVE RFP, pLOVE FHHR, pLOVE FHHB, pCXLE FHHR and pCXLE FHHB). (B) Bright Field, RFP and GFP images after HEK293T cells were infected with RLL (GFP control), pLOVE RFP (RFP control) and overexpression plasmids. (C) Bright Field, RFP and GFP images after HEK293T cells were transfected with pCXLE eGFP (GFP control) and overexpression plasmids.

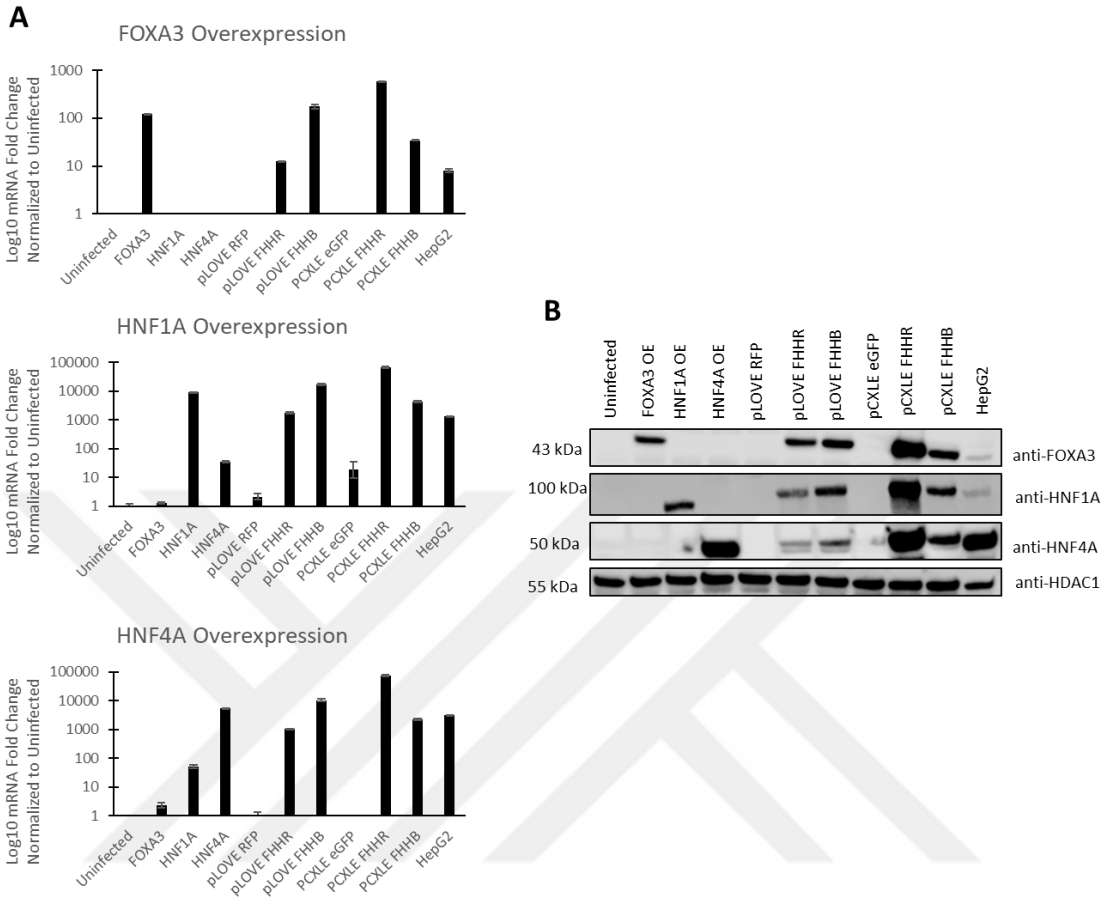

Figure 3.2 Conformation of FOXA3, HNF1A and HNF4A overexpression

(A) RT-qPCR analysis to confirm FOXA3, HNF1A and HNF4A overexpression. HepG2 cells were used as positive controls. (B) Western Blot to confirm FOXA3, HNF1A, HNF4A overexpression at HEK293T cells with related antibodies. HDAC1 was used as loading control. HepG2 cells were used as positive controls. (n=2 technical replicates; error bars, ± s.d.)

3.2 Our Albumin reporter is specific for Albumin expression

To monitor transdifferentiation efficiency on a per cell basis, we generated a reporter construct for Albumin expression. Albumin is a liver-specific protein and this reporter allows us to distinguish transdifferentiated cells which expresses Albumin (GFP-positive) from uninfected fibroblasts and those that are infected but do not exhibit hepatic gene expression (GFP-negative). For this purpose, Albumin promoter sequences were cloned it to pENTR1A-UBE2C-eGFP plasmid by restriction enzyme-based cloning. We chose this backbone to modify because it contains two insulator elements flanking the albumin-GFP cassette which improves specificity of the reporter. The cassette was then moved to the promoterless lentiviral backbone pLENTIX1 Puro DEST by Gateway cloning (Figure 3.2A).

To be able to quantify the total cell number by fluorescence imaging, we used PGK-H2B-mCherry plasmid that provides nuclear localized mCherry signal. All cells transduced with this vector express a fusion H2B-mCherry protein in the nucleus, which can be detected with TexasRed channel (Figure 3.2A). We first infected the fibroblasts with PGK-H2B-mCherry lentiviruses, and sequentially performed pALB-GFP-Puro (PGP) infection and Puromycin selection. Thus, we ensured that every cell would have mCherry signal but only transdifferentiated and Albumin expressing cells would be GFP positive (Figure 3.3B).

First, we confirmed that starting fibroblast cells and HepG2 cells do not express GFP and mCherry signals under fluorescent microscopy (Figure 3.3C). Cells were then transduced with H2B-mCherry construct, and imaged two days later with Cytation5 Imaging Reader to confirm that all cells were expressing mCherry, but not GFP (Figure 3.3C). H2B-mCherry expressing cells were transduced with Albumin-GFP reporter and selected for 3 days with 2 µg/ml Puromycin (Figure 3.3C). After the selection, 67% of HepG2 cells were GFP positive whilePGP-dH1f cells had no detectable GFP signal (Figure 3.3D). These results indicated that Albumin reporter was specifically turned on in cells that express Albumin and could serve as a useful readout of transdifferentiation.

To assess if Albumin reporter can be turned on upon transdifferentiation, PGP-dH1f cells were infected with pLOVE-FHHB. Uninfected dH1f, PGP-dH1f, dH1f FHHB and HepG2 cells were used as negative controls while PGP HepG2 cells were used as a positive control. After 12 days of incubation in hepatocyte medium, GFP expression was detected only in PGP-dH1f cells infected with pLOVE FHHB and the positive control PGP-HepG2 cells (Figure 3.3D). dH1f cells that did not contain the reporter or pLOVE-FHHB had no detectable GFP signal, confirming the specificity of the assay system.

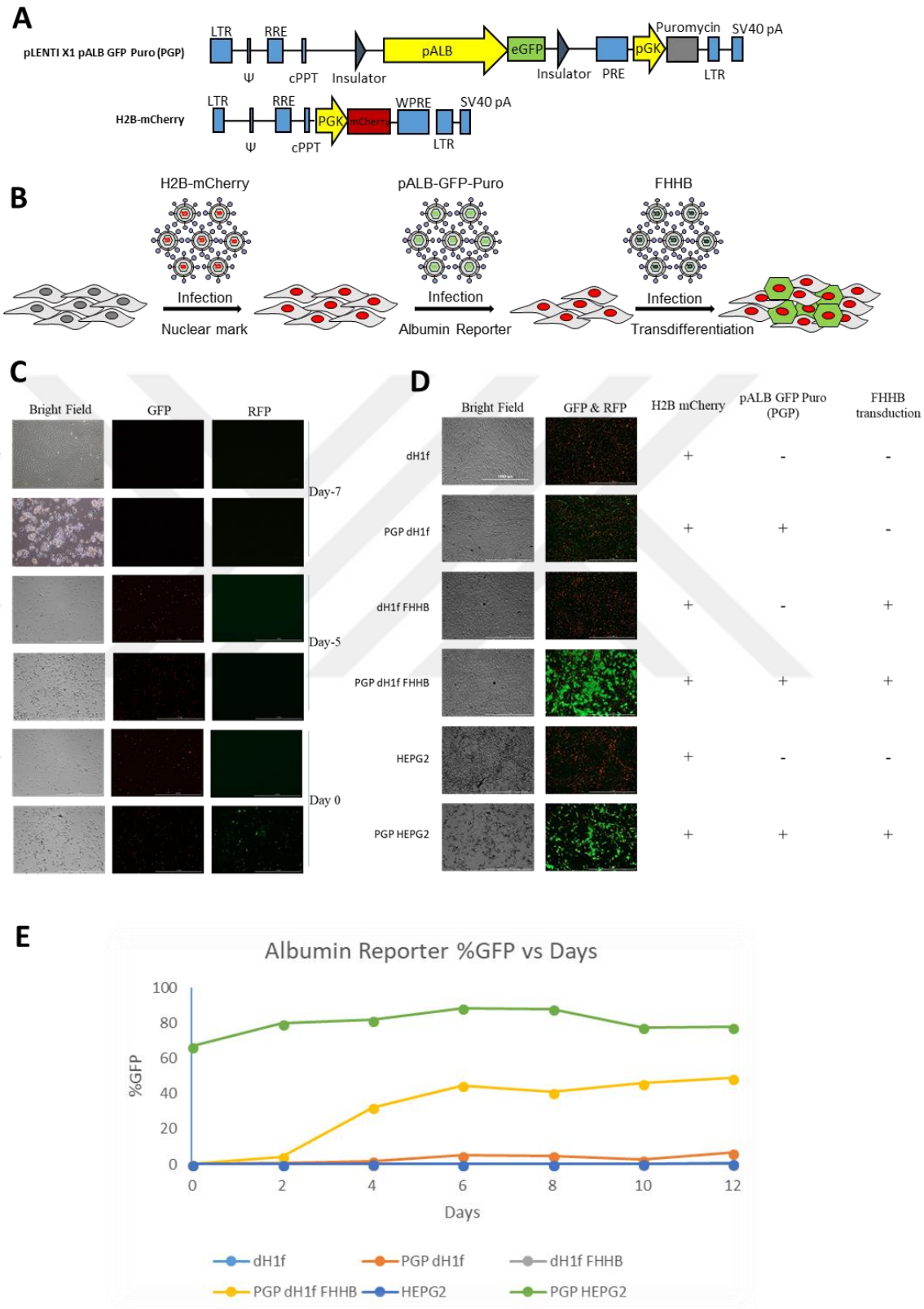
A
pLENTI X1 pALB GFP Puro (PGP)
LTR
RRE
Ψ
cPPT
Insulator
pALB
eGFP
Insulator
PRE
pGK
Puromycin
SV40 pA
LTR
H2B-mCherry
LTR
RRE
Ψ
cPPT
PGK
mCherry
WPRE
SV40 pA
LTR
B
H2B-mCherry
Infection
Nuclear mark
pALB-GFP-Puro
Infection
Albumin Reporter
FHHB
Infection
Transdifferentiation
C
Bright Field
GFP
RFP
dH1f
HEPG2
dH1f
HEPG2
dH1f
HEPG2
Day-7
Day-5
Day 0
D
Bright Field
GFP & RFP
H2B mCherry
pALB GFP Puro (PGP)
FHHB transduction
dH1f + - -
PGP dH1f + + -
dH1f FHHB + - +
PGP dH1f FHHB + + +
HEPG2 + - -
PGP HEPG2 + + +
E
Albumin Reporter %GFP vs Days
%GFP
100
80
60
40
20
0
0
2
4
6
8
10
12
Days
dH1f
PGP dH1f
dH1f FHHB
PGP dH1f FHHB
HEPG2
PGP HEPG2

Figure 3.3 Albumin expression with pALB GFP Puro

(A) Plasmid map schematics of pALB-GFP-Puro (PGP) and H2B-mCherry. (B) Experimental setup of PGP-H2BmCherry dH1f cells preparation. (C) Bright Field, GFP and RFP Images of dH1f and HepG2 cells. (B) Bright Field, GFP and RFP Images of dH1f and HepG2 at different timepoints before transdifferentiation. Naive forms of dH1f and HepG2 were imaged with Nikon ECLIPSE TS100. H2B mCherry Infected and pALB GFP Puro infected cells were imaged with Cytation5 Image Reader. (D) Bright Field and Merged (GFP and RFP) images of dH1f (wild-type), PGP dH1f, dH1f infected with pLOVE FHHB (dH1f FHHB), PGP dH1f infected with pLOVE FHHB (PGP dH1f FHHB), HepG2 (wild-type) and PGP HepG2. (E) Time course %GFP analysis with Albumin Reporter.

Next, we wanted the assess the dynamics of Albumin reporter activity upon transcription factor expression. To this end, a time course experiment was performed with CYTATION5 image analysis every two days. We observed a gradual increase in the percentage of GFP-positive cells until day 6, after which the % GFP cells remained steady at around 40%. In this experiment, HepG2 cells continuously had 80% GFP between days 2 and 12. In Huang et al.'s protocol, transdifferentiation requires nearly 12 days (Huang et al., 2014); however, these results indicated that most of the cells starts to express Albumin at an earlier timepoint. This result prompted us to analyze the direct lineage conversion rates both on day 6 and day 12 (Figure 3.3E).

3.3 CRISPR-Cas9 mediated knockout of DOT1L significantly reduced H3K79me2 mark

To investigate the role of DOT1L and the associated H3K79me2 mark in fibroblast to hepatocyte transdifferentiation, we created CRISPR-Cas9 mediated DOT1L knockouts in PGP-dH1f cells. We designed guideRNAs that target exons 5 of *DOT1L* gene (Figure 3.4A). Previous work has indicated that conditional knock-out of exon 5 resulted in complete loss of the protein's catalytic function (Chang et al., 2010). Selected guideRNAs were cloned into lentiCRISPRv2 plasmids (Figure 3.4B), and dH1f cells were infected with concentrated lentiviruses and selected with 2 µg/ml Puromycin (Figure 3.4C). Polyclonal puromycin resistant cell populations were then sequentially infected with PGP and H2B-mCherry lentiviruses.

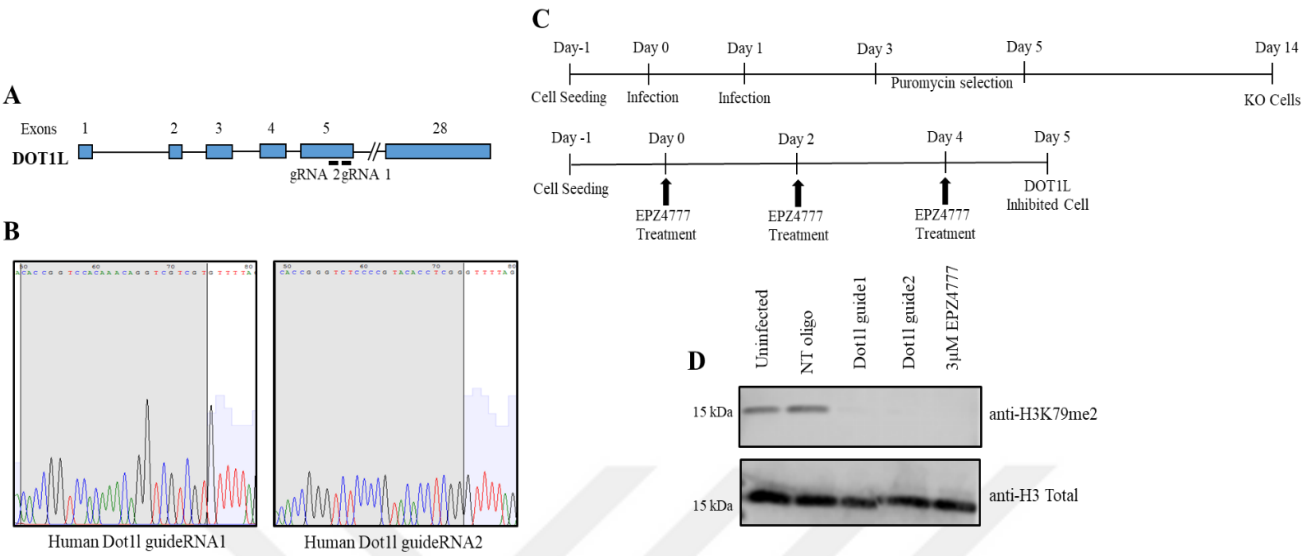

Figure 3.4 CRISPR-Cas9 mediated DOT1L Knockout

(A) Schematic of designed guideRNAs to target Exon 5 of DOT1L at human genome. (B) Sanger sequencing of guideRNAs cloned in lentiCRISPRv2 plasmid. (C) Experimental setup for DOT1L knockout and inhibition with wild-type dH1f cells. (D) Functional confirmation of DOT1L knockout and inhibition with Western Blot as H3K79me2 mark is disappeared.

To confirm the loss of DOT1L activity in CRISPR/Cas infected cells, we extracted histones and performed Western blot with a H3K79me2-specific antibody. It was previously known that 5 days of treatment with 3 μM EPZ004777 (a DOT1L chemical inhibitor) significantly reduces H3K79me2, which served as our positive control. We observed similar levels of reduction with guideRNA 1 (HD1) and guideRNA 2 (HD2), and non-targeting guideRNA (NT) transduced cells had the same level of H3K79me2 as uninfected dH1f cells (Figure 3.4D). These results indicated that we were able to catalytically inactivate DOT1L with this knockout, and the resulting cells could be used to determine the role of DOT1L's H3K79 methyltransferase role in fibroblast to hepatocyte transdifferentiation in human cells.

3.4 DOT1L knockout increases transdifferentiation efficiency to Hepatocytes on day 6

After we confirmed that we can quantify Albumin expression in PGP-dH1f cells on a per cell basis upon transdifferentiation, we seeded control (NT), and two DOT1L gRNA expressing cells (HD1 and HD2) on Collagen Type 1 coated 6 well plates, infected them with concentrated pLOVE FHHB viruses, and cultured them in Hepatocyte maintenance medium (HMM). On day 6, infected cells started to display an epithelial morphology (Figure 3.5A). As expected, we observed mCherry signal in both uninfected and infected cells, but only the FHHB infected cells

displayed GFP signal (Figure 3.5B). With Cytation5 Imaging Reader, we performed fluorescent imaging with TexasRed and GFP channels. We observed that GFP percentage was significantly higher in DOT1L knockout cells HD1 (25.7%) and HD2 (20.2%) compared to controls (14.6%) ($p<0.01$, three independent biological replicate experiments). The background GFP positivity in uninfected wells were 1.4% which most likely is due to autofluorescence of the cells (Figure 3.5C).

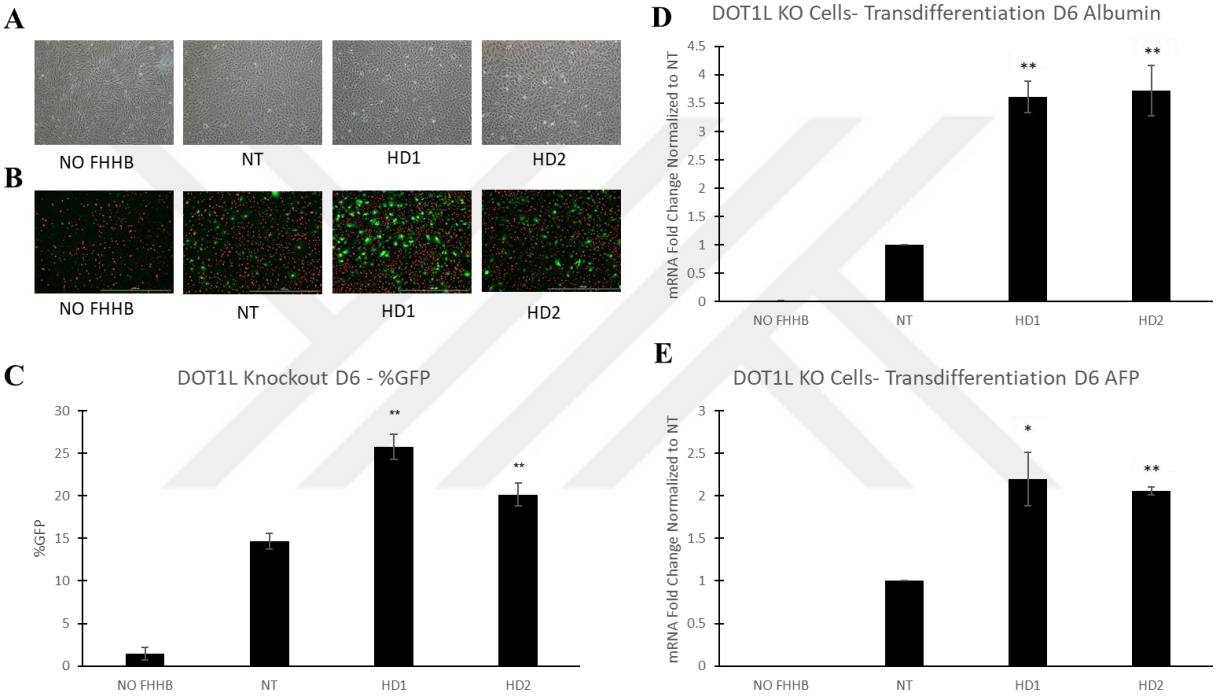

Figure 3.5 Transdifferentiation efficiency of DOT1L knockout cells at day 6

(A) Transdifferentiated PGP-H2BmCherry dH1f cells show typical epithelial morphology. (B) mCherry expression from H2BmCherry and GFP expression from PGP of DOT1L knockout dH1f cells on day 6. (C) %GFP analysis of DOT1L knockout cells at day 6. (n=6) (D) Increasing Albumin mRNA expression at DOT1L knockout cells, measured by quantitative PCR (qPCR). (E) Increasing AFP mRNA expression at DOT1L knockout cells, measured by qPCR. *$p<0.05$ and **$p<0.01$ (n=3; error bars, ± s.err.)

We next wanted to validate the increase in Albumin reporter activity by examining the mRNA level of Albumin. Cell pellets were collected on day 6 and RNAs were isolated. qPCR analysis indicated a significant increase in Albumin mRNA expression in DOT1L knockout cells. Albumin expression was 3.5-fold higher in HD1 and HD2 cells compared to controls, while PGP-dH1f cells that were not infected with pLOVE FHHB had no detectable albumin expression (Figure 3.5D). These results indicated that the Albumin-GFP reporter activity faithfully mirrors

Albumin mRNA expression and that inhibition of Dot1L results higher Albumin levels after 6 days of transdifferentiation.

Next, we checked levels of Alpha-fetoprotein (AFP) which is a glycoprotein expressed in early liver development. In the literature, unlike mature hepatocytes, iHep cells have high levels of AFP expression (Sekiya and Suzuki, 2011). According to qPCR analysis, both HD1 and HD2 cells had 2-fold higher AFP mRNA expression than NT cells. Again, we did not observe significant AFP mRNA expression with PGP-dH1f cells uninfected with pLOVE FHHB (Figure 3.5E). Taken together, these results suggest that transdifferentiation efficiency of fibroblasts to hepatocytes is increased when DOT1L is knocked out.

3.5 Effect of knocking-out DOT1L on transdifferentiation efficiency decreases at later stages

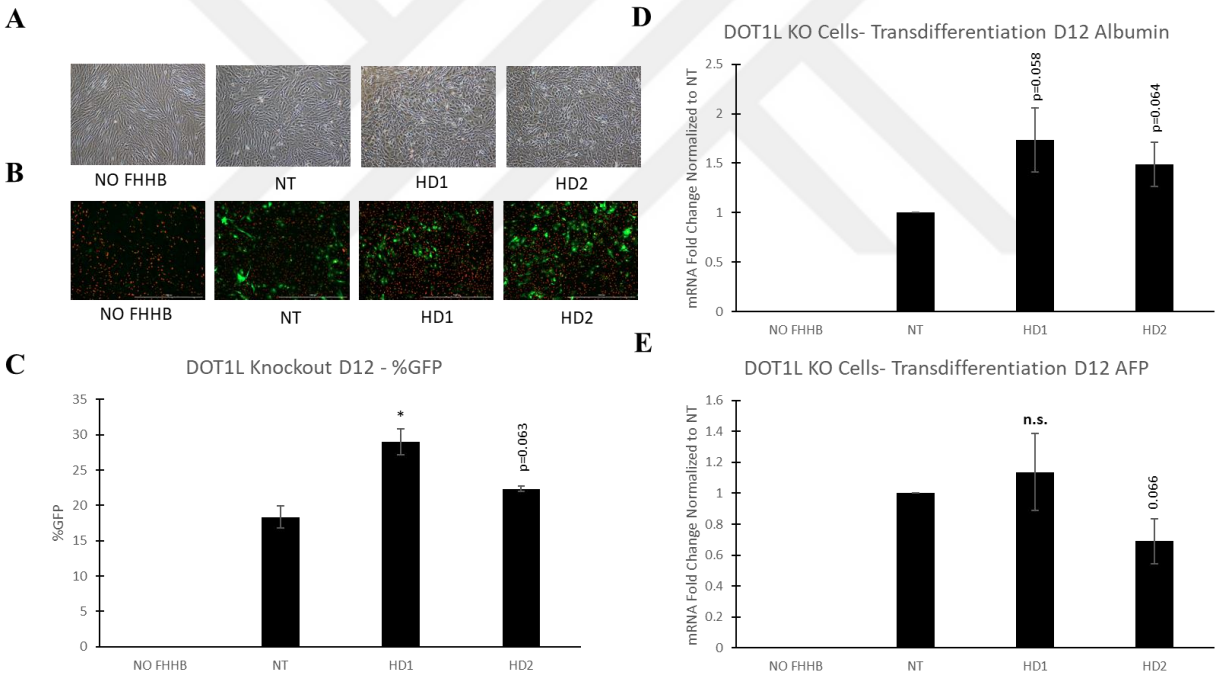

Figure 3.6 Knocking out DOT1L slightly increases transdifferentiation efficiency in later stages

(A) Epithelial morphology of transdifferentiated PGP-H2BmCherry dH1f cells at day 12. (B) mCherry and GFP expression of transdifferentiated DOT1L knockout PGP-H2BmCherry dH1f cells at day 12. (C) %GFP analysis of DOT1L knockout cells at day 12. (D) qPCR analysis of Albumin mRNA expression at DOT1L knockout cells at day 12. (E) qPCR analysis of AFP mRNA expression at DOT1L knockout cells at day 12. *$p<0.05$ (n=3; error bars, ± s.err.)

According to Huang et al., direct lineage conversion to hepatocytes requires 10-14 days (Huang et al., 2014). Because of this reason, we performed GFP percentage analysis also on day 12 after FHHB transduction. On day 12, GFP positive cells still displayed an epithelial morphology (Figure 3.6A). In general, since we did not passage the cells, wells were more crowded compared to day 6. However, it is known that hiHeps do not proliferate, a challenge Huang et al. overcame by lentivirus-mediated SV40 large T antigen expression (Huang et al., 2014). As we did not infect cells with SV40 large T antigen, while transdifferentiated cells ceased to proliferate, remaining dH1f cells continued to divide. As such, the GFP-positive percentage on day 12 were similar to day 6 with only a slight increase (Figure 3.6B). However, we still observed higher GFP positivity in HD1 cells (28.98%) and HD2 cells (22.35%) compared to NT cells (18.37%) (Figure 3.6C).

qPCR analysis of Albumin mRNA expression indicated a trend for increase in both HD1 (1.73-fold) and HD2 (1.48-fold) cells, but the difference compared to NT cells did not reach statistical significance (Figure 3.6D). qPCR for AFP indicated the observed effect of DOT1L was lost as HD1 and HD2 cells had a similar or lower level of mRNA expression (Figure 3.6E). This indicates that the effect of knocking out DOT1L decreases in later stages of transdifferentiation.

3.6 Chemical inhibition of Dot1L with EPZ004777 slightly increases Transdifferentiation efficiency at early stages

As alternative approach to inhibit DOT1L and to test whether the effect we observed with DOT1L knockout cell-lines was dependent on the loss of DOT1L catalytic activity, we utilized the small molecule EPZ004777 to inhibit DOT1L. DMSO was used as a negative control. Since the removal of histone marks from chromatin may require some time, we pre-treated our cells for 5 days with EPZ004777 followed by FHHB infection. 6 days post-infection morphologies of the cells were similar to CRISPR/CAS-based knockout cells (Figure 3.7A).

With Cytation5 Imaging Reader, we were able to detect the mCherry and GFP signals with these cells as well (Figure 3.7B). Percentage of GFP positive cells increased significantly with EPZ004777 treatment (13.99% compared to 9.57% for DMSO treated) (Figure 3.7C). The overall lower percentage of GFP in these sets of experiments might be due to lower viral titer or nonspecific effects of chemical treatment on GFP brightness.

qPCR analysis for Albumin mRNA expression showed an increasing trend when the cells were treated with EPZ004777 (1.4-fold) although not at significance (Figure 3.7D). Similarly, EPZ004777 treated cells had 1.44-fold increase at AFP mRNA expression at the day 6 qPCR analysis (Figure 3.7E). These results, taken together with the GFP-percentage analysis, suggest that chemical inhibition of Dot1L may have a positive effect on transdifferentiation efficiency.

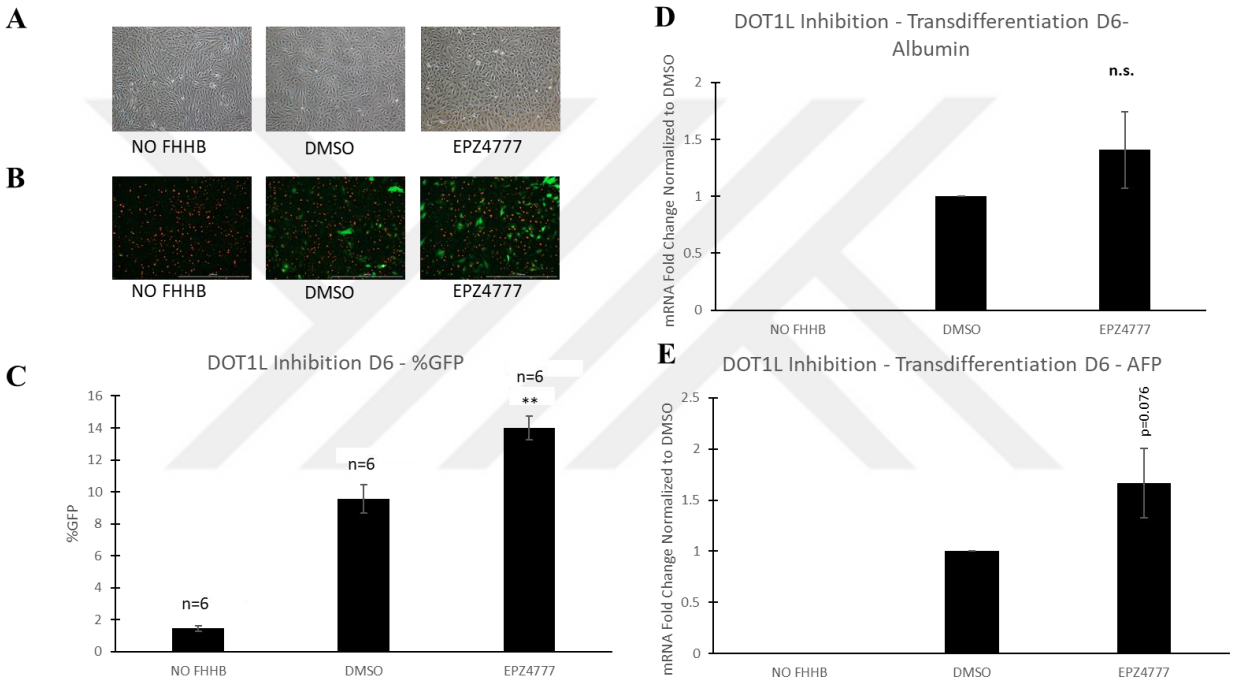

Figure 3.7 Dot1L inhibition's effect on transdifferentiation at day 6

(A) Morphologies of chemical treated cells PGP-H2BmCherry dH1f cells at day 6 of transdifferentiation. (B) mCherry and GFP expression at chemical treated PGP-H2BmCherry dH1f cells at day 6 of transdifferentiation. (C) %GFP analysis of DOT1L inhibited cells at day 6. (D) qPCR analysis of Albumin mRNA expression and (E) AFP mRNA expression at DOT1L inhibited cells at day 6. **p<0.01 (n=3; error bars, ± s.err.)

3.7 Inhibition of Dot1L with EPZ004777 has no effect at later stages of transdifferentiation

To understand if there is an effect of inhibiting DOT1L at the later stages of transdifferentiation, we analyzed our samples at the day 12 after pLOVE FHHB infection. Both DMSO and EPZ004777 treated cells had epithelial-like morphology (Figure 3.8A). However, cells were more stressed than DOT1L knockout cells. The reason for this might be treating the cells for 17 days with the chemicals. Even though cell death was apparent for both DMSO and

EPZ004777 conditions, all living cells had mCherry expression, while transdifferentiated cells had GFP signal (Figure 3.8B).

GFP percentage analysis showed no significant difference between DMSO-treated cells (30%) and EPZ004777-treated cells (28.88%) (Figure 3.8C). We observed a decrease in Albumin mRNA expression level with EPZ004777 (0.88-fold) compared to DMSO treated cells (Figure 3.8D). Even though we observed an increasing trend for AFP mRNA levels at EPZ004777 treated cells (1.24-fold), this was not significant (Figure 3.8E). These results indicate that there is no clear effect of inhibiting DOT1L with EPZ004777 at later stages of transdifferentiation.

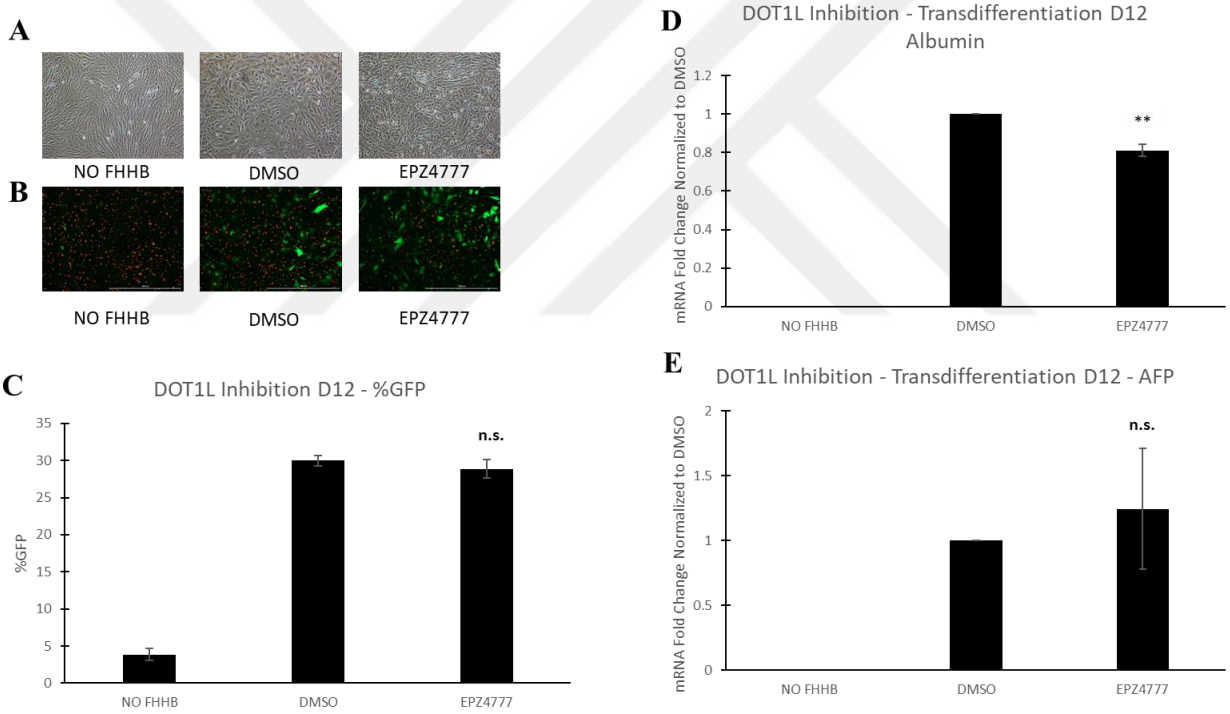

Figure 3.8 Dot1L inhibition's effect on transdifferentiation efficiency at day 12

(A) Epithelial-like morphologies of chemical treated cells at day 12 of transdifferentiation. (B) mCherry and GFP expression of chemical treated PGP-H2BmCherry dH1f cells at day 12 of transdifferentiation. (C) Dot1L inhibition's effect on %GFP of transdifferentiated cells. (D) qPCR analysis of Albumin mRNA expression and (E) AFP mRNA expression at DOT1L inhibited cells at day 12. **p<0.01 (n=3; error bars, ± s.err.)

3.8 DOT1L Knockout Accelerates Expression of Hepatocyte Markers

To investigate how gene expression network shifts from fibroblasts to hepatocytes, we selected 5 hepatocyte markers: CK8, CK18, ASGR1, APOB, ITIH2. First, we confirmed that these markers were not expressed in uninfected dH1f cells except for ASGR1 (Figure 3.9A). However, they were highly expressed in HepG2 cells, which were used as positive controls. On day 6 after FHHB transduction, hepatocyte markers were expressed at higher levels in DOT1L knockout cells HD1 (2.43-fold, 1.44-fold, 1.02-fold, 3.02-fold and 1.52-fold, respectively) and HD2 (3.06-fold, 1.58-fold, 0.83-fold, 3.02-fold and 1.18-fold, respectively) compared to NT controls (Figure 3.9B).However, on day 12 there were no significant differences in hepatic marker expression between DOT1L knockout and control cells (Figure 3.9C). Generally, the mRNA levels of hepatocyte markers followed the same trend of Albumin and AFP which shows that DOT1L knockout accelerates transdifferentiation of fibroblast cells hepatocytes at early stages, but the effect is diminished on day 12.

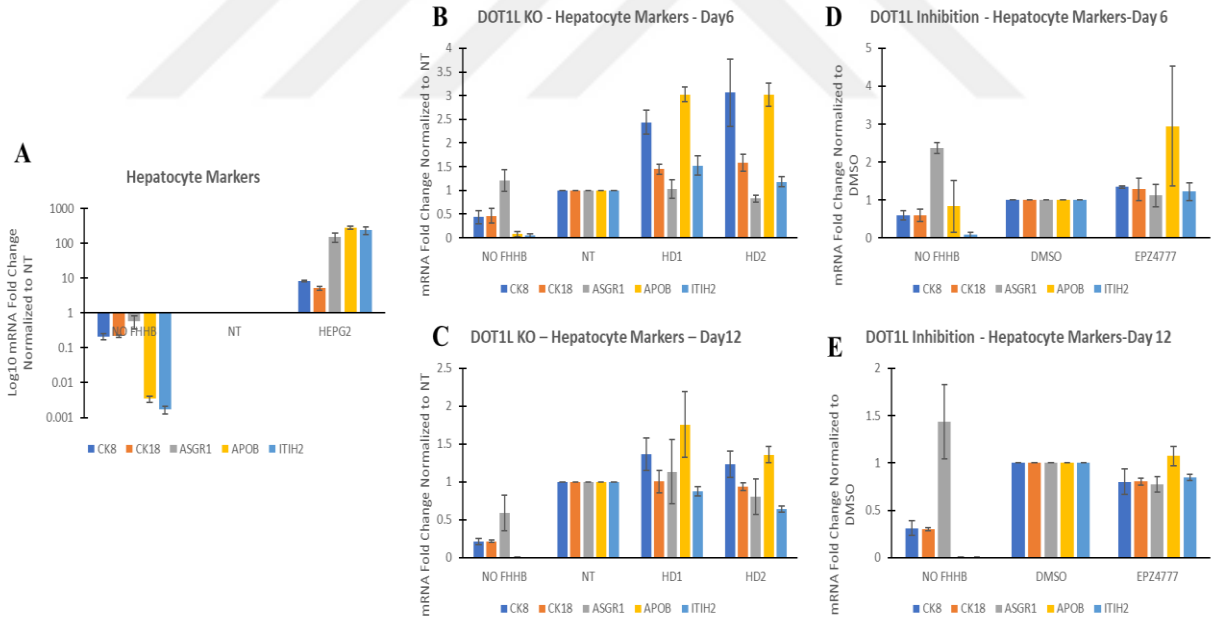

Figure 3.9 Hepatocyte marker genes' mRNA expression increases when DOT1L is knocked out

(A) qPCR analysis of Hepatocyte marker genes at dH1f cells without pLOVE FHHB infection, NT and HepG2. (B) Hepatocyte marker genes' mRNA expression increases at DOT1L KO cells on day 6 and (C) day 12 of transdifferentiation. (D) Hepatocyte marker genes mRNA expression slightly increases on day 6 and (E) at a similar level with NT on day 12. (n=3; error bars, ± s.err.)

To assess the effect of Dot1L inhibition, we compared EPZ004777 treated cells with DMSO treated cells at day 6 and day 12. On day 6, we observed a slight increase at EPZ004777 cells (1.34-fold, 1.28-fold, 1.11-fold, 2.94-fold and 1.22-fold, respectively), which was similar to Albumin and AFP (Figure 3.9D). At day 12 samples, hepatocyte markers genes' mRNA expression slightly decreased with EPZ004777 treatment (0.80-fold, 0.80-fold, 0.77-fold, 1.07-fold and 0.84-fold, respectively) when compared to DMSO-treated samples (Figure 3.9E). However, this again can be caused by prolonged treatment of cells with chemicals, which is a stress-inducing process.

3.9 Removal of H3K79me2 mark allows for better closing of fibroblast markers

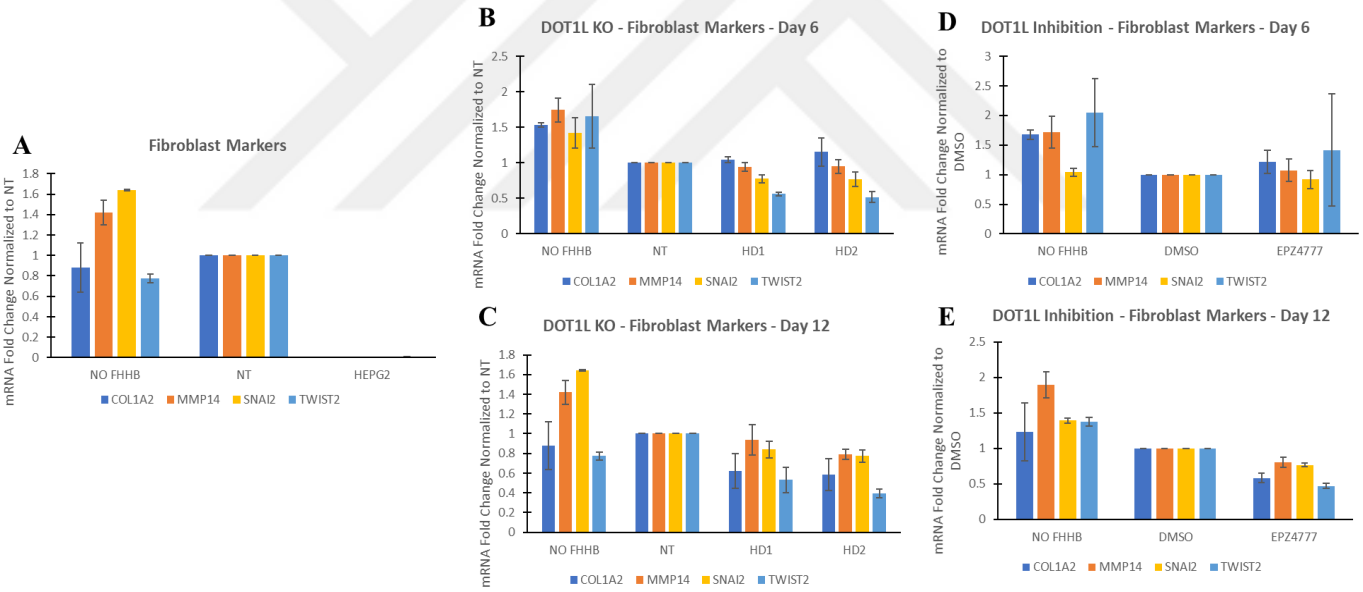

Figure 3.10 Knocking out and inhibition of Dot1L allows for easier shutdown of Fibroblast marker genes' mRNA expression

(A) qPCR analysis of Fibroblast marker genes shows uninfected dH1f cells have higher expression than NT and HepG2 cells. On day 6, mRNA expressions of Fibroblast marker genes do not drastically change with (B) DOT1L knockout or (D) Dot1L inhibition but decreases when (D) DOT1L is knocked out or (E). (n=3; error bars, ± s.err.)

As gene expression network shifts from fibroblast to hepatocytes during transdifferentiation, we expect downregulation of fibroblast marker expression downregulated as hepatocyte marker genes' expression upregulated. These expression changes would allow iHeps to have a more hepatocyte-like phenotype than fibroblasts. For this analysis, we investigated

COL1A2, MMP14, SNAI2 and TWIST2 genes expressions, which are highly known fibroblast marker genes. With qPCR analysis, were able to confirm these markers are highly expressed in wild-type dH1f cells and not in HepG2 cells. (Figure 3.10A).

On day 6, mRNA expressions of these genes in HD1 (1.05-fold, 0.94-fold, 0.78-fold and 0.56-fold, respectively) and HD2 (1.15-fold, 0.95-fold, 0.77-fold and 0.52-fold, respectively) cells were at a similar level to NT cells (normalized to 1) (Figure 3.10B). However, on day 12, the expression of these markers was downregulated in HD1 (0.62-fold, 0.94-fold, 0.84-fold and 0.53-fold, respectively) and HD2 cells (0.59-fold, 0.79-fold, 0.77-fold and 0.39-fold, respectively) compared to NT cells (normalized to 1) (Figure 3.10C). This might be an indicator that removal of H3K79me2 mark facilitated the shift from fibroblast marker genes' expression to hepatocyte marker genes' expression.

To assess if this effect was related with H3K79me2 mark's removal, we did the same analysis with DOT1L-inhibited samples. On day 6, these genes mRNA expression at EPZ004777 treated cells (1.22-fold, 1.07-fold, 0.92-fold and 1.41-fold, respectively) were close to DMSO treated cells (normalized to 1), just like DOT1L knockout cells (Figure 3.10D). However, similar to DOT1L knockout cells, we observed a lower mRNA expression of these genes with EPZ004777 treatment (0.58-fold, 0.80-fold, 0.77-fold and 0.47-fold, respectively) than DMSO treatment (normalized to 1) on day 12 (Figure 3.10E).

3.10 DOT1L Knockout does not induce transdifferentiation without FOXA3, HNF1A and HNF4A overexpression

To test if DOT1L knockout can on its own cause transdifferentiation, we applied the same procedure without the overexpression of FOXA3, HNF1A and HNF4A for 12 days. Morphology of the cells were similar to wild-type dH1f cells on day 12 (Figure 3.11A). As before, when the cells were infected with pLOVE FHHB viruses, there were high level of GFP expression at NT (40.15%), HD1 (58.46%) and HD2 (45.51%) cells. However, when the cells were not infected with pLOVE FHHB viruses, %GFP analysis showed background levels of GFP positive cells in HD1 (3.78%) and HD2 knockout (3.01%) similar to NT control (2.96%) on day 12 (Figure 3.11B-D).

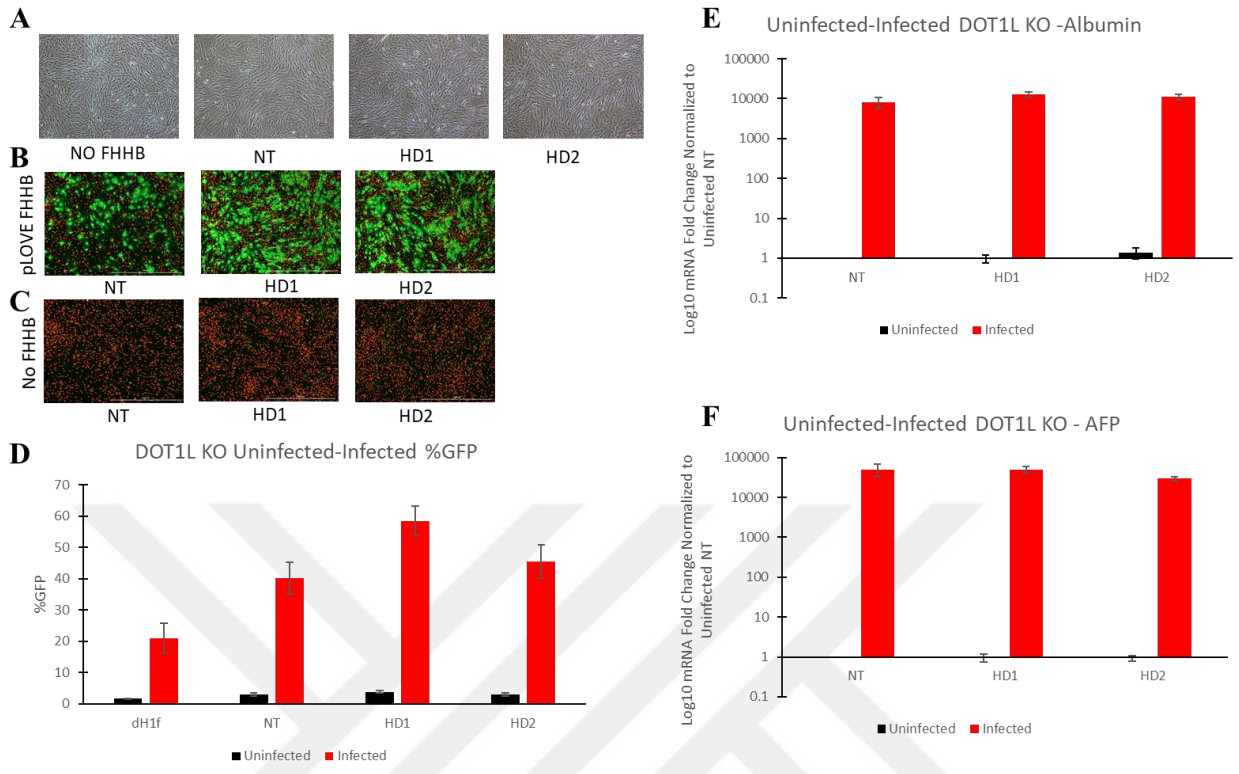

Figure 3.11 DOT1L knockout does not cause transdifferentiation if FOXA3, HNF1A and HNF4A is not overexpressed

(A) Morphology of NT, HD1 and HD2 is similar to wild-type dH1f cells. (B) pLOVE FHHB infection causes GFP expression via Albumin reporter. However, (C) DOT1L knockout does not activate Albumin reporter. (D) GFP expression is minimal without FOXA3, HNF1A and HNF4A overexpression. No expression of (E) Albumin or (F) AFP at uninfected NT, HD1 and HD2 PGP-H2B mCherry dH1f cells. (n=3; error bars, ± s.err.)

We compared Albumin mRNA expression of pLOVE FHHB infected and uninfected cells for further analysis. Compared to their uninfected versions, pLOVE FHHB infected NT, HD1 and HD2 cells had nearly 10000-fold increase at Albumin mRNA expression (Figure 3.11E). A similar expression pattern was observed with AFP mRNA, which infected NT, HD1 and HD2 cells had nearly 50000-fold increase when they are compared to their uninfected versions (Figure 3.11F). These data indicate that knocking out DOT1L alone is not sufficient for transdifferentiation of cells to iHeps.

3.11 EPZ004777 treatment does not induce fibroblast to hepatocyte transdifferentiation by itself

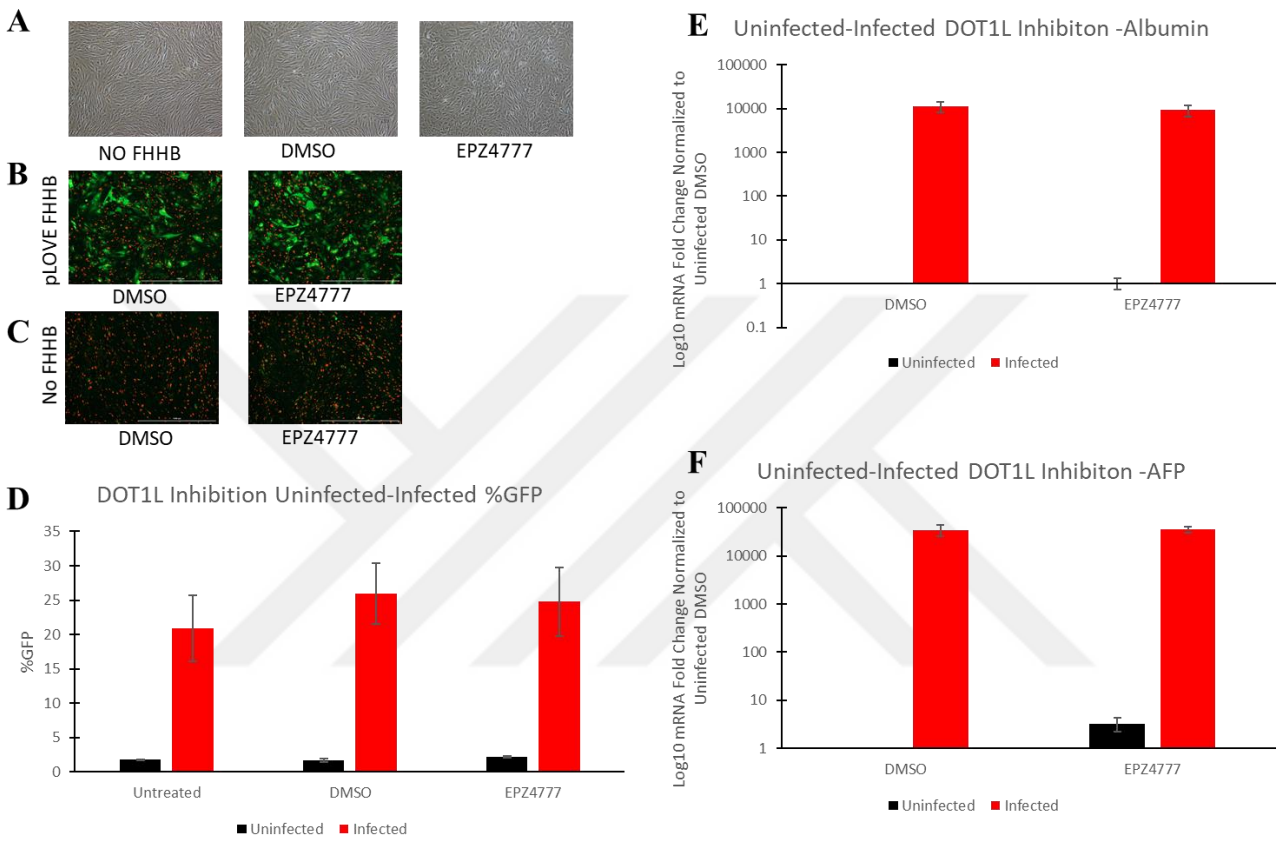

Figure 3.12 Dot1L inhibition does not solely transdifferentiate fibroblast cells into iHeps

(A) Morphology of dH1f cells does not change after DMSO and EPZ004777 treatment. (B-C) DMSO and EPZ004777 treated do not express GFP if not infected with pLOVE FHHB PGP-H2B mCherry dH1f (D) GFP expression is minimal without FOXA3, HNF1A and HNF4A overexpression. No expression of (E) Albumin or (F) AFP at uninfected PGP-H2B mCherry dH1f cells when treated with DMSO and EPZ004777. (n=3; error bars, ± s.err.)

It is known that some small molecule inhibitors can be used for chemical reprogramming of the cells. EPZ004777 was one of the seven components to obtain extra-embryonic endoderm-like (XEN) at Li et al. protocol(Li et al., 2017). Because of this reason, we wanted to check if EPZ004777 treatment without FOXA3, HNF1A and HNF4A overexpression can induce transdifferentiation to iHeps. Morphologies of the cells were same as wild-type dH1f (Figure 3.12A). We observed minimal GFP expression in uninfected DMSO-treated (2.20%) and EPZ004777-treated (1.67%) cells, which were at a close level of untreated cells (1.77%). However, same set of cells expressed high level of GFP when they were infected with pLOVE

FHHB (Figure 3.12B-D). Albumin mRNA expression of uninfected but chemically treated cells were 10000-fold less than the infected versions (Figure 3.12E). In AFP mRNA expression, there was a 35000-fold deference between uninfected and infected versions of chemically treated cells (Figure 3.12F). This shows that EPZ004777 treatment or DMSO treatment did not cause a transdifferentiation from fibroblast cells to iHeps.

3.12 DOT1L Knockout or Inhibition Does Not Increase Infectibility or FOXA3, HN1A and HNF4A (HFF) mRNA Expression

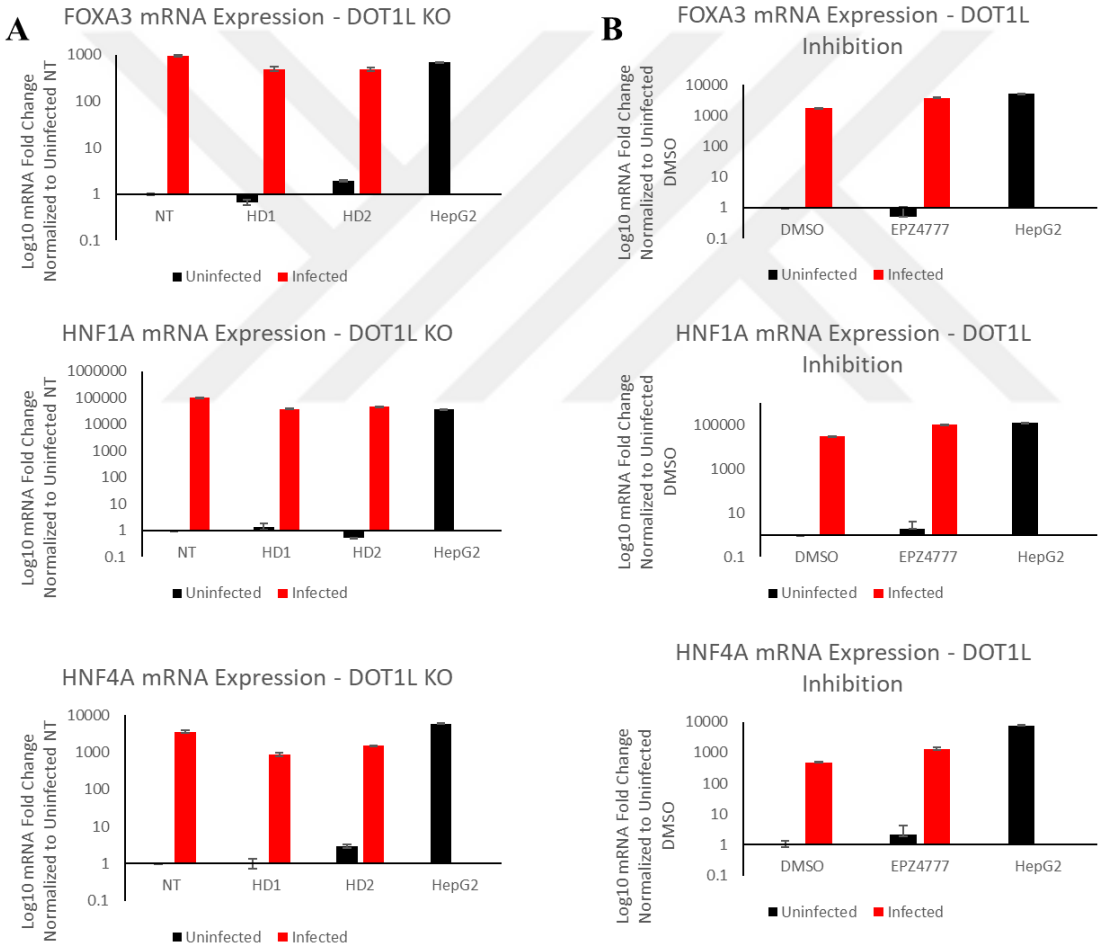

Figure 3.13 DOT1L Knockout and Inhibition Does Not Affect FOXA3, HNF1A and HNF4A Expressions

(A) qPCR analysis of FOXA3, HNF1A and HNF4A mRNA expressions at DOT1L Knockout cells with and without individual transcription factors' infection. (B) qPCR analysis of FOXA3, HNF1A and HNF4A mRNA expressions at Dot1L inhibition with or without individual transcription factors' infection. (n=2 technical replicates; error bars, ± s.d.)

We checked whether DOT1L knockout or inhibition affects lentiviral infection efficiency or transgene expression. qPCR analysis for exogenous transcription factor mRNA levels with and without individual FOXA3, HN1A and HNF4A lentiviruses indicated no significant differences between control and DOT1L-inhibited cells (Figure3.13A and B). Moreover, overexpression of these transcription factors was at a similar to HepG2. These results indicated that removal of H3K79me2 accelerates transdifferentiation independent of an effect on lentiviral infection or transgene expression level.

3.13 Loss of DOT1L Increases Expression of Epithelial Marker Genes

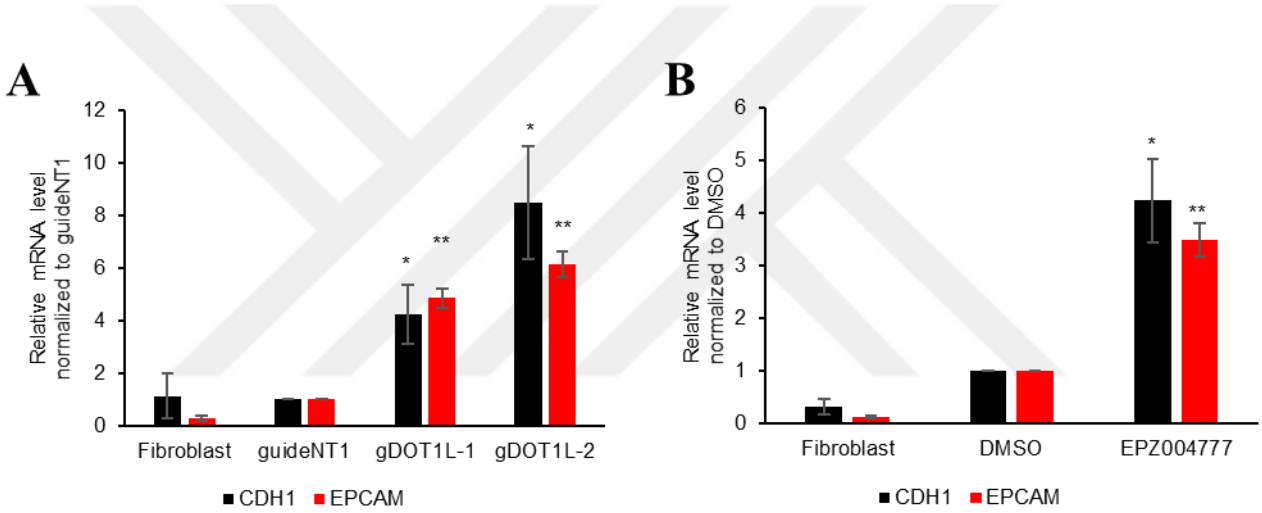

Figure 3.14 Relative mRNA Expressions of Epithelial Marker Genes
qPCR analysis of CHD1 and EPCAM mRNA expressions at (A) DOT1L knockout cells and (B) DOT1L inhibited cells. *p<0.05, **p<0.01 (n=3; error bars, ± s.err.)

As transdifferentiation of fibroblasts into hepatocytes requires mesenchymal to epithelial transition, we checked expressions of two epithelial marks: CDH1 and EPCAM. We observed both knockout of DOT1L (Figure3.14A) and inhibition of Dot1L (Figure3.14B) significantly increases mRNA expression of these epithelial marks. Therefore, loss of DOT1L can allow an easier shift from mesenchymal to epithelial gene expression network after the overexpression of required transcription factors.

3.14 Loss of DOT1L Allows for Higher Albumin Secretion

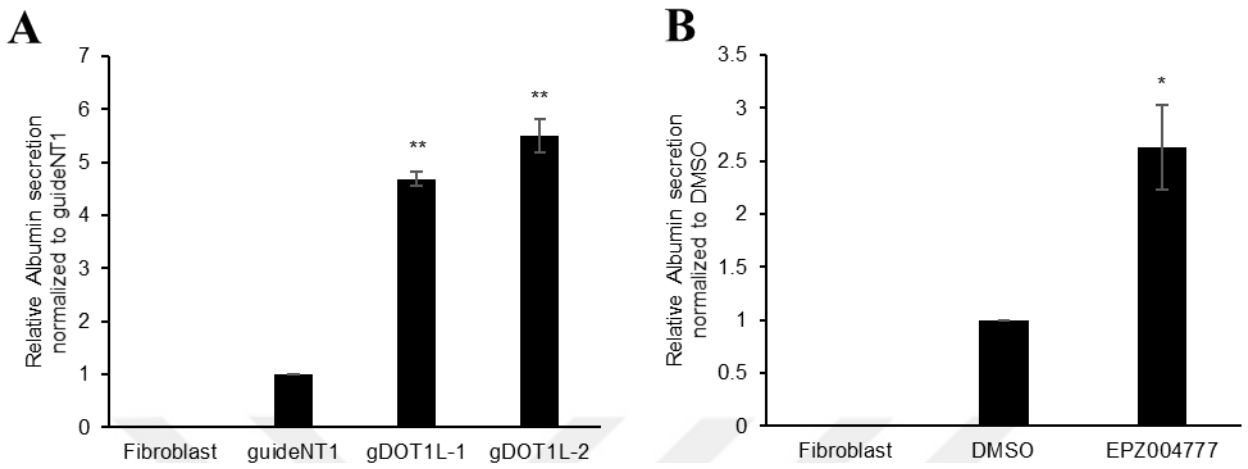

Figure 3. 15 Loss of DOT1L Increases Albumin Secretion
ELISA analysis for Albumin secretion of (A) DOT1L knockout and (B) Dot1L inhibition compared to related controls. *p<0.05, **p<0.01 (n=3; error bars, ± s.err.)

As we observed an increase in Albumin mRNA expression with the loss of DOT1L, we wanted to check Albumin secretion with ELISA as iHeps secrete Albumin just like mature hepatocytes. We did not detect any Albumin secretion from the wild-type dH1f cells. We observed a significant increase with DOT1L knockout cells compared to NT control (Figure3.15A). In addition, Dot1L inhibition by EPZ4777 treatment significantly increased Albumin secretion compared to DMSO treated cells (Figure3.15B).

3.15 Acceleration in Transdifferentiation Is Not Due to Proliferation Caused by the loss of DOT1L

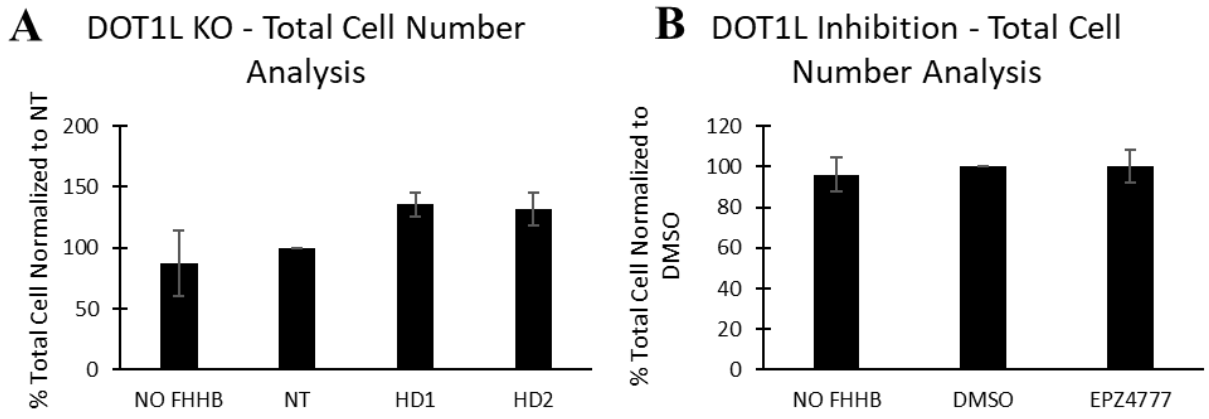

Figure 3.16 Total Cell Number Analysis on Day 6
Total cell number analysis by Cytation5 Image Reader on Day6 with (A) DOT1L knockout compared to NT and (B) DOT1L inhibited cells compared to DMSO treated cells. (n=6; error bars, ± s.err)

To check the effect we observe in transdifferentiation efficiency on day 6 is not due to changes in proliferation due to inhibition of Dot1L, we calculated the total cell numbers on day 6 analysis with Cytation5 Image Reader with H2B-mCherry signal from the cells. We normalized the total cell number of our control cells (NT for knockout and DMSO for inhibition) to 100%. As we saw an increase of 3-fold in Albumin mRNA expression and 5-fold in Albumin secretion, but total cell numbers were not significantly different, we can conclude that the affect we observe is not due to proliferation caused by DOT1L knockout or inhibition.

3.16 Functional Analysis of iHeps

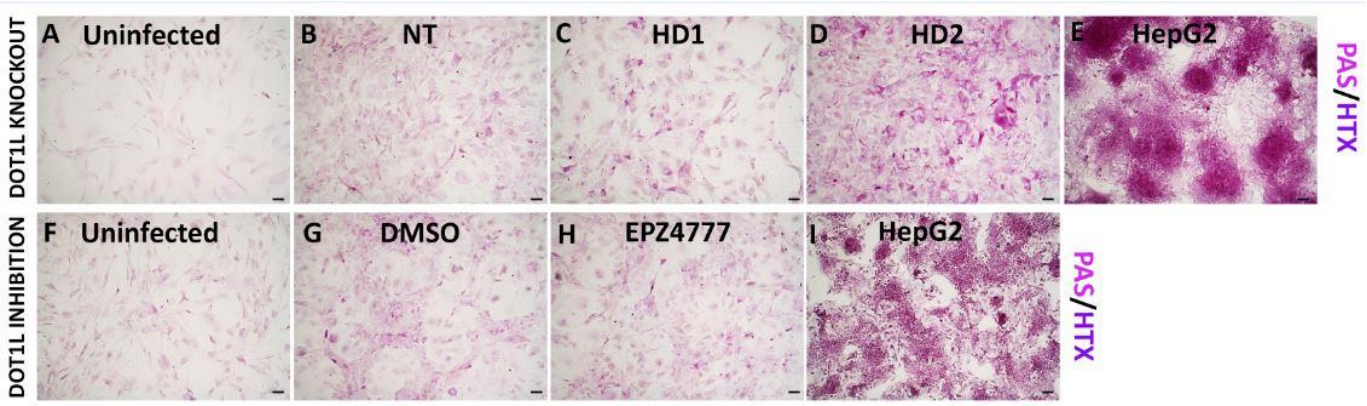

Figure 3.17 Glycogen storage of DOT1L knockout and inhibition hiHeps at day 6 of transdifferentiation

Glycogen storage was confirmed by PAS staining. (B) NT, (C) HD1, (D) HD2, (G) DMSO and (H) EPZ4777 conditions did not affect iHeps glycogen storage while Uninfected cells (A and F) were negative control and HepG2 (E and I) cells were positive control of the staining. (Scale Bars=50μM)

To confirm that the lineage converted iHeps have hepatic functions, we performed PAS (Figure 3.17) and Oil Red O staining (Figure 3.18). PAS staining is a method to detect glycogen storage in a cell, which is a hallmark function of mature hepatocytes. As periodic acid oxidizes glycosidic bonds, free aldehydes give a magenta color when exposed to Schiff's reagent. Since we observed high Albumin expression in addition to other hepatocyte markers at day 6, we tested if our cells also show hepatic functions at this early stage of transdifferentiation. As expected, NT, HD1 and HD2 cells were positive for PAS staining while uninfected cells were our negative control and HepG2 were positive control. In addition, DMSO and EPZ00477 treated cells were also PAS-positive, which shows DOT1L knockout or inhibition does not affect iHeps glycogen storage.

We next confirmed the lipid accumulation in iHeps which is another hallmark function of mature hepatocytes. Oil red O is a lysochrome that allows detection of triglycerides and lipids. With this staining, we confirmed our iHeps were able to store lipids at day 6 of transdifferentiation, while uninfected cells were our negative controls and HepG2 cells were positive controls. These stainings showed that we were able to obtain hepatocyte like cells on day 6 and DOT1L knockout or inhibition does not affect iHeps glycogen or lipid storage functions.

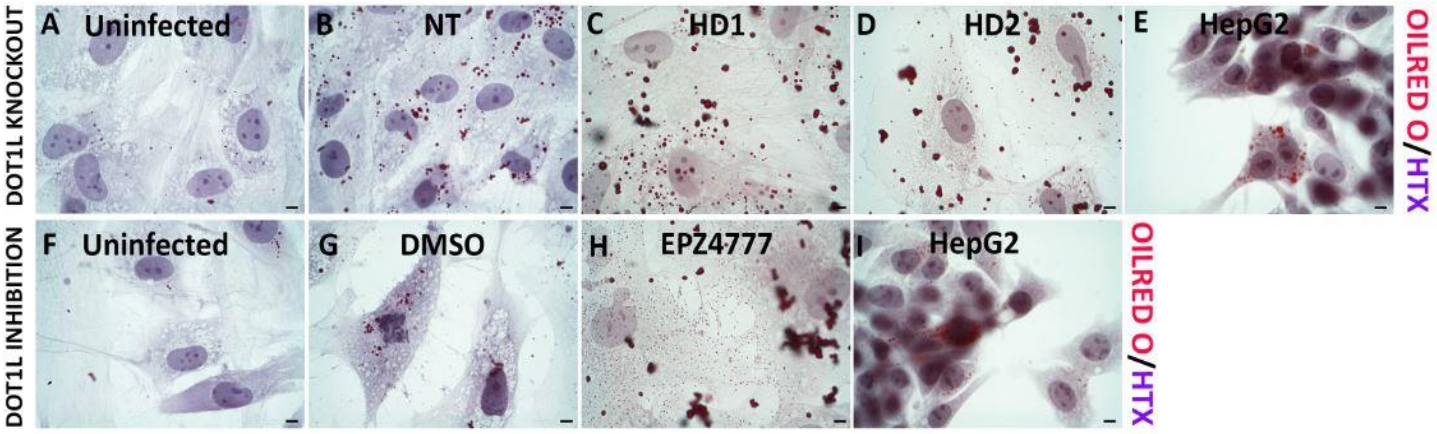

Figure3.18 Lipid accumulation of DOT1L knockout and inhibition hiHeps at day 6 of transdifferentiation
Triglycerides and lipid storage of was confirmed by Oil Red O staining. (B) NT, (C) HD1, (D) HD2, (G) DMSO and (H) EPZ4777 conditions did not affect lipid accumulation in iHeps. Uninfected cells (A and F) were negative control and HepG2 (E and I) cells were positive control of the staining. (Scale Bars=5μM)

3.17 Compound Screen Allows to Identify Small Molecule Hits That Can Increase Transdifferentiation Efficiency

To identify other chromatin modifiers which may have a functional role in transdifferentiation, we performed a compound screen with PGP-H2BmCherry dH1f cells. Compound library was a gift from Udo Oppermann (Oxford University) and consisted of molecules targeting a broad range of chromatin writers, erasers and readers (Table 2.7). To minimize the amount of compound used and allow for a high-throughput screen, we adopted the transdifferentiation assay to a 96-well format. Unlike Dot1L inhibition with EPZ004777, we did not pre-treat our cells with compounds before the screen as the compounds can have an effect on cell proliferation. As Albumin reporter (PGP) reaches its maximum %GFP at day 6, we set our analysis at day 6, day 9 and day 12 (Figure 3.19).

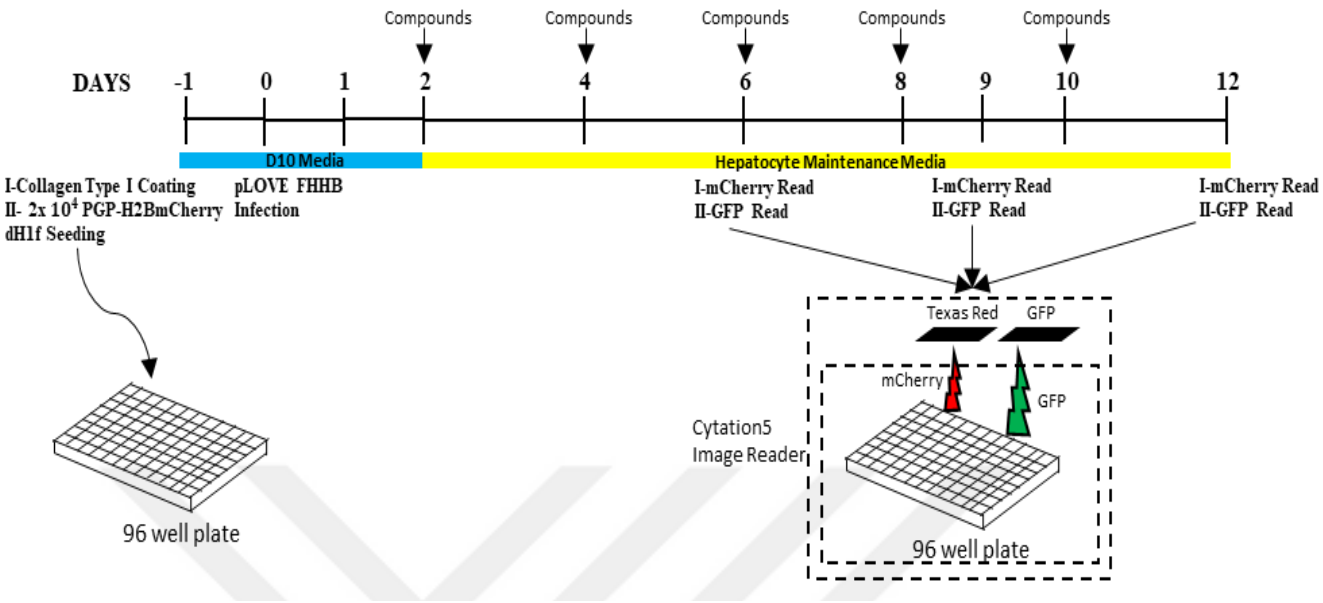

Figure3. 19 Compound screen with pLOVE FHHB infection
Experimental setup for compound screen.

Day 6 analysis showed 8.77% of DMSO treated cells were GFP positive. Our top hits were Rocilinostat (HDAC6 Inhibitor), SAHA (HDAC Inhibitor), GSK8815 (Bromodomains, ATAD2 Inhibitor), MS023 (Arginine Methyltransferase Inhibitor), Valproic Acid (HDAC Inhibitor), GSK8814 (Bromodomains, ATAD2 Inhibitor), LP99 (Bromodomains-BRD9, BRD7) and IOX2 (Prolyl-Hydroxylases - PHD2 (EGLN1) Inhibitor). All these compounds significantly increased percentage of GFP-positive cell (Figure 3.20A and D). Generally, HDAC inhibitors and Bromodomain inhibitors caused the highest % GFP compared to DMSO.

Although our time-course analysis showed there is no significant increase in %GFP with our Albumin reporter after day 6, to see the consistency of our data and identify compounds that might have a role in later stages of transdifferentiation, we did %GFP analysis at day 9. DMSO treated cells had 11.28% GFP and our top hits were 3-DZNEP (EZH2 inhibitor), Repsox (TGF-β receptor inhibitor), Rocilinostat, SAHA, Valproic acid, GSK8815, MS023 and IOX2, which all significantly increased %GFP (Figure 3.20B and E). While most of the top hits were also the top hits at day 6, we identified 3-DZNEP and Repsox, which was interesting since EZH2 inhibition, which is a methyltransferase for H3K27me3 mark, has been linked with reducing reprogramming efficiency at iPSC generation.

Finally, for our compound screen, we did a %GFP analysis at day 12 which was the end-point for our transdifferentiation protocol. On day 12, 11.86% of DMSO treated cells were

measured to be GFP-positive. Our top hits were 3-DZNEP, Repsox, CHR-6494, MS023, SAHA, Rocilinostat, Valproic acid and GSK8815 (Figure 3.20C and F). All compounds were consistent with day 9 analysis except CHR-6494 which is a Haspin inhibitor that function as a Serine/threonine-protein kinase.

Our compound screen suggests that while Rocilinostat, SAHA, GSK8815, MS023, Valproic Acid, GSK8814, LP99 and IOX2 can increase transdifferentiation efficiency at early stages; 3-DZNEP, Repsox and CHR-6494 can have a role in later stages. Mainly, HDAC and Bromodomain systems can be investigated to increase the efficiency of transdifferentiation. However, further analysis required to prove these chemicals truly increase transdifferentiation and not only actives Albumin reporter. For this purpose, mRNA expression of hepatocyte markers can be analyzed and functional test such as PAS staining, and Oil Red O staining can be performed to show iHeps that we obtain has hepatic functions.

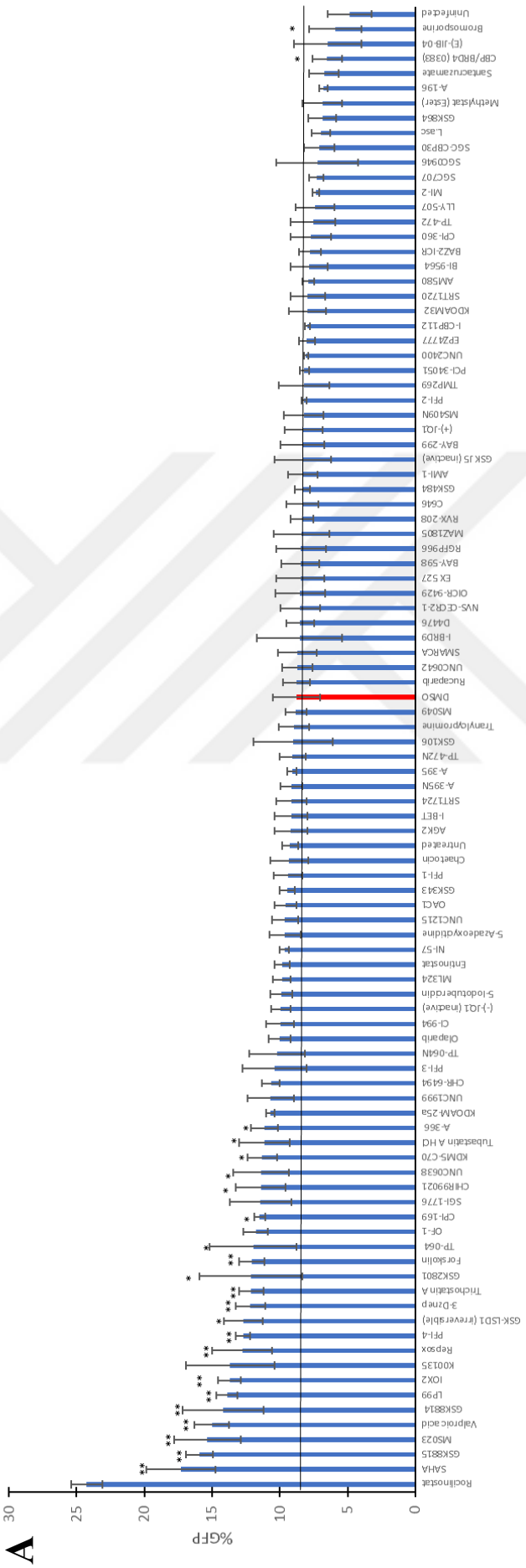
A
%GFP
0
5
10
15
20
25
30
Compound Screen - %GFP- Day 6
Rociinostat
SAHA
GSK8815
IMS0123
Valproic acid
GSK8814
LP99
IOX2
K00135
Repsox
PFI-4
GSK-LSD1 (irreversible)
3-D2nep
Trichostatin A
GSK2801
Forskolin
TP-064
OF-1
CPI-169
SGI-1776
CHIR99021
UNC0638
KDM5-C70
Tubastatin A HCl
A-366
KDOAM-25a
UNC1999
CHR-6494
PFI-3
TP-064N
Olaparib
CI-994
(-)-JQ1 (inactive)
5-Iodotubercidin
ML324
Entinostat
NI-57
5-Azadeoxycytidine
UNC1215
OACI
GSK343
PFI-1
Chaetocin
Untreated
AGK2
I-BET
SRT1724
A-395N
A-395
TP-472N
GSK106
TranylcypromineIMS049
DMSO
Rucaparib
UNC0642
SIMARCA
I-BRD9
D4476
NVS-CDK2-1
OICR-9429
EX 527
BAY-598
RGFP966
MAZ1805
RVX-208
C646
GSK484
AMI-1
GSK J5 (inactive)
BAY-299
(+)-JQ1
MS409N
PFI-2
TMP269
PCI-34051
UNC2400
EPZ4777
I-CBP112
KDOAM32
SRT1720
AM580
BI-9564
BAZ2-ICR
CPI-360
TP-472
LLY-507
MI-2
SGC707
SGC0946
SGC-CBP30
L-asc
GSK864
Mettylstat (Ester)
A-196
Sanbacruzamate
CBP/BRD4 (0383)
(E)-JIB-04
Bromosporine
Uninfected

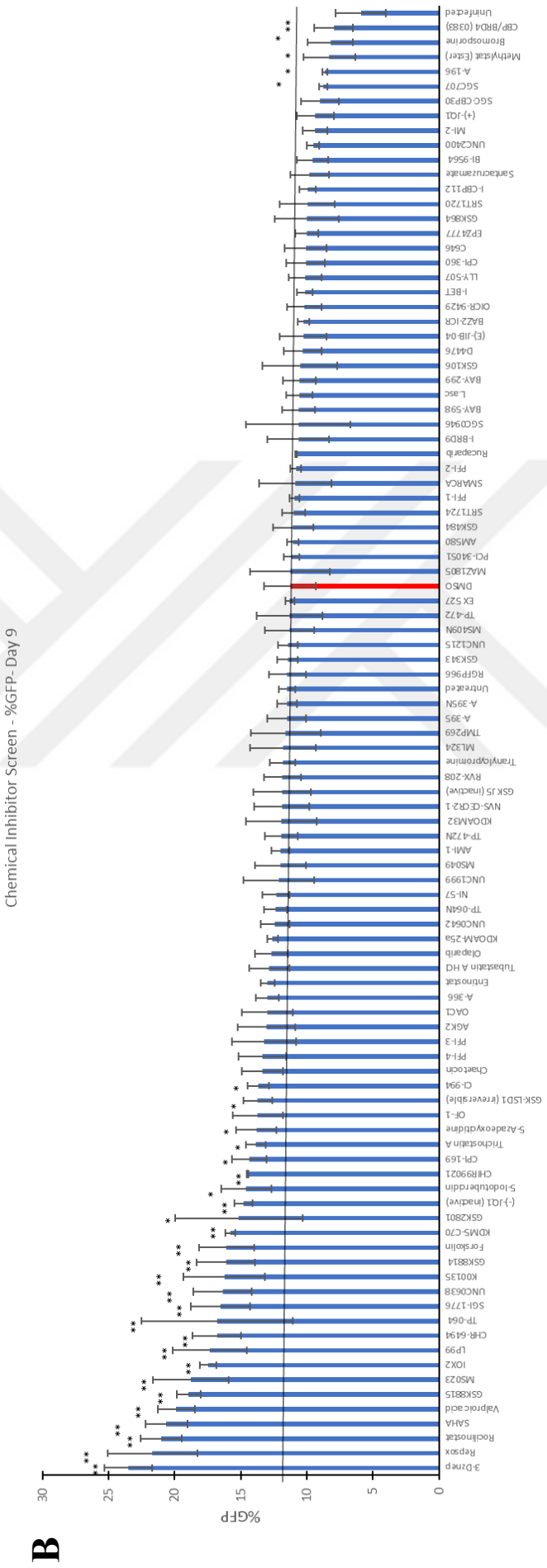
B
Chemical Inhibitor Screen - %GFP- Day 9
%GFP
0
5
10
15
20
25
30
3-Deaza-neplanocin A
Repsox
Rociletinostat
SAHA
Valproic acid
GSK8815
MS023
IOX2
LP99
CHR-6494
TP-064
SGI-1776
UNC0638
K00135
GSK8814
Forskolin
KDM5-C70
GSK2801
(+)-JQ1 (inactive)
5-Iodotubercidin
CHIR99021
CPI-169
Trichostatin A
5-Azadeoxycytidine
OF-1
GSK-LSD1 (irreversible)
CI-994
Chaetocin
PFI-4
PFI-3
AGK2
OAC1
A-366
Entinostat
Tubastatin A HCl
Olaparib
KDOAM-25a
UNC0642
TP-064N
NI-57
UNC1999
MS049
AMI-1
TP-472N
KDOAM32
NVS-CECR2-1
GSK J5 (inactive)
RVX-208
Tranylcypromine
ML324
TMP269
A-395
A-395N
Untreated
RGFP966
GSK343
UNC1215
MS409N
TP-472
EX 527
DMSO
MAZ1805
PC-340S1
AM580
GSK484
SRT1720
PFI-1
SMARCA
PFI-2
Rucaparib
I-BRD9
SGC0946
BAY-598
L-asc
BAY-299
GSK106
D4476
(E)-JIB-04
BAZ2-ICR
OICR-9429
I-BET
LLY-507
CPI-360
C646
EPZ4777
GSK864
SRT1720
I-CBP112
Santacruzamate
BI-9564
UNC2400
MI-2
(+)-JQ1
SGC-CBP30
SGC707
A-196
Methylstat (Ester)
Bromosporine
CBP/BRD4 (0383)
Uninfected

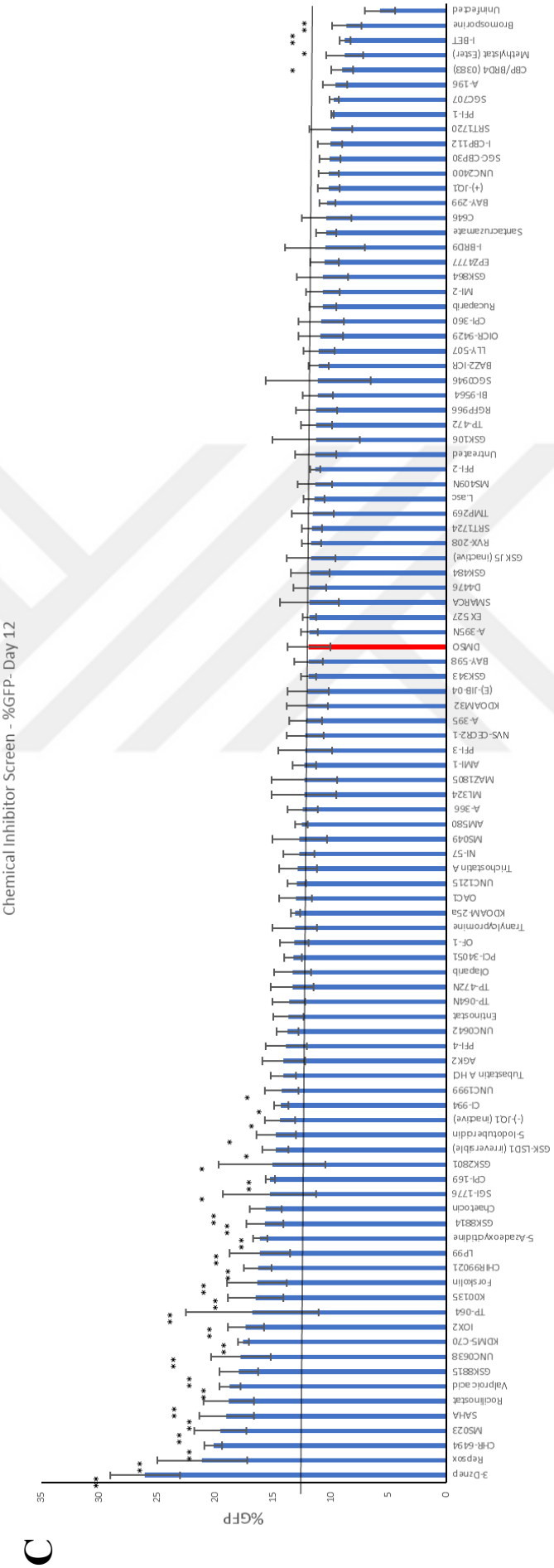
Chemical Inhibitor Screen - %GFP - Day 12
%GFP
0
5
10
15
20
25
30
35
3-Dznep
Repsox
CHR-6494
MS023
SAHA
Rocilinostat
Valproic acid
GSK8815
UNC0638
KDM5-C70
IOX2
TP-064
KO0135
Forskolin
CHIR99021
LP99
5-Azadeoxycytidine
GSK8814
Chaetocin
SGI-1776
CPI-169
GSK2801
GSK-LSD1 (irreversible)
5-Iodotuberadin
(-)-JQ1 (inactive)
CI-994
UNC1999
Tubastatin A HCl
AGK2
PFI-4
UNC0642
Entinostat
TP-064N
TP-472N
Olaparib
PCI-34051
OF-1
Tranylcypromine
KDOAM-25a
OACI
UNC1215
Trichostatin A
NI-57
MS049
AM580
A-366
ML324
MAZ1805
AMI-1
PFI-3
NVS-CECR2-1
A-395
KDOAM32
(E)-JIB-04
GSK343
BAY-598
DMSO
A-395N
EX 527
SMARCA
D4476
GSK484
GSK J5 (inactive)
RVX-208
SRT1724
TMP269
L-asc
MS409N
PFI-2
Untreated
GSK106
TP-472
RGFP966
BI-9564
SGC0946
BAZ2-ICR
LLY-507
OICR-9429
CPI-360
Rucaparib
MI-2
GSK854
EPZ4777
I-BRD9
Santacruzamate
C646
BAY-299
(+)-JQ1
UNC2400
SGC-CBP30
I-CBP112
SRT1720
PFI-1
SGC707
A-196
CBP/BRD4 (0383)
Methylstat (Ester)
I-BET
Bromosporine
Uninfected

C

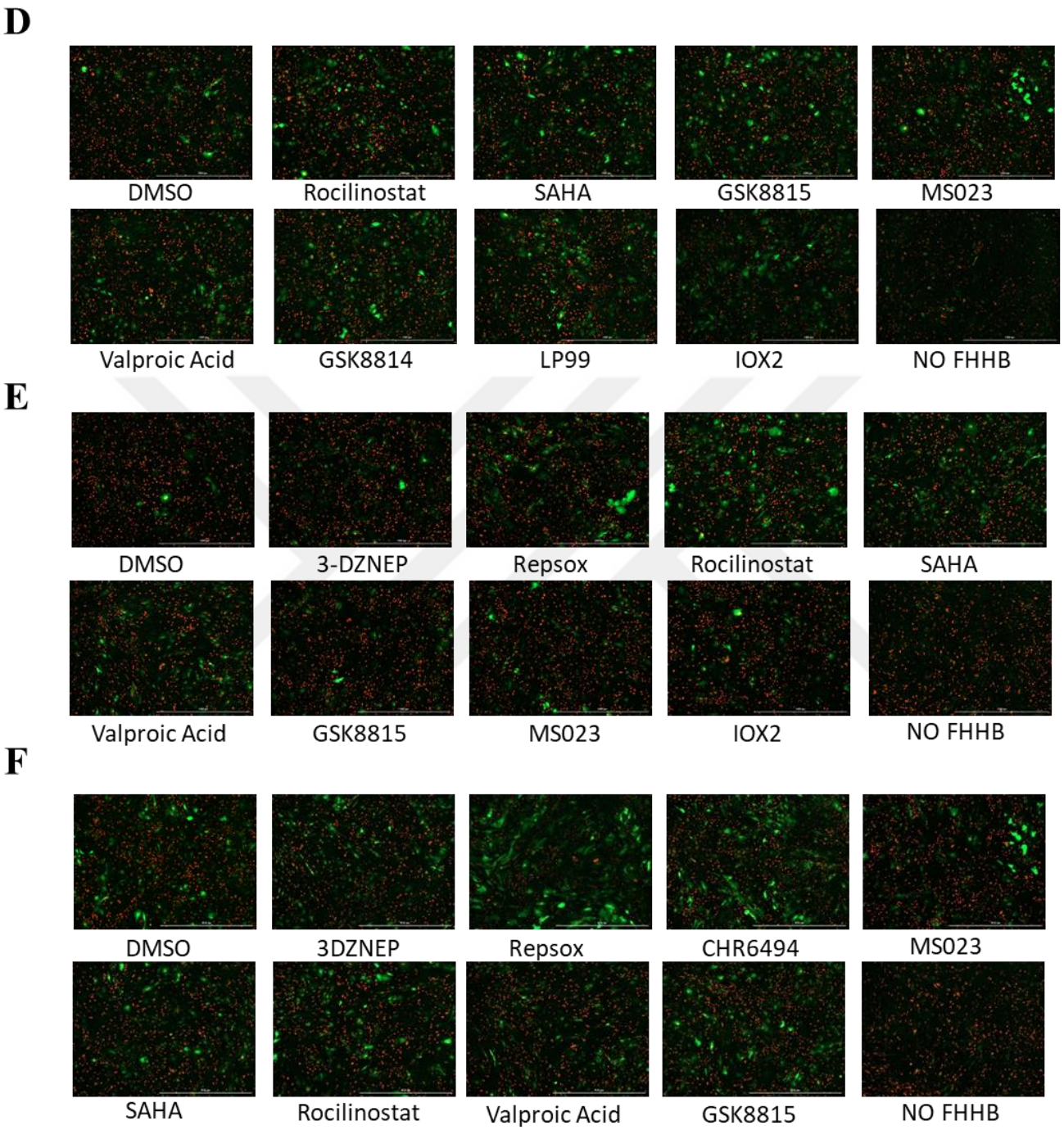

Figure3.20 Compound screen with pLOVE FHHB infection

Compound screen % GFP analysis at (A) day 6, (B) day 9 and (C) day 12. (Each compound has 3 technical replicas, except DMSO control. error bars, ± s.d.) DMSO, Top 8 hits and Uninfected cells mCherry and GFP merged images at (D) day 6, (E) day 9 and (F) day 12.

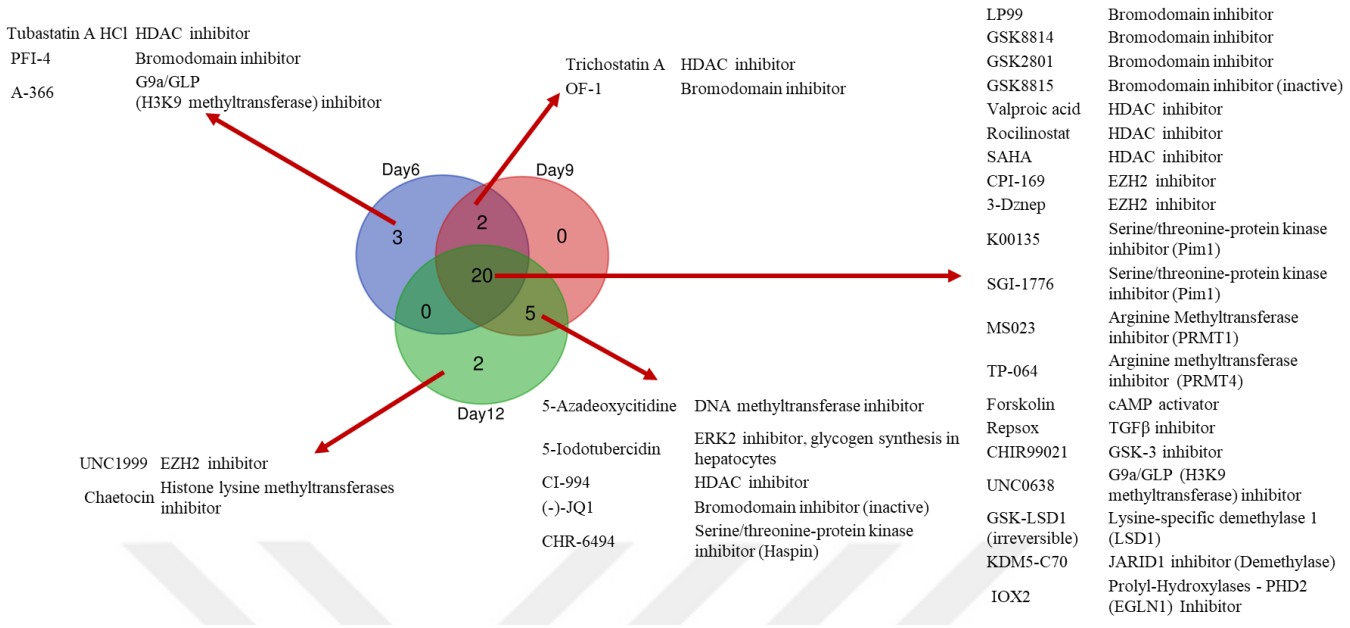

Figure3.21 Analysis of Compounds that Significantly Increased %GFP
Compounds that significantly increased %GFP on day 6, day 9 and day 12 and their targets

% GFP analysis showed that 20 compounds significantly increased the number of Albumin expressing on day 6, day 9 and day 12. Mainly, we observed bromodomain inhibitors (LP99, GSK8814, GSK2801), HDAC inhibitors (Valproic acid, Rocilinostat, SAHA), EZH2 inhibitors (CPI-169, 3-DZNep), Serine/Threonine-protein kinase inhibitors (K00135, SGI-1776), Arginine Methyltransferase (MS023, TP-064) and G9a/GLP methyltransferase inhibitors (UNC0638) can increase the transdifferentiation efficiency. In addition, certain signaling pathway inhibitors (Repsox, CHIR99021) or activators (Forskolin) significantly increased %GFP-positive cells. Tubastatin A HCl (HDAC inhibitor), PFI-4 (Bromomodomain inhibitor) and A-366 (G9a inhibitor) had only effect on day 6. Likewise, 2 shared inhibitors of day 6 and day 9 were HDAC (Trichostatin A) and Bromodomain (OF-1) inhibitors. 5-Azadeoxcitidine, 5-Iodotubercidin, CI-994 and CHR-6494 significantly increased %GFP both on day 9 and day 12 which might indicate that the targets may have a role in later stages of transdifferentiation or they required more than 6 days to show their effect and for example remove the marks from histones or DNA. Again, we observed an EZH2 inhibitor (UNC1999) and a non-specific Histone Lysine Methyltransferase inhibitor (Chaetocin) significantly increased %GFP only on day 12. Our confidence to our compound screen was increased as we repeatedly observed the inhibitors targets the same classes. However, as 2 inactive controls of the inhibitors ((-)-JQ1 and GSK8815) came up as hits, this shows that our inhibitors might also have an off-target effect and activate only Albumin reporter but do not increase the transdifferentiation efficiency.

A

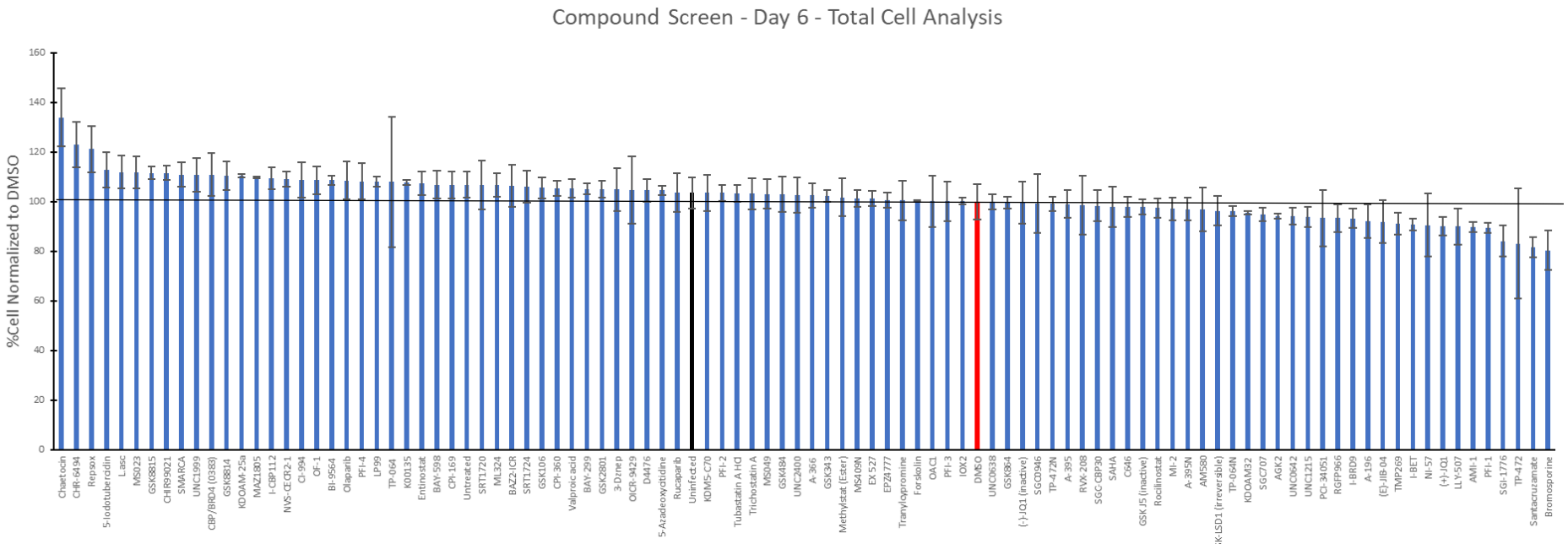
Compound Screen - Day 6 - Total Cell Analysis
%Cell Normalized to DMSO
0
20
40
60
80
100
120
140
160
Chaetocin
CHR-6494
Repsox
5-Iodotubercidin
Lasc
MS023
GSK8815
CHIR99021
SMARCA
UNC1999
CBP/BRD4 (0388)
GSK8814
KDOAM-25a
MAZ1805
I-CBP112
NVS-CECR2-1
CI-994
OF-1
BI-9564
Olaparib
PFI-4
LP99
TP-064
K00135
Entinostat
BAY-598
CPI-169
Untreated
SRT1720
ML324
BAZ2-ICR
SRT1724
GSK106
CPI-360
Valproic acid
BAY-299
GSK2801
3-Deaza
OICR-9429
D4476
5-Azadeoxycytidine
Rucaparib
Uninfected
KDM5-C70
PFI-2
Tubastatin A HCl
Trichostatin A
MS049
GSK484
UNC2400
A-366
GSK343
Methylstat (Ester)
MS409N
EX 527
EPZ4777
Tranylcypromine
Forskolin
OAC1
PFI-3
IOX2
DMSO
UNC0638
GSK864
(-)-JQ1 (inactive)
SGC0946
TP-472N
A-395
RVX-208
SGC-CBP30
SAHA
C646
GSK J5 (inactive)
Rocilinostat
MI-2
A-395N
AM580
GSK-LSD1 (irreversible)
TP-064N
KDOAM32
SGC707
AGK2
UNC0642
UNC1215
PCI-34051
RGFP966
I-BRD9
A-196
(E)-JIB-04
TMP269
I-BET
NI-57
(+)-JQ1
LLY-507
AMI-1
PFI-1
SGI-1776
TP-472
Santacruzamate
Bromosporine

B

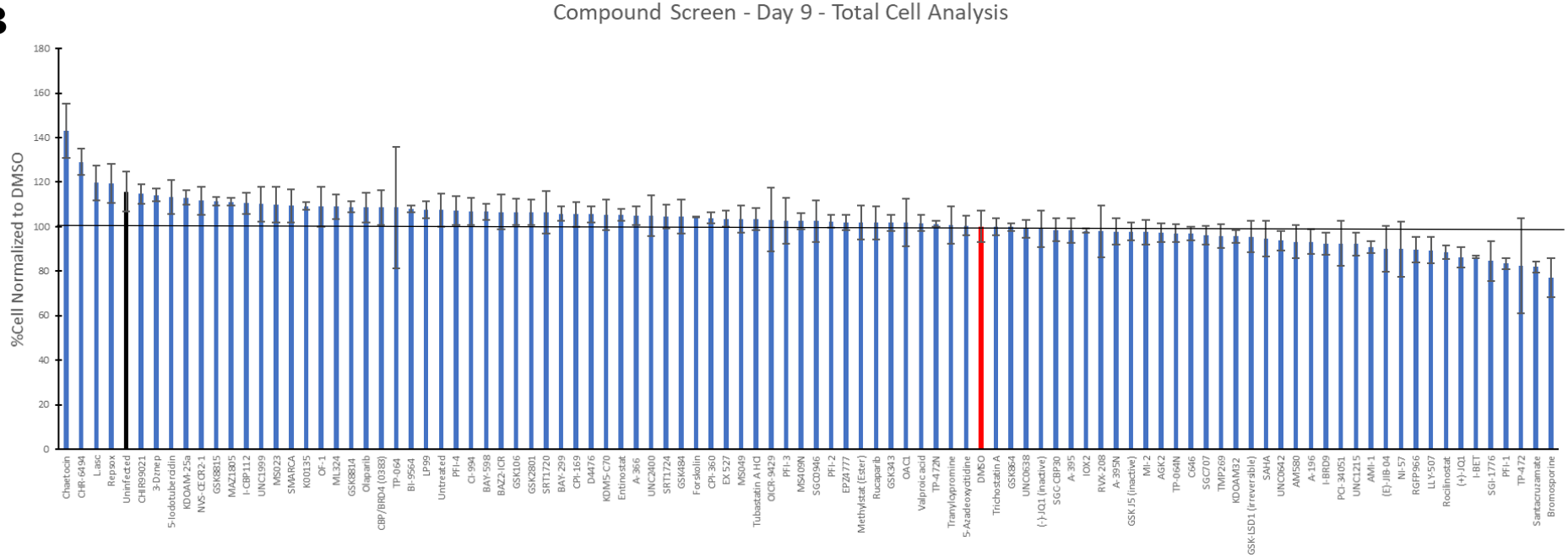
Compound Screen - Day 9 - Total Cell Analysis
%Cell Normalized to DMSO
0
20
40
60
80
100
120
140
160
180
Chaetocin
CHR-6494
Lasc
Repsox
Uninfected
CHIR99021
3-DzNep
5-Iodotubercidin
KDOAM-25a
NVS-CER2-1
GSK8815
MAZ1805
I-CBP112
UNC1999
MS023
SMARCA
K00135
OF-1
ML324
GSK8814
Olaparib
CBP/BRD4 (0388)
TP-064
BI-9564
LP99
Untreated
PFI-4
CI-994
BAY-598
BAZ2-ICR
GSK106
GSK2801
SRT1720
BAY-299
CPI-169
D4476
KDM5-C70
Entinostat
A-366
UNC2400
SRT1724
GSK484
Forskolin
CPI-360
EX 527
MS049
Tubastatin A HCl
OICR-9429
PFI-3
MS409N
SGC0946
PFI-2
EPZ4777
Methylstat (Ester)
Rucaparib
GSK343
OACL
Valproic acid
TP-472N
Tranylcypromine
5-Azadeoxycytidine
DMSO
Trichostatin A
GSK864
UNC0638
(-)-JQ1 (inactive)
SGC-CBP30
A-395
IOX2
RVX-208
A-395N
GSK J5 (inactive)
MI-2
AGK2
TP-064N
C646
SGC707
TMP269
KDOAM32
GSK-LSD1 (irreversible)
SAHA
UNC0642
AMS80
A-196
I-BRD9
PCI-34051
UNC1215
AMI-1
(E)-JIB-04
NI-57
RGFP966
LLY-507
Rocilinostat
(+)-JQ1
I-BET
SGI-1776
PFI-1
TP-472
Santacruzamate
Bromosporine

C

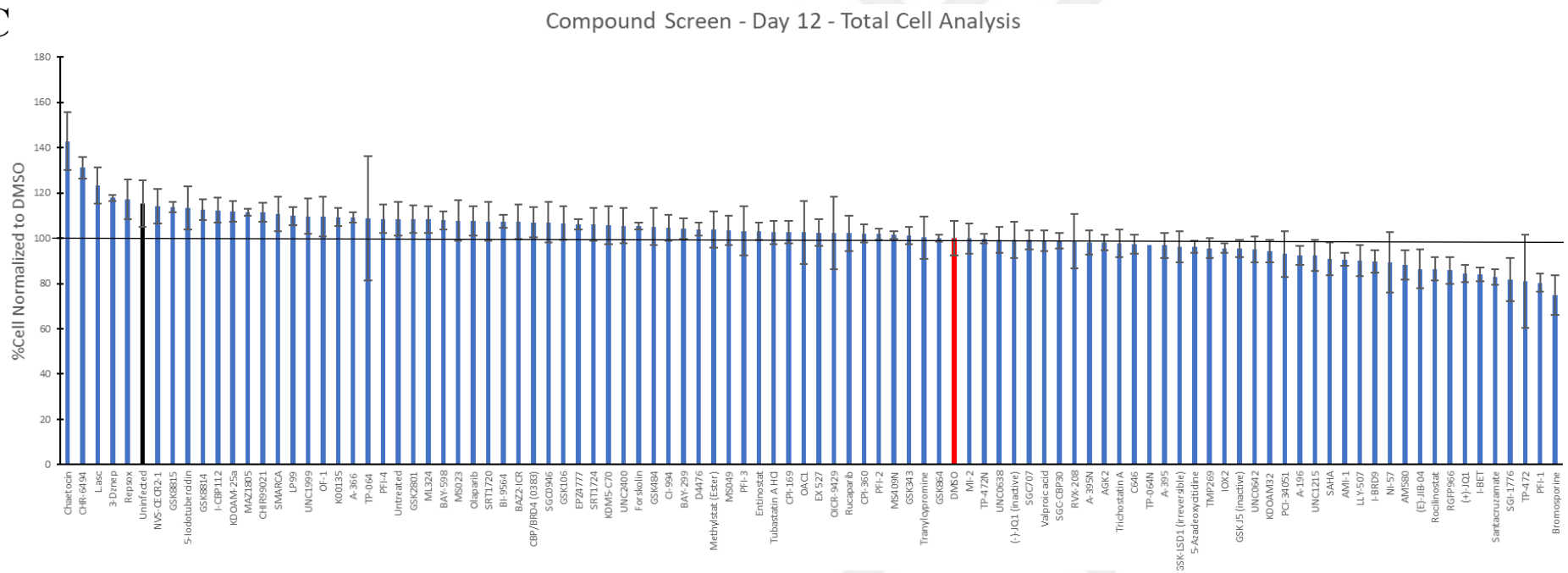
Compound Screen - Day 12 - Total Cell Analysis
%Cell Normalized to DMSO
180
160
140
120
100
80
60
40
20
0
Chaetocin
CHR-6494
Lasc
3-Dinep
Repsox
Uninfected
NVS-CECR2-1
GSK8815
5-Iodotubercidin
GSK8814
I-CBP112
KDOAM-25a
MAZ1805
CHR9021
SMARCA
LP99
UNC1999
OF-1
K00135
A-366
TP-064
PFI-4
Untreated
GSK2801
ML324
BAY-598
MS023
Olaparib
SRT1720
BI-9564
BAZ2-ICR
CBP/BRD4 (0383)
SGC0946
GSK106
EPZ4777
SRT1724
KDM5-C70
UNC2400
Forskolin
GSK484
CI-994
BAY-299
D4476
Methylstat (Ester)
MS049
PFI-3
Entinostat
Tubastatin A HCl
CPI-169
OAC1
EX 527
OICR-9429
Rucaparib
CPI-360
PFI-2
MS409N
GSK343
Tranylcypromine
GSK864
DMSO
MI-2
TP-472N
UNC0638
(-)-JQ1 (inactive)
SGC707
Valproic acid
SGC-CBP30
RVX-208
A-395N
AGK2
Trichostatin A
C646
TP-064N
A-395
GSK-LSD1 (irreversible)
5-Azadeoxycytidine
TMP269
IOX2
GSK J5 (inactive)
UNC0642
KDOAM32
PCI-34051
A-196
UNC1215
SAHA
AMI-1
LLY-507
I-BRD9
NI-57
AM580
(E)-JIB-04
Roclinostat
RGFP966
(+)-JQ1
I-BET
Santacruzamate
SGI-1776
TP-472
PFI-1
Bromosporine

Figure3. 22 Total Cell Number Analysis on Day 6, Day 9 and Day 12 for Compound Screen

Total cell number analysis by Cytation5 Image Reader on (A) Day6, (B) Day 9 and (C) Day 12. Cell numbers were normalized to to DMSO treated cells (100%). (n=2 technical replicate; error bars, ± s.d)

To check the effect we observe in %GFP analysis with compound screen is not due to changes in proliferation, we calculated the total cell numbers on day 6, day 9 and day 12 analyses with Cytation5 Image Reader with H2B-mCherry signal from the cells. We normalized the total cell number of our control cells (DMSO treated) to 100%. As the top hits change in %GFP-positive cells higher than changes in total cell numbers, we can conclude that the effects we observe is not due to proliferation (Figure3.22).

Chapter 4

DISCUSSION

In this study, we investigated the role of histone methyltransferase DOT1L in transdifferentiation of human fibroblasts into induced hepatocytes (iHeps) by the overexpression of FOXA3, HNF1A and HNF4A. We observed that when DOT1L is knocked out or inhibited, the expression of Albumin, AFP and other hepatocyte markers increase on day 6. Conversely, we observed that Dot1L inhibition results in the downregulation of fibroblast marker genes on day 12 compared to control cells. We also showed DOT1L knockout or inhibition on its own is not sufficient to cause transdifferentiation of fibroblasts into iHeps. By PAS and Oil Red O stainings, we confirmed the cells we obtained had some hepatic functions. In addition, we performed a compound screen with albumin reporter and identified other chromatin modifiers that can have a role at transdifferentiation.

4.1 Assessment of Chromatin Modifying Enzymes Role in Direct Lineage Conversion

To this date, many studies revealed the interplay between reprogramming factors and molecules that influence chromatin state during cellular reprogramming (Orkin and Hochedlinger, 2011). These studies showed that reprogramming factors directly interact with histone modifying enzymes such as histone methyltransferases, histone acetyltransferases, histone demethylases and histone deacetylases (Apostolou and Hochedlinger, 2013). When the reprogramming transcription factors are overexpressed in the cell, these enzymes act as the co-activators and co-repressors and they are either required for the maintenance of somatic state or they assist transcriptional factors in reprogramming (Apostolou and Hochedlinger, 2013). As chromatin marks can be potential barriers to reprogramming, researchers investigated the combination of required transcriptional factors with inhibition or overexpression of chromatin modifying enzymes to achieve higher efficiencies. These studies yielded information on how chromatin remodelers affect iPSC generation. However, the functions of these molecules in transdifferentiation are largely unknown.

Previous studies showed DOT1L and PCR2 is responsible for the downregulation somatic genes in reprogramming (Fragola et al., 2013; Onder et al., 2012). Moreover, it was found that loss of DOT1L increases iPSC generation efficiency, but loss of PCR2 decreases it (Fragola et al., 2013; Onder et al., 2012). For this reason, we questioned if H3K79me2 mark can also be a

barrier for direct lineage conversion and loss or inhibition of Dot1L can enhance the transdifferentiation efficiency. Moreover, as there are clear links between reprogramming factors and signaling pathway components (LIF, TGFβ, Gsk3, MEK, BMP, Wnt), architectural proteins (Mediator, cohesion, Ctcf, Lamin A), RNAs and RBPs (Lin28, Ago2, let-7, miR-34), DNA methylation (Tet1, Tet2, AID, Parp1, Dnmt1, Dnmt3a) and Chromatin remodelers (Brg1, Baf155, Brm, Chd1, Hdac1) that has influence on chromatin states (Apostolou and Hochedlinger, 2013), we performed a compound screen to broadly target these molecules.

The reason why we chose to use this method to investigate the role of chromatin modifiers in transdifferentiation was, it only requires the overexpression of three transcription factors to obtain functional iHeps with a relatively high efficiency (Huang et al., 2014). However, in that study, cells were transduced with lentiviruses expressing SV40 large T expression. As iHeps reported to be not proliferating, if we combined DOT1L knockout or inhibition with SV40 large T expression, we would obtain more iHeps. However, the efficiency of transdifferentiation would not change since we compare our cells with NT or DMSO treated cells.

There are other protocols for direct lineage conversion of fibroblasts to additional cell type such as induced neurons (Vierbuchen et al., 2010),(Qiang et al., 2011),(Marro et al., 2011), induced motor neurons(Son et al., 2011), induced dopaminergic neurons (Ulrich et al., 2011), multilineage blood progenitors (Schnerch et al., 2010) and cardiomyocytes (Efe et al., 2011; Ieda et al., 2010). These protocols can be used to assess the role of chromatin modifier enzymes in other direct lineage conversions and to show the effects we observed are not specific for hepatocyte conversions.

4.2 Role of DOT1L in Direct Lineage Conversion

In this study, DOT1L knockout or inhibition resulted in higher transdifferentiation efficiency on day 6, but efficiency did not significantly increase on day 12. The reason for this can be the efficiency of our procedure was already too high to observe the effect of DOT1L at later timepoints. Huang et al. reported that 36.2% of their hiHeps were Albumin positive (Huang et al., 2014). This efficiency is significantly higher when compared to Sekiya et al.'s first protocol in which only 0.3% of starting MEF cells were converted to iHeps (Sekiya and Suzuki, 2011). At high MOI conditions, we were able to quantify nearly 60% of DOT1L knockout cells as Albumin positive. A suboptimal transdifferentiation protocol may be more sensitive to observe a more pronounced effect upon DOT1L knockout or inhibition. Such a method would

also allow us to answer if DOT1L and H3K79me2 mark have roles in late stages of transdifferentiation.

Generally, transdifferentiation efficiency was higher in DOT1L knockout cells compared to NT than Dot1L inhibition with EPZ004777 compared to DMSO treated cells. The reason for this can be the prolonged chemical treatment of the cells. The complete removal of H3K79me2 mark requires 5 days of pretreatment with 3 µM EPZ004777 followed by 12 days of transdifferentiation which resulted in a total of 17 days treatment. Such prolonged treatment may have resulted in cellular toxicity. Although this inhibitor has been shown to be quite specific, it may have off-target effects (Daigle et al., 2011). Another reason for this can be that the binding partners of DOT1L might also have a role in transdifferentiation. It is known that DOT1L is a part of complex required for H3K79me1/2 which is an active mark associated with RNA Pol II-mediated transcriptional elongation. CRISPR-Cas9 mediated knockout can cause a frameshift and binding sites for Dot1L-interacting proteins might be affected. However, when DOT1L is inhibited, the complex can still form.

DOT1L is the only methyltransferase responsible for the activating H3K79me2 mark (Chang et al., 2010). A possible mechanism of DOT1L's knockout or inhibition during transdifferentiation could be that it allows for more extensive silencing of fibroblast specific genes when the H3K79me2 is removed. When we tested fibroblast specific gene expression by qPCR, there was no significant difference on day 6 but most were downregulated by day 12. It is possible that silencing of fibroblast specific genes requires more time than 6 days. Transdifferentiation is caused by the shift in gene expression network of the cells when transcription factors are overexpressed, therefore it is easier to detect the increment in hepatocyte specific markers at the early stages. When we did a qPCR analysis to hepatocyte marker genes expression, both in DOT1L knockout and inhibition, they were expressed higher than NT or DMSO treated cells. Therefore, it can be argued that removal of H3K79me2 mark enabled an easier shift in gene expression network when transcription factors were overexpressed.

To understand the role of DOT1L in transdifferentiation to hepatocytes, we investigated the mRNA expression of epithelial marker genes since mesenchymal to epithelial transition is required at the conversion of fibroblasts (mesenchymal) to hepatocytes (epithelial). We observed that mRNA expressions of CHD1 and EPCAM were significantly increased, which might

indicate that inhibition of Dot1L may allowed transcription factors to inhibit mesenchymal regulators even further and allowed an easier shift for hepatocyte markers.

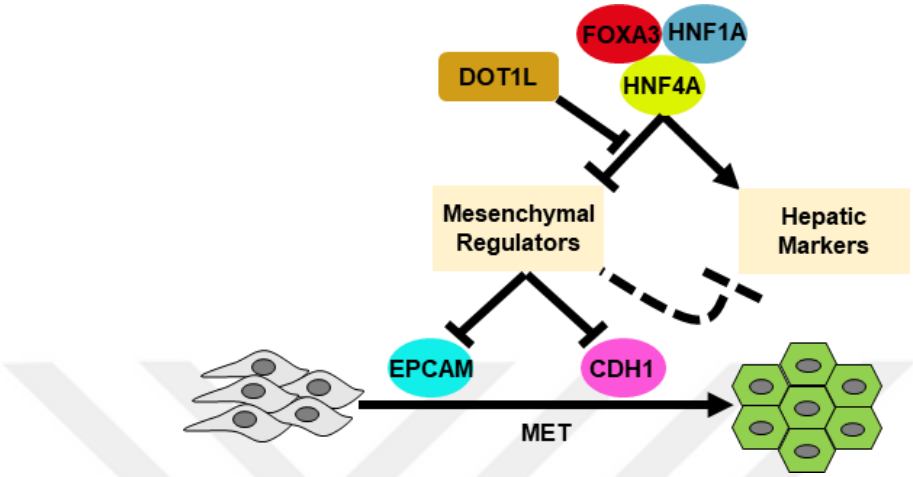

Figure4.1 Working Model of How Loss of DOT1L Affects Transdifferentiation of Fibroblasts into Hepatocytes

Sekiya et al. showed that iHeps continue to express fibroblast specific genes aberrantly after transdifferentiation, which are normally expressed in low levels in primary hepatocytes (Sekiya and Suzuki, 2011). Huang et al. showed that fibroblast specific gene (COL1A2, SNAI1, TWIST2, MMP14, WISP2) expression significantly drops with their protocol (Huang et al., 2014). However, fibroblasts in their study were derived from limbs of human fetuses (HFF) or adult fibroblasts (HAF) derived from human skin biopsy(Huang et al., 2014). In this study, we used dH1f cells, to further validate our results, we can perform the same experiments with a cell line derived from human skin such as BJ1 or human adult fibroblasts.

4.3 Possible Mechanisms of Top Hits from Compound Screen on Transdifferentiation

Compound screen allowed us to identify the molecules that increased the ratio of GFP-positive cells to the total number of cells after the pLOVE FHHB infection. As GFP expression was caused by Albumin reporter, this was an indicator of transdifferentiation efficiency per-cell basis. We identified that classes of bromodomain inhibitors, HDAC inhibitors, EZH2 inhibitors, Serine/Threonine-protein kinase inhibitors, Arginine Methyltransferase and G9a/GLP methyltransferase inhibitors and certain pathway activators and inhibitors can increase the transdifferentiation efficiency at different time points.

Earlier studies identified H3K4me2/3, and acetylation facilitates transdifferentiation of fibroblasts into neurons and cardiomyocytes while H3K9me2/3 inhibits (Qin et al., 2016). In

addition, inhibitors of chromatin modifiers for these histone marks directly affect the transdifferentiation efficiency such as Parnate (H3K4me2/3 by targeting Histone Demethylases), BIX-01294 (H3K9me2/3 by targeting G9a methyltransferase) and VPA (Acetylation by selectively inhibiting HDACs) (Qin et al., 2016). In addition, inhibition of HDAC7 (pre-B cells into macrophages) and EHZ2 (HSC into myofibroblasts) was shown to be essential for certain transdifferentiation protocols. These studies increase our confidence to our compound screen as we identified that inhibition of the same enzymes can increase efficiency of transdifferentiation from fibroblasts into hepatocytes. Recently, Li et al. performed a chemical screen and identified HDAC3 is important for hepatic differentiation of iPSCs and treating the cells with CI-994 significantly improved differentiation (Li et al., 2018). We also identified CI-994 as a hit that significantly increases transdifferentiation efficiency on day 9 and day 12.

HDACs are linked with TGFβ signaling which is important for epithelial-mesenchymal transition EMT (Shan et al., 2008). Smad proteins are key regulators TGFβ pathway and HDAC enzymes bind to Smad multiprotein and regulate transcriptional activity at Smad-responsive genes (Joanna et al., 2009). As EMT/MET transitions are important for cell reprogramming (Li et al., 2014), this might be the possible mechanism for HDAC inhibition on transdifferentiation. This can also explain the effect we observe with Repsox treatment which is a TGFβR inhibitor. Another study supports this possible mechanism as Tricostatin A, which is another HDAC inhibitor, suppressed EMT transition and inhibited transdifferentiation of hepatic stellate cells into myofibroblasts by inhibiting TGFβ/Smad2 and Jagged/Notch signaling pathways (Chen et al., 2013). These reports show that HDAC inhibitors block signaling pathways and overcome the epigenetic barrier for transdifferentiation.

We also identified class of bromodomain inhibitors can significantly increase number of GFP-positive cells at different time points. Recently, the link between BRD4, which is a bromodomain containing transcription regulator is required for TGFβ-induced Nox4 expression which causes myofibroblast transdifferentiation. Moreover, a study with full chemical approach for induced neurons reported that iBET151 which is a Bromodomain and extraterminal inhibitor disrupted the fibroblast-specific program and allowed for transdifferentiation (Li et al., 2015). On contrary, another study reported that JQ1 and iBET151 blocks Prox1 and Hnf4a induction which is required for liver regeneration (Ko et al., 2017). However, both of these reports show that

bromodomains are important for transcriptional regulation of fibroblast and hepatocyte marker genes, and therefore inhibition of bromodomains increased the transdifferentiation efficiency.

MS023 is an Arginine-methyltransferase inhibitor. A study revealed that regulation of Arginine-Methyltransferases is important for cellular reprogramming and AMI-5, which is an Arginine-Methyltransferase inhibitor enabled Oct4-induced reprogramming with A-83-01, which is a TGFβ inhibitor (Yuan et al., 2011). This might be an indicator that inhibition of Arginine-Methyltransferases removes the epigenetic barrier between different types of cells and allowed for higher transdifferentiation efficiencies.

3-DNZEP is an EZH2 inhibitor which is a part of PRC2 complex that is responsible for H3K27me3. H3K27me3 is a repressive mark and recruitment of PRC2 complex has been associated with downregulation of somatic genes in reprogramming (Fragola et al., 2013). However, it was found that loss of PCR2 complex inhibits iPSC generation (Fragola et al., 2013). In addition, a study showed H3K27me3 does not control lineage specific markers when cells were differentiated from hESC to hepatocytes (Vanhove et al., 2016). One possible explanation of increased Albumin-positive cell number is that inhibition of Ezh2 removed the H3K27me3 marks on hepatocyte marker genes which required more than 6 days and allowed a stronger activation when required transcription factors were overexpressed.

To support our findings, many of HDAC, TGFβ and Methyltransferase inhibitors were a part of chemical cocktails that are used for chemical reprogramming (Xie et al., 2017). Two of our top hits (Valproic acid and 3-DZNEP) was in the cocktail of first full chemical induction of iPSC (Hou et al., 2013). In addition, reprogramming of fibroblasts to XEN-like state requires Valproic acid and EPZ004777, which we observed both of them increased transdifferentiation efficiency (Li et al., 2017). Moreover, it was reported that chemical induced Neural progenitor cells can be generated from fibroblasts with the cocktail of CHIR99021, Valproic acid and Repsox; which were in our top hits.

Generally, our top hits were either related with mesenchymal-epithelial transition promotion by blocking TGFβ signaling pathway or they removed the epigenetic barriers between the cells for higher transdifferentiation efficiencies.

4.4 Future Directions

As a future direction, rescue experiments can be performed by overexpression of wild-type and catalytically inactive versions of DOT1L. This way, we can understand if the effect we

observe is caused by the absence or truncated version of DOT1L or removal of the H3K79me2 mark. To understand the mechanism of how transdifferentiation efficiency increases with DOT1L knockout or inhibition, Chromatin immunoprecipitation (ChIP) and RNA sequencing can be performed. By validating the upregulated and downregulated genes, as new hits can be identified to increase the transdifferentiation efficiency, we can also understand the underlying mechanism how DOT1L knockout or inhibition affects transdifferentiation.

While expression of hepatocyte markers, morphology of the cells and the decrease in fibroblast marker genes expressions are important indicators of transdifferentiation, it is vital to show the iHeps that we obtain have hepatic functions at the end of this process. For this purpose, we performed PAS and Oil Red O stainings to show our iHeps can store glycogen and lipids like HepG2. However, to show AAT secretion by ELISA, indocyanine green uptake and release, and drug metabolism with the measurement of CYP enzymes activities would be crucial for the comparison to normal hepatocyte functions. In addition, functionality of our iHeps can be determined by liver recovery after acute liver injury. If iHeps that we obtained can engraft themselves and increase the survivability of the mice after acute liver injury such as fulminant hepatitis, it would show us that the cells have sufficient hepatic functions.

Like DOT1L, the hits from compound screen can be validated by mRNA expression of hepatocyte markers, ELISA for proteins that are secreted from iHeps and functional tests such as PAS and Oil Red O stainings; targets of the compounds can be knocked out or knocked down to show the effects are truly caused by targets. We can also combine them with DOT1L knockout and inhibition to achieve higher transdifferentiation efficiencies.

Recently, a research group performed a genetic and chemical screen to identify the key regulators in hepatic differentiation by recombining Albumin reporter into endogenous ALB gene (Li et al., 2018). We can also improve our technique by creating a similar reporter cell line to assess the activation of endogenous ALB gene instead of a lentiviral vector that may be influenced by its integration site. In addition, moving the overexpression cassette into a Dox-inducible system may allow us to identify components that do not show an acute phenotype, such as EPZ004477, which requires pretreatment for 5 days and therefore did not come up as a hit in our compound screen. By doing this, we can eliminate the changes in proliferation when cells are pretreated with compounds since the overexpression will occur after we give the Dox to the system.

In summary, we showed that epigenetic modifications can affect transdifferentiation efficiency of human fibroblast to hepatocyte-like cells. Our results indicate that, especially at the early stages of transdifferentiation, removal of the H3K79me2 mark can accelerate the conversion and increase the expression of hepatocyte markers after the overexpression of the required transcriptional factors.

APPENDIX

Appendix A: Rocilinostat Treatment Does Not Increase Albumin and AFP mRNA Expressions

To verify the effect of Rocilinostat treatment from compound screen, we seeded $4x10^5$ PGP-H2BmCherry dH1f cells and infected the cells with pLOVE FHHB lentiviruses. Infected cells had epithelial-like morphologies and expressed mCherry and GFP (Figure A.1A and B). However, we observed Rocilinostat at 10μM concentration caused cell deaths. Rocilinostat treatment significantly increased the number of GFP-positive cells on day 6, especially at 3μM and 10μM concentrations. (Figure A.1C) However, qPCR analysis on day 6 showed a significant decrease at mRNA expression levels of Albumin (Figure A.1D) and AFP (Figure A.1E) compared to DMSO treated cells.

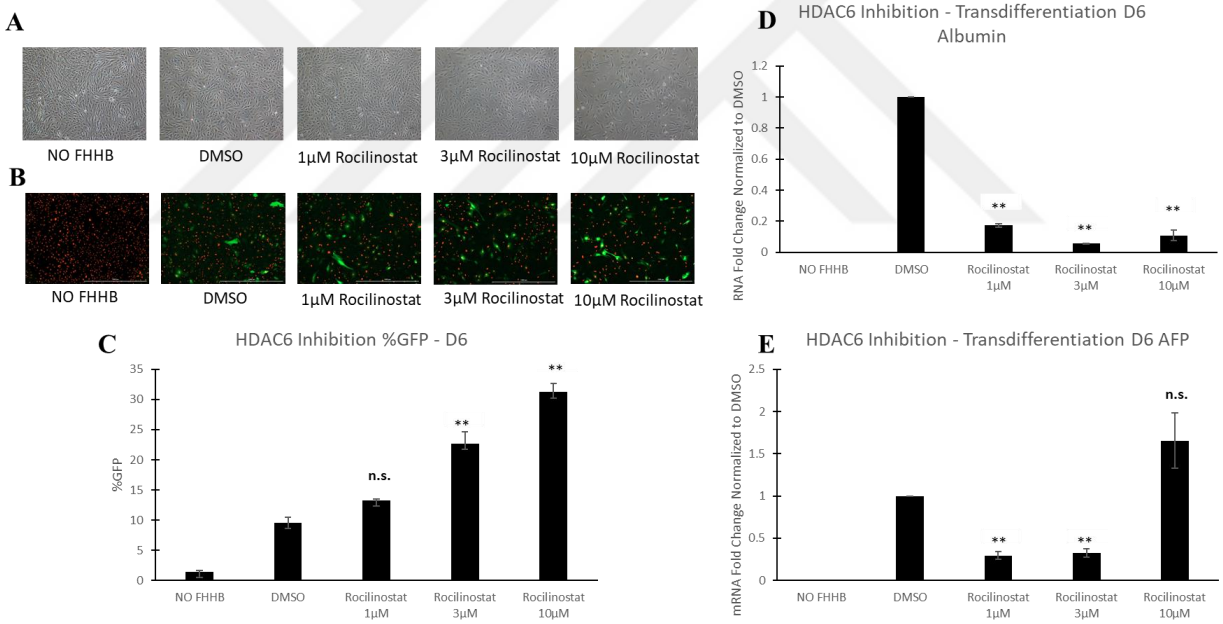

Figure A. 1 HDAC6 inhibition's effect on transdifferentiation efficiency on day 6
(A) Epithelial-like morphologies of Rocilinostat treated cells when they are infected with pLOVE FHHB. (B) mCherry and GFP expression of Rocilinostat treated cells 6 days after infected with pLOVE FHHB. (C) HDAC6 inhibition's effect on %GFP of transdifferentiated cells. (D) Albumin and (E) AFP mRNA expression of HDAC6 inhibited cells at day 6. **p<0.01 (n=3; error bars, ± s.err.)

On day 12, morphologies of cells were similar to day 6 and infected cells continued to express mCherry and GFP (Figure A.2A and B). Interestingly, we observed %GFP decreases when cells are treated with Rocilinostat compared to DMSO treatment (Figure A.2C). Consistent

with day 6 data, qPCR analysis at day 12 showed Rocilinostat treatment caused lower levels of Albumin (Figure A.2D) and AFP mRNA expression compared to DMSO (Figure A.2E).

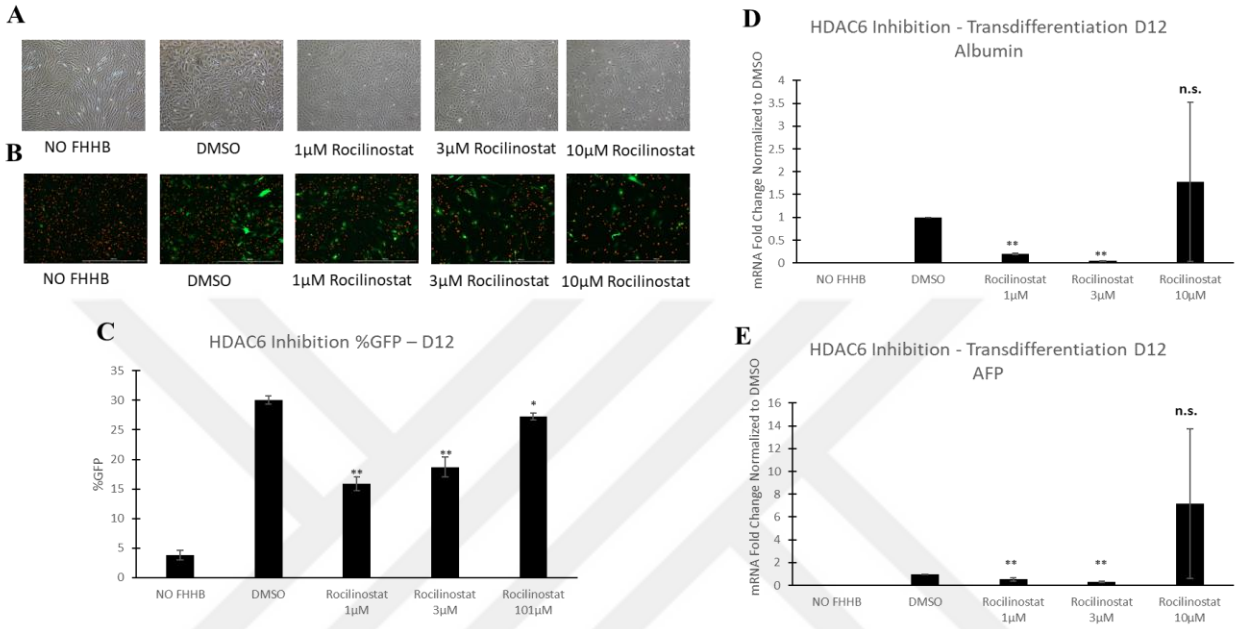

Figure A. 2 HDAC6 inhibition's effect on transdifferentiation efficiency at day 12
(A) Morphologies of Rocilinostat treated cells at day 12 of transdifferentiation (B) mCherry and GFP expression at Rocilinostat treated cells at day 12. (C) HDAC6 inhibition's effect on %GFP of transdifferentiated cells at day 12. (D) Albumin and (E) AFP mRNA expression of HDAC6 inhibited cells at day 12. **p<0.01 (n=3; error bars, ± s.err.)

Appendix B: CRISPR-Cas9 Mediated HDAC6 Knockout Does Not Increase mRNA Expression Levels of Albumin and AFP

To further investigate of HDAC6's role in transdifferentiation, we designed guideRNAs to target HDAC6 in human genome, and cloned into LentiCRISPRv2 plasmid (Figure B.1A) . We confirmed the cloning by Sanger Sequencing (Figure B.1B). 14 days after the infection with LentiCRISPRv2 viruses, we performed functional confirmation of HDAC6 knockout by Western Blot. We observed an inhibition at HDAC6g1 and HDAC6g2 samples with HDAC6 antibody. As Hdac6 is required for deacetylation of tubulins, we checked and observed levels of acetylated tubulin increased with HDAC6 knockout (Figure B.1C).

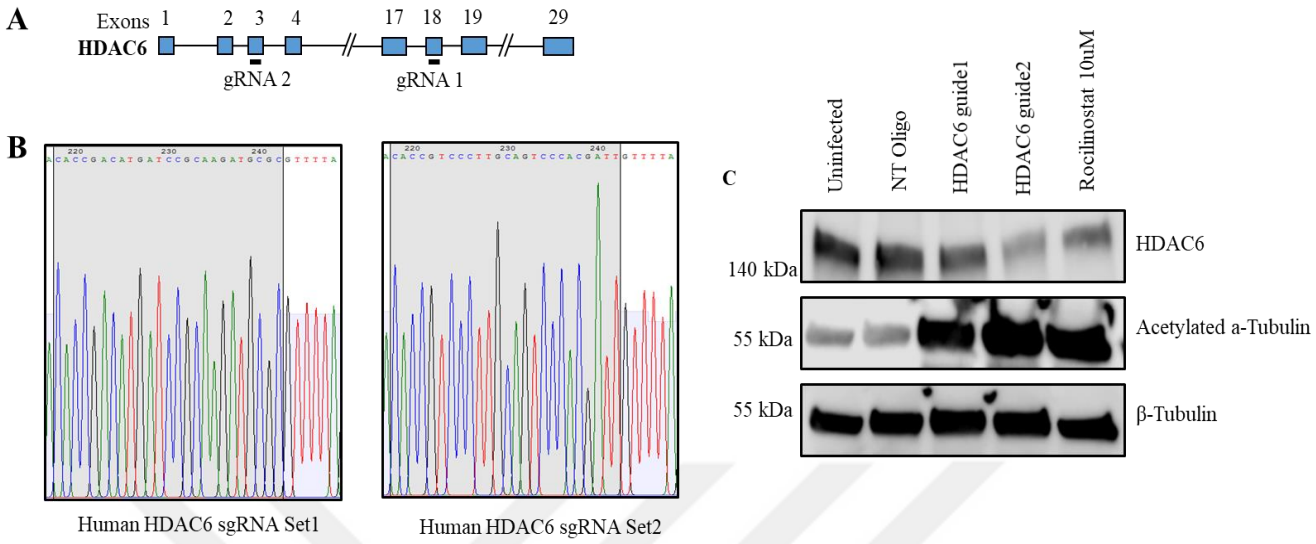

Figure B. 1 CRISPR-Cas9 mediated HDAC6 knockout
(A) Schematic of designed guideRNAs to target HDAC6 at human genome. (B) Sanger sequencing confirmed the guideRNAs were cloned in lentiCRISPRv2 plasmid. (D) Western Blot of HDAC6 and functional confirmation of HDAC6 knockout with acetylated tubulin increase.

Morphologies of HDAC6 knockout cells were epithelial-like on day 6 (Figure B.2 A). We detected mCherry and GFP expression from transdifferentiated cells (Figure B.2 B). Day 6 analysis showed knocking out HDAC6 slightly increased the number of GFP-positive cells and nearly half of the total cells were expressing GFP (Figure B.2 C). However, there was no significant increase at mRNA expression levels of Albumin (Figure B.2 D) and AFP (Figure B.2 E), compared to NT on day 6.

Day 12 analysis results were consistent with day 6. Infected cells continued to have epithelial-like morphology (Figure B.3A), mCherry and GFP expressions (Figure B.3B). Again, half of the infected HDAC6 knockout cells were GFP positive at day 12 (Figure B.3C). However, we observed HDAC6 knockout cells had lower levels of Albumin (Figure B.3D) and AFP (Figure B.3E) mRNA expression than NT cells at day 12.

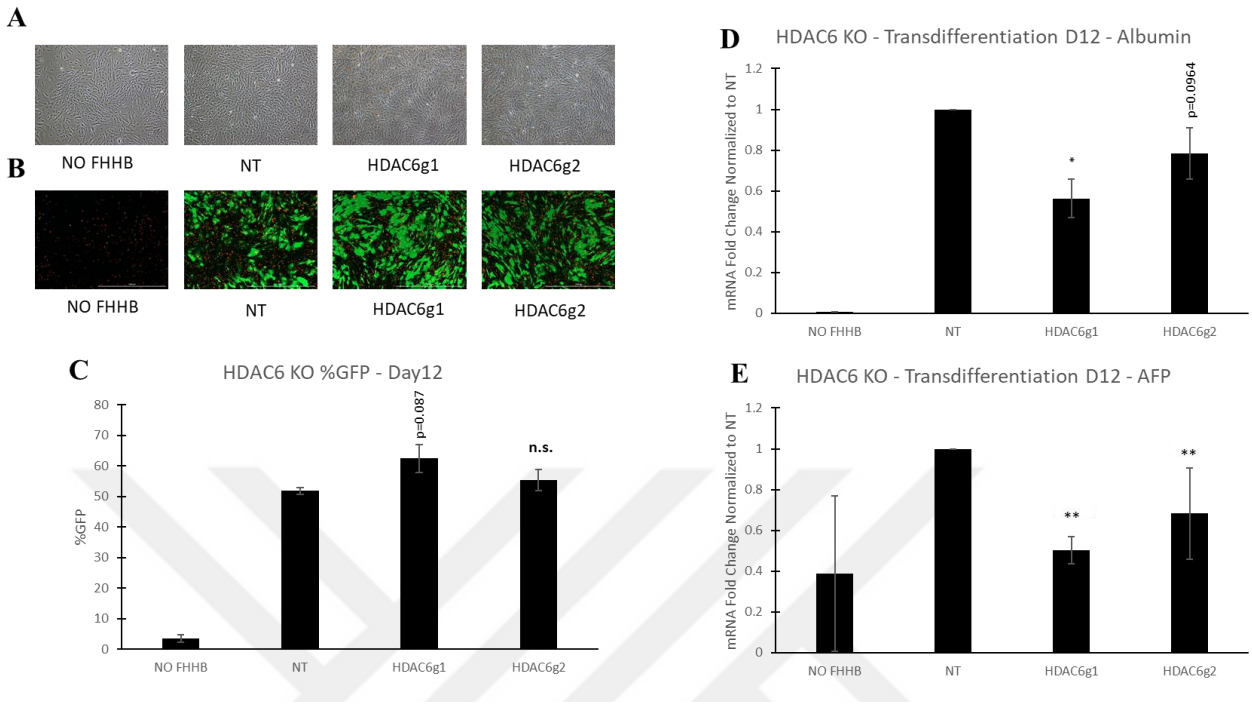

Figure B. 2 HDAC6 knockout does not increase transdifferentiation efficiency at day 12
(A) Morphologies of HDAC6 Knockout cells at day 12 (B) pLOVE FHHB infected HDAC6 knockout cells Express mCherry and GFP at day 12. (C) Day 12 %GFP analysis for HDAC6 Knockout cells at day 12 (D) Albumin and (E) AFP mRNA expression levels of HDAC6 knockout cells at day 6. **p<0.01 (n=3; error bars, ± s.err.)

Appendix C: Rocilinostat Treatment Activates Albumin Reporter without FHH Overexpression

Next, we tested if the effect of Rocilinostat treatment on %GFP was independent from transdifferentiation. As expected, Rocilinostat treated cells expressed GFP when they were infected with pLOVE FHHB viruses (Figure C.1A). However, we also observed nearly 10% of cells were detected as GFP-positive when the cells were not infected with pLOVE FHHB viruses (Figure C.1B and C). This indicated that Rocilinostat treatment alone was sufficient to active Albumin reporter.

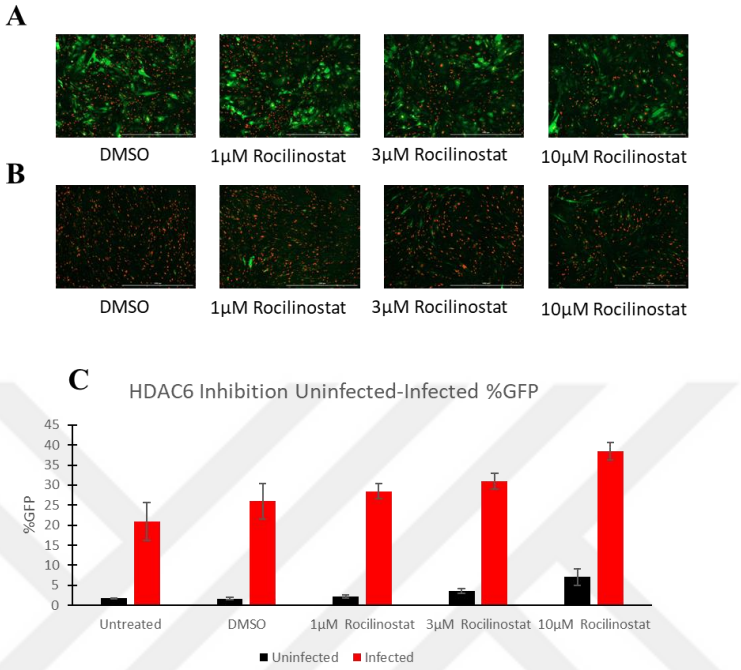

Figure C. 1 Rocilinostat treatment activates Albumin reporter without FHH overexpression
(A) mCherry and GFP expression of Rocilinostat treated cells at day 12 of transdifferentiation. (B) mCherry and GFP expression of Rocilinostat treated cells without FHHB infection. (C) %GFP analysis of Rocilinostat treated cells with and without pLOVE FHHB infection. (n=3; error bars, ± s.err.)

To understand if HDAC6 inhibition was the reason of Albumin reporter activation when cells were treated with Rocilinostat, we checked the Albumin reporter activity at HDAC6 knockout cells. pLOVE FHHB infected cells were GFP positive as expected (Figure C.2A). However, when we did not infect the cells with pLOVE FHHB viruses, we did not observe a significant increase at %GFP analysis with HDAC6 knockout cells compared to NT cells (Figure C.2B and C). Therefore, activation of Albumin reporter at Rocilinostat treatment was not caused by the inhibition of Hdac6.

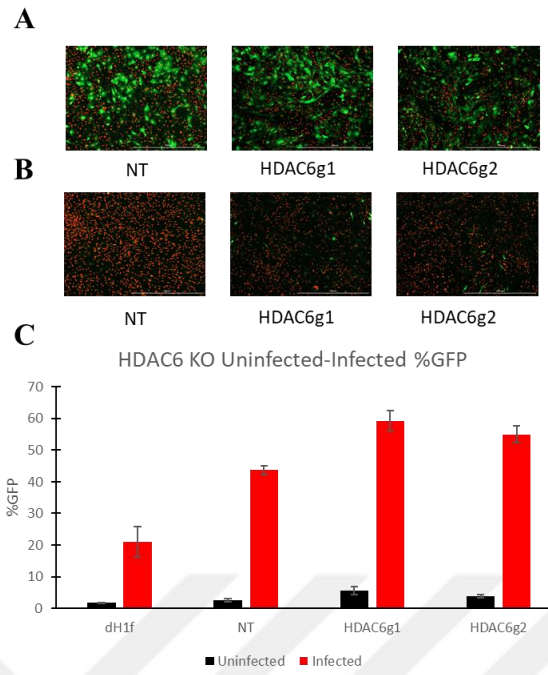

Figure C. 2 HDAC6 does not cause non-specific activation of Albumin reporter
(A) mCherry and GFP expression of HDAC6 knockout cells at day 12 of transdifferentiation. (B) mCherry and GFP expression of HDAC6 Knockout cells without FHHB infection. (C) %GFP analysis of HDAC6 knockout cells with and without pLOVE FHHB infection. (n=3; error bars, ± s.err.)

Appendix D: CRISPR-Cas9 Mediated EZH2 Knockout Causes a Decreases at H3K27me3 Levels

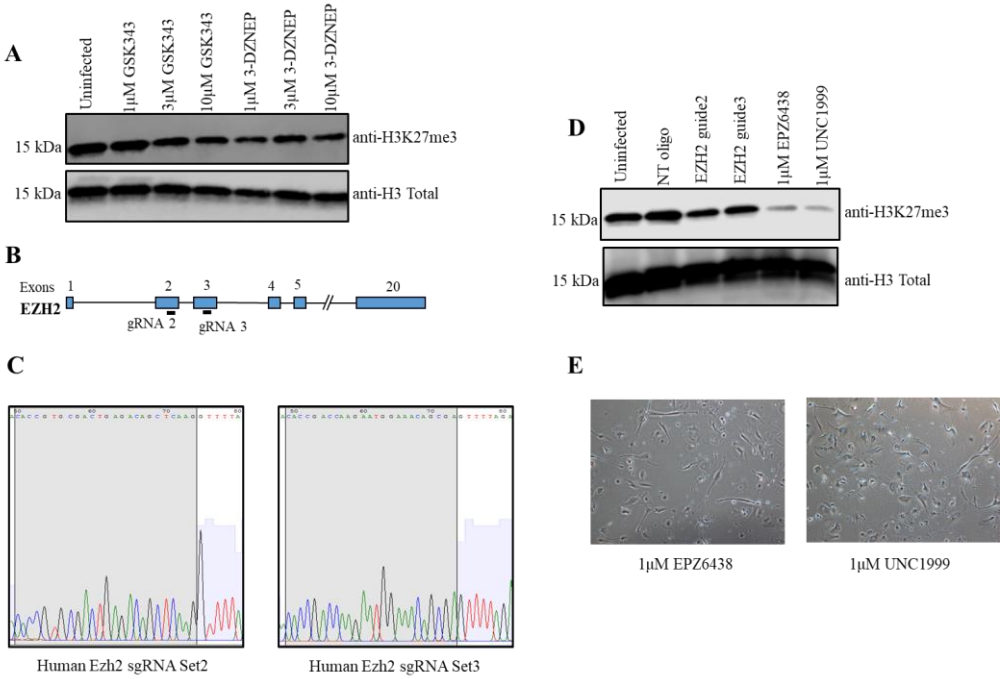

Figure D. 1 CRISPR-Cas9 mediated EZH2 knockout
(A) Functional test of EZH2 inhibitiors with H3K27me3 Western Blot. (B) Schematic of designed guideRNAs to target EZH2 at human genome. (C) Sanger sequencing of guideRNAs cloned in lentiCRISPRv2 plasmid. (D) Functional confirmation of EZH2 inhibition with Western Blot. (E) Morphologies of cells after treatment with EPZ6438 and UNC1999 for 7 days.

To test if the effect of 3-DNZEP on transdifferentiation efficiency was related with the decrease at H3K27me3 level, we treated our cells with EZH2 inhibitors (GSK343 and 3-DNZEP) for 5 days and performed H3K27me3 Western Blot (Figure D.1A). However, with these concentrations, we could not observe a significant decrease at H3K27me3 levels. Then, we designed guideRNAs to target EZH2 in human genome, and cloned into LentiCRISPRv2 plasmid (Figure D.1B). Sanger sequencing to these plasmids confirmed the cloning (Figure D.1C). After 14 days, we performed a Western Blot and observed a decrease at H3K27me3 levels but not total removal(Figure D.1D). In addition to this, EPZ6438 and UNC1999 caused a significant decrease at H3K27me3 levels. However, 7-day treatment with these EZH2 inhibitors caused cell deaths (Figure D.1E).

References

Akiyama, T., Wakabayashi, S., Soma, A., Sato, S., Nakatake, Y., Oda, M., Murakami, M., Sakota, M., Chikazawa-Nohtomi, N., Ko, S.B.H., et al. (2016). Transient ectopic expression of the histone demethylase JMJD3 accelerates the differentiation of human pluripotent stem cells. Development *143*, 3674–3685.

Ang, S.L., and Rossant, J. (1994). HNF-3β is essential for node and notochord formation in mouse development. Cell *78*, 561–574.

Apostolou, E., and Hochedlinger, K. (2013). Chromatin dynamics during cellular reprogramming.

Banas, A., Teratani, T., Yamamoto, Y., Tokuhara, M., Takeshita, F., Quinn, G., Okochi, H., and Ochiya, T. (2007). Adipose tissue-derived mesenchymal stem cells as a source of human hepatocytes. Hepatology *46*, 219–228.

Boyer, L.A., Plath, K., Zeitlinger, J., Brambrink, T., Medeiros, L.A., Lee, T.I., Levine, S.S., Wernig, M., Tajonar, A., Ray, M.K., et al. (2006). Polycomb complexes repress developmental regulators in murine embryonic stem cells. Nature *441*, 349–353.

Bracken, A.P., Dietrich, N., Pasini, D., Hansen, K.H., and Helin, K. (2006). Genome-wide mapping of polycomb target genes unravels their roles in cell fate transitions. Genes Dev. *20*, 1123–1136.

Buganim, Y., Itskovich, E., Hu, Y.C., Cheng, A.W., Ganz, K., Sarkar, S., Fu, D., Welstead, G.G., Page, D.C., and Jaenisch, R. (2012). Direct reprogramming of fibroblasts into embryonic sertoli-like cells by defined factors. Cell Stem Cell *11*, 373–386.

Caiazzo, M., Dell'Anno, M.T., Dvoretskova, E., Lazarevic, D., Taverna, S., Leo, D., Sotnikova, T.D., Menegon, A., Roncaglia, P., Colciago, G., et al. (2011). Direct generation of functional dopaminergic neurons from mouse and human fibroblasts. Nature *476*, 224.

Campbell, K.H.S., McWhir, J., Ritchie, W.A., and Wilmut, I. (1996). Sheep cloned by nuclear transfer from a cultured cell line. Nature *380*, 64.

Campos, E.I., and Reinberg, D. (2009). Histones: Annotating Chromatin. Annu. Rev. Genet. *43*, 559–599.

Cao, R., Wang, L., Wang, H., Xia, L., Erdjument-Bromage, H., Tempst, P., Jones, R.S., and Zhang, Y. (2002). Role of Histone H3 Lysine 27 Methylation in Polycomb-Group Silencing. Science (80-.). *298*, 1039–1043.

Chang, M.J., Wu, H., Achille, N.J., Reisenauer, M.R., Chou, C.W., Zeleznik-Le, N.J., Hemenway, C.S., and Zhang, W. (2010). Histone H3 Lysine 79 Methyltransferase Dot1 Is Required for Immortalization by MLL Oncogenes. Cancer Res. *70*, 10234–10242.

Chen, W.S., Manova, K., Weinstein, D.C., Duncan, S.A., Plump, A.S., Prezioso, V.R., Bachvarova, R.F., and Darnell, J.E. (1994). Disruption of the HNF-4 gene, expressed in visceral endoderm, leads to cell death in embryonic ectoderm and impaired gastrulation of mouse embryos. Genes Dev. *8*, 2466–2477.

Chen, X., Xiao, W., Chen, W., Luo, L., Ye, S., and Liu, Y. (2013). The epigenetic modifier trichostatin A , a histone deacetylase inhibitor , suppresses proliferation and epithelial – mesenchymal transition of lens epithelial cells. 1–12.

Chen, Z., Niu, M., Sun, M., Yuan, Q., Yao, C., Hou, J., Wang, H., Wen, L., Fu, H., Zhou, F., et al. (2017). Transdifferentiation of human male germline stem cells to hepatocytes in vivo via the transplantation under renal capsules. Oncotarget.

Cheng, L., Hu, W., Qiu, B., Zhao, J., Yu, Y., Guan, W., Wang, M., Yang, W., and Pei, G. (2014). Generation of neural progenitor cells by chemical cocktails and hypoxia. Cell Res. *24*, 665–679.

Daigle, S.R., Olhava, E.J., Therkelsen, C.A., Majer, C.R., Sneeringer, C.J., Song, J., Johnston, L.D., Scott, M.P., Smith, J.J., Xiao, Y., et al. (2011). Selective Killing of Mixed Lineage Leukemia Cells by a Potent Small-Molecule DOT1L Inhibitor. Cancer Cell *20*, 53–65.

Dal-Pra, S., Hodgkinson, C.P., Mirotsou, M., Kirste, I., and Dzau, V.J. (2017). Demethylation of H3K27 Is Essential for the Induction of Direct Cardiac Reprogramming by miR Combo. Circ. Res.

Davis, R.L., Weintraub, H., Lassar, A.B., Alitalo, K., Bishop, J.M., Smith, D.H., Chen, E.Y., Colby, W.W., Levinson, A.D., Bader, D., et al. (1987). Expression of a single transfected cDNA converts fibroblasts to myoblasts. Cell *51*, 987–1000.

Du, Y., Wang, J., Jia, J., Song, N., Xiang, C., Xu, J., Hou, Z., Su, X., Liu, B., Jiang, T., et al.

(2014). Human hepatocytes with drug metabolic function induced from fibroblasts by lineage reprogramming. Cell Stem Cell *14*, 394–403.

Duncan, S.A., Nagy, A., and Chan, W. (1997). Murine gastrulation requires HNF-4 regulated gene expression in the visceral endoderm: tetraploid rescue of Hnf-4(-/-) embryos. Development *124*, 279–287.

Efe, J.A., Hilcove, S., Kim, J., Zhou, H., Ouyang, K., Wang, G., Chen, J., and Ding, S. (2011). Conversion of mouse fibroblasts into cardiomyocytes using a direct reprogramming strategy. Nat. Cell Biol. *13*, 215–222.

Faralli, H., Wang, C., Nakka, K., Benyoucef, A., Sebastian, S., Zhuang, L., Chu, A., Palii, C.G., Liu, C., Camellato, B., et al. (2016). UTX demethylase activity is required for satellite cell-mediated muscle regeneration. J. Clin. Invest. *126*, 1555–1565.

Feng, Q., Wang, H.H.H.H., Ng, H.H., Erdjument-Bromage, H., Tempst, P., Struhl, K., Zhang, Y., Xu, M., Wang, W., Chen, S., et al. (2012). Methylation of H3-Lysine 79 Is Mediated by a New Family of HMTases without a SET Domain. Nature *6*, 737–738.

Feng, R., Desbordes, S.C., Xie, H., Tillo, E.S., Pixley, F., Stanley, E.R., and Graf, T. (2008). PU.1 and C/EBPalpha/beta convert fibroblasts into macrophage-like cells. Proc. Natl. Acad. Sci. U. S. A. *105*, 6057–6062.

Fragola, G., Germain, P., Laise, P., Cuomo, A., Blasimme, A., Gross, F., Signaroldi, E., Bucci, G., Sommer, C., Pruneri, G., et al. (2013). Cell Reprogramming Requires Silencing of a Core Subset of Polycomb Targets. *9*.

Gao, Y., Zhang, X., Zhang, L., Cen, J., Ni, X., Liao, X., Yang, C., Li, Y., Chen, X., Zhang, Z., et al. (2017). Distinct Gene Expression and Epigenetic Signatures in Hepatocyte-like Cells Produced by Different Strategies from the Same Donor. Stem Cell Reports *9*, 1813–1824.

Grompe, M. (2001). Liver repopulation for the treatment of metabolic diseases. J. Inherit. Metab. Dis. *24*, 231–244.

Guo, R., Tang, W., Yuan, Q., Hui, L., Wang, X., and Xie, X. (2017). Chemical Cocktails Enable Hepatic Reprogramming of Mouse Fibroblasts with a Single Transcription Factor. Stem Cell Reports *9*, 499–512.

Hou, P., Li, Y., Zhang, X., Liu, C., Guan, J., Li, H., Zhao, T., Ye, J., Yang, W., Liu, K., et al. (2013). Pluripotent stem cells induced from mouse somatic cells by small-molecule compounds. Science (80-.). *341*, 651–654.

Hu, W., Qiu, B., Guan, W., Wang, Q., Wang, M., Li, W., Gao, L., Shen, L., Huang, Y., Xie, G., et al. (2015). Direct Conversion of Normal and Alzheimer's Disease Human Fibroblasts into Neuronal Cells by Small Molecules. Cell Stem Cell *17*, 204–212.

Huang, P., He, Z., Ji, S., Sun, H., Xiang, D., Liu, C., Hu, Y., Wang, X., and Hui, L. (2011). Induction of functional hepatocyte-like cells from mouse fibroblasts by defined factors. Nature *475*, 386–389.

Huang, P., Zhang, L., Gao, Y., He, Z., Yao, D., Wu, Z., Cen, J., Chen, X., Liu, C., Hu, Y., et al. (2014). Direct reprogramming of human fibroblasts to functional and expandable hepatocytes. Cell Stem Cell *14*, 370–384.

Huangfu, D., Maehr, R., Guo, W., Eijkelenboom, A., Snitow, M., Chen, A.E., and Melton, D.A. (2008). Induction of pluripotent stem cells by defined factors is greatly improved by small-molecule compounds. Nat. Biotechnol. *26*, 795–797.

Ieda, M., Fu, J.D., Delgado-Olguin, P., Vedantham, V., Hayashi, Y., Bruneau, B.G., and Srivastava, D. (2010). Direct reprogramming of fibroblasts into functional cardiomyocytes by defined factors. Cell *142*, 375–386.

Iwase, S., Lan, F., Bayliss, P., de la Torre-Ubieta, L., Huarte, M., Qi, H.H., Whetstine, J.R., Bonni, A., Roberts, T.M., and Shi, Y. (2007). The X-Linked Mental Retardation Gene SMCX/JARID1C Defines a Family of Histone H3 Lysine 4 Demethylases. Cell *128*, 1077–1088.

Joanna, F., A, V.G.L., Mathieu, V., Sarah, S., Sarah, D., Karin, V., Tamara, V., and Vera, R. (2009). Histone deacetylase inhibition and the regulation of cell growth with particular reference to liver pathobiology. *13*, 2990–3005.

Jones, B., Su, H., Bhat, A., Lei, H., Bajko, J., Hevi, S., Baltus, G.A., Kadam, S., Zhai, H., Valdez, R., et al. (2008). The histone H3K79 methyltransferase Dot1L is essential for mammalian development and heterochromatin structure. PLoS Genet. *4*.

Kaestner, K.H., Hiemisch, H., and Schütz, G. (1998). Targeted disruption of the gene encoding

hepatocyte nuclear factor 3gamma results in reduced transcription of hepatocyte-specific genes. Mol. Cell. Biol. *18*, 4245–4251.

Kaestner, K.H., Katz, J., Liu, Y., Drucker, D.J., and Schütz, G. (1999). Inactivation of the winged helix transcription factor HNF3?? affects glucose homeostasis and islet glucagon gene expression in vivo. Genes Dev. *13*, 495–504.

Kanherkar, R.R., Bhatia-Dey, N., Makarev, E., and Csoka, A.B. (2014). Cellular reprogramming for understanding and treating human disease. Front. Cell Dev. Biol. *2*.

Kass, S.U., Pruss, D., and Wolffe, A.P. (1997). How does DNA methylation repress transcription? *13*, 444–449.

Katayama, H., Yasuchika, K., Miyauchi, Y., Kojima, H., Yamaoka, R., Kawai, T., Yukie Yoshitoshi, E., Ogiso, S., Kita, S., Yasuda, K., et al. (2017). Generation of non-viral, transgene-free hepatocyte like cells with piggyBac transposon. Sci. Rep. *7*, 44498.

Katsuda, T., Kawamata, M., Hagiwara, K., Takahashi, R. u., Yamamoto, Y., Camargo, F.D., and Ochiya, T. (2017). Conversion of Terminally Committed Hepatocytes to Culturable Bipotent Progenitor Cells with Regenerative Capacity. Cell Stem Cell *20*, 41–55.

Ko, S., Choi, T., Russell, J.O., So, J., and Shin, D. (2017). Bromodomain and extraterminal (BET) proteins regulate biliarydriven liver regeneration. *64*, 316–325.

Kouzarides, T. (2007). Chromatin Modifications and Their Function. Cell *128*, 693–705.

Kuzmichev, A., Nishioka, K., Erdjument-Bromage, H., Tempst, P., and Reinberg, D. (2002). Histone methyltransferase activity associated with a human multiprotein complex containing the Enhancer of Zeste protein. Genes Dev. *16*, 2893–2905.

Lai, E., Prezioso, V.R., Smith, E., Litvin, O., Costa, R., and Darnell J. E., J. (1990). HNF3A, a hepatocyte -enriched transcription factor of novel structure is regulated transcriptionally. Genes Dev. *4*, 1427–1436.

Lai, E., Prezioso, V.R., Tao, W., Chen, W.S., and Darnell, J.E. (1991). Hepatocyte nuclear factor 3α belongs to a gene family in mammals that is homologous to the Drosophila homeotic gene fork head. Genes Dev. *5*, 416–427.

Lassar, A.B., Paterson, B.M., and Weintraub, H. (1986). Transfection of a DNA locus that mediates the conversion of 10T1 2 fibroblasts to myoblasts. Cell *47*, 649–656.

Lawrence, M., Daujat, S., and Schneider, R. (2016). Lateral Thinking: How Histone Modifications Regulate Gene Expression. Trends Genet. *32*, 42–56.

Lee, K.-D., Kuo, T.K.-C., Whang-Peng, J., Chung, Y.-F., Lin, C.-T., Chou, S.-H., Chen, J.-R., Chen, Y.-P., and Lee, O.K.-S. (2004). In vitro hepatic differentiation of human mesenchymal stem cells. Hepatology *40*, 1275–1284.

Lee, T.I., Jenner, R.G., Boyer, L.A., Guenther, M.G., Levine, S.S., Kumar, R.M., Chevalier, B., Johnstone, S.E., Cole, M.F., Isono, K. ichi, et al. (2006). Control of Developmental Regulators by Polycomb in Human Embryonic Stem Cells. Cell *125*, 301–313.

Lee, Y.H., Sauer, B., and Gonzalez, F.J. (1998). Laron dwarfism and non-insulin-dependent diabetes mellitus in the Hnf- 1alpha knockout mouse. Mol. Cell. Biol. *18*, 3059–68.

Li, J., Ning, G., and Duncan, S.A. (2000). Mammalian hepatocyte differentiation requires the transcription factor HNF-4?? Genes Dev. *14*, 464–474.

Li, S., Li, M., Liu, X., Yang, Y., Wei, Y., Chen, Y., Qiu, Y., Zhou, T., Feng, Z., Ma, D., et al. (2018). Genetic and Chemical Screenings Identify HDAC3 as a Key Regulator in Hepatic Differentiation of Human Pluripotent Stem Cells. Stem Cell Reports *11*, 22–31.

Li, X., Pei, D., and Zheng, H. (2014). Transitions between epithelial and mesenchymal states during cell fate conversions. *5*, 580–591.

Li, X., Zuo, X., Jing, J., Ma, Y., Wang, J., Liu, D., Zhu, J., Du, X., Xiong, L., Du, Y., et al. (2015a). Small-Molecule-Driven Direct Reprogramming of Mouse Fibroblasts into Functional Neurons. Cell Stem Cell *17*, 195–203.

Li, X., Zuo, X., Jing, J., Ma, Y., Wang, J., Liu, D., Zhu, J., and Du, X. (2015b). Small-Molecule-Driven Direct Reprogramming of Mouse Fibroblasts into Functional Neurons Short Article Small-Molecule-Driven Direct Reprogramming of Mouse Fibroblasts into Functional Neurons. Stem Cell *17*, 195–203.

Li, X., Liu, D., Ma, Y., Du, X., Jing, J., Wang, L., Xie, B., Sun, D., Sun, S., Jin, X., et al. (2017).

Direct Reprogramming of Fibroblasts via a Chemically Induced XEN-like State. Cell Stem Cell *21*, 264–273.e7.

Lim, K.T., Lee, S.C., Gao, Y., Kim, K.P., Song, G., An, S.Y., Adachi, K., Jang, Y.J., Kim, J., Oh, K.J., et al. (2016). Small Molecules Facilitate Single Factor-Mediated Hepatic Reprogramming. Cell Rep. *15*, 814–829.

Liu, Z., Chen, O., Wall, J.B.J., Zheng, M., Zhou, Y., Wang, L., Ruth Vaseghi, H., Qian, L., and Liu, J. (2017). Systematic comparison of 2A peptides for cloning multi-genes in a polycistronic vector. Sci. Rep. *7*, 1–9.

Ma, X., Kong, L., and Zhu, S. (2017). Reprogramming cell fates by small molecules. Protein Cell *8*, 328–348.

Margueron, R., and Reinberg, D. (2011). The Polycomb complex PRC2 and its mark in life. Nature *469*, 343–349.

Marro, S., Pang, Z.P., Yang, N., Tsai, M.C., Qu, K., Chang, H.Y., Südhof, T.C., and Wernig, M. (2011). Direct lineage conversion of terminally differentiated hepatocytes to functional neurons. Cell Stem Cell *9*, 374–382.

Mcdonald, T.J., Colclough, K., Brown, R., Shields, B., Shepherd, M., Bingley, P., Williams, A., Hattersley, A.T., and Ellard, S. (2011). Islet autoantibodies can discriminate maturity-onset diabetes of the young (MODY) from Type1 diabetes. Diabet. Med. *28*, 1028–1033.

Metzger, E., Wissmann, M., Yin, N., Müller, J.M., Schneider, R., Peters, A.H.F.M., Günther, T., Buettner, R., and Schüle, R. (2005). LSD1 demethylates repressive histone marks to promote androgen-receptor-dependent transcription. Nature.

Mohn, F., Weber, M., Rebhan, M., Roloff, T.C., Richter, J., Stadler, M.B., Bibel, M., and Schübeler, D. (2008). Lineage-Specific Polycomb Targets and De Novo DNA Methylation Define Restriction and Potential of Neuronal Progenitors. Mol. Cell *30*, 755–766.

Morris, S.A., Cahan, P., Li, H., Zhao, A.M., San Roman, A.K., Shivdasani, R.A., Collins, J.J., and Daley, G.Q. (2014). Dissecting engineered cell types and enhancing cell fate conversion via Cellnet. Cell *158*, 889–902.

Odom, D.T. (2004). Control of Pancreas and Liver Gene Expression by HNF Transcription Factors. Science (80-.). *303*, 1378–1381.

Onder, T.T., Kara, N., Cherry, A., Sinha, A.U., Zhu, N., Bernt, K.M., Cahan, P., Marcarci, B.O., Unternaehrer, J., Gupta, P.B., et al. (2012). Chromatin-modifying enzymes as modulators of reprogramming. Nature *483*, 598–602.

Ooga, M., Inoue, A., Kageyama, S., Akiyama, T., Nagata, M., and Aoki, F. (2008). Changes in H3K79 Methylation During Preimplantation Development in Mice. Biol. Reprod. *78*, 413–424.

Orkin, S.H., and Hochedlinger, K. (2011). Review Chromatin Connections to Pluripotency and Cellular Reprogramming. Cell *145*, 835–850.

Park, I.H., Zhao, R., West, J.A., Yabuuchi, A., Huo, H., Ince, T.A., Lerou, P.H., Lensch, M.W., and Daley, G.Q. (2008). Reprogramming of human somatic cells to pluripotency with defined factors. Nature *451*, 141–146.

Pereira, C.F., Piccolo, F.M., Tsubouchi, T., Sauer, S., Ryan, N.K., Bruno, L., Landeira, D., Santos, J., Banito, A., Gil, J., et al. (2010). ESCs require PRC2 to direct the successful reprogramming of differentiated cells toward pluripotency. Cell Stem Cell *6*, 547–556.

Pontoglio, M., Barra, J., Hadchouel, M., Doyen, A., Kress, C., Bach, J.P., Babinet, C., and Yaniv, M. (1996). Hepatocyte nuclear factor 1 inactivation results in hepatic dysfunction, phenylketonuria, and renal Fanconi syndrome. Cell *84*, 575–585.

Qiang, L., Fujita, R., Yamashita, T., Angulo, S., Rhinn, H., Rhee, D., Doege, C., Chau, L., Aubry, L., Vanti, W.B., et al. (2011). Directed conversion of Alzheimer's disease patient skin fibroblasts into functional neurons. Cell *146*, 359–371.

Qin, H., Zhao, A., Zhang, C., and Fu, X. (2016). Epigenetic Control of Reprogramming and Transdifferentiation by Histone Modifications. Stem Cell Rev. Reports 708–720.

Quiring, R., Walldorf, U., Kloter, U., and Gehring, W.J. (1994). Homology of the eyeless gene of Drosophila to the Small eye gene in mice and Aniridia in humans. Science (80-.). *265*, 785 LP-789.

Reddy, J.K., Rao, M.S., Qureshi, S.A., Reddy, M.K., Scarpelli, D.G., and Lalwani, N.D. (1984).

Induction and origin of hepatocytes in rat pancreas. J. Cell Biol. *98*, 2082–2090.

Sancho-Martinez, I., Baek, S.H., and Izpisua Belmonte, J.C. (2012). Lineage conversion methodologies meet the reprogramming toolbox. Nat. Cell Biol. *14*, 892–899.

De Santa, F., Totaro, M.G., Prosperini, E., Notarbartolo, S., Testa, G., and Natoli, G. (2007). The Histone H3 Lysine-27 Demethylase Jmjd3 Links Inflammation to Inhibition of Polycomb-Mediated Gene Silencing. Cell *130*, 1083–1094.

Scarpelli, D.G., and Rao, M.S. (1981). Differentiation of regenerating pancreatic cells into hepatocyte-like cells. Proc. Natl. Acad. Sci. U. S. A. *78*, 2577–2581.

Schnerch, A., Mitchell, R., Fiebig-comyn, A., Szabo, E., Rampalli, S., and Risuen, R.M. (2010). Direct conversion of human fibroblasts to multilineage blood progenitors.

Schneuwly, S., Klemenz, R., and Gehring, W.J. (1987). Redesigning the body plan of Drosophila by ectopic expression of the homoeotic gene Antennapedia. Nature *325*, 816–818.

Sekiya, S., and Suzuki, A. (2011). Direct conversion of mouse fibroblasts to hepatocyte-like cells by defined factors. Nature *475*, 390–393.

Servitja, J.-M., Pignatelli, M., Maestro, M.A., Cardalda, C., Boj, S.F., Lozano, J., Blanco, E., Lafuente, A., McCarthy, M.I., Sumoy, L., et al. (2009). Hnf1 (MODY3) Controls Tissue-Specific Transcriptional Programs and Exerts Opposed Effects on Cell Growth in Pancreatic Islets and Liver. Mol. Cell. Biol. *29*, 2945–2959.

Shan, B., Yao, T., Nguyen, H.T., Zhuo, Y., Levy, D.R., Klingsberg, R.C., Tao, H., Palmer, M.L., Holder, K.N., and Lasky, J.A. (2008). Requirement of HDAC6 for Transforming Growth. *283*, 21065–21073.

Sommer, C.A., Stadtfeld, M., Murphy, G.J., Hochedlinger, K., Kotton, D.N., and Mostoslavsky, G. (2016). iPS Cell Generation Using a Single Lentiviral Stem Cell Cassette. *27*, 543–549.

Son, E.Y., Ichida, J.K., Wainger, B.J., Toma, J.S., Rafuse, V.F., Woolf, C.J., and Eggan, K. (2011). Conversion of mouse and human fibroblasts into functional spinal motor neurons. Cell Stem Cell *9*, 205–218.

Song, G., Pacher, M., Balakrishnan, A., Yuan, Q., Tsay, H.C., Yang, D., Reetz, J., Brandes, S.,

Dai, Z., Pützer, B.M., et al. (2016). Direct Reprogramming of Hepatic Myofibroblasts into Hepatocytes in Vivo Attenuates Liver Fibrosis. Cell Stem Cell *18*, 797–808.

Stride, A., and Hattersley, A.T. (2002). Different genes, different diabetes: lessons from maturity-onset diabetes of the young. Ann. Med. *34*, 207–216.

Takahashi, K., and Yamanaka, S. (2006). Induction of Pluripotent Stem Cells from Mouse Embryonic and Adult Fibroblast Cultures by Defined Factors. Cell *126*, 663–676.

Taylor, S.M., and Jones, P.A. (1979). Multiple new phenotypes induced in 10T 1 2 and 3T3 cells treated with 5-azacytidine. Cell *17*, 771–779.

Tsukada, Y., Fang, J., Erdjument-Bromage, H., Warren, M.E., Borchers, C.H., Tempst, P., and Zhang, Y. (2005). Histone demethylation by a family of JmjC domain-containing proteins. Nature *439*, 811–816.

Ulrich, P., Kirkeby, A., Torper, O., Wood, J., Nelander, J., Dufour, A., Björklund, A., Lindvall, O., Jakobsson, J., and Parmar, M. (2011). Direct conversion of human fi broblasts to dopaminergic neurons. *108*, 10343–10348.

Vanhove, J., Pistoni, M., Welters, M., Eggermont, K., Vanslembrouck, V., Helsen, N., Boon, R., Najimi, M., Sokal, E., Collas, P., et al. (2016). H3K27me3 Does Not Orchestrate the Expression of Lineage-Specific Markers in hESC-Derived Hepatocytes In Vitro. Stem Cell Reports *7*, 192–206.

Vassilopoulos, G., Wang, P.-R., and Russell, D.W. (2003). Transplanted bone marrow regenerates liver by cell fusion. Nature *422*, 901–904.

Vierbuchen, T., Ostermeier, A., Pang, Z.P., Kokubu, Y., Südhof, T.C., and Wernig, M. (2010). Direct conversion of fibroblasts to functional neurons by defined factors. Nature *463*, 1035–1041.

Walker, E., Chang, W.Y., Hunkapiller, J., Cagney, G., Garcha, K., Torchia, J., Krogan, N.J., Reiter, J.F., and Stanford, W.L. (2010). Polycomb-like 2 Associates with PRC2 and Regulates Transcriptional Networks during Mouse Embryonic Stem Cell Self-Renewal and Differentiation. Cell Stem Cell *6*, 153–166.

Wang, X., Willenbring, H., Akkari, Y., Torimaru, Y., Foster, M., Al-Dhalimy, M., Lagasse, E.,

Finegold, M., Olson, S., and Grompe, M. (2003). Cell fusion is the principal source of bone-marrow-derived hepatocytes. Nature *422*, 897–901.

Wang, Y., Qin, J., Wang, S., Zhang, W., Duan, J., Zhang, J., Wang, X., Yan, F., Chang, M., Liu, X., et al. (2016). Conversion of Human Gastric Epithelial Cells to Multipotent Endodermal Progenitors using Defined Small Molecules. Cell Stem Cell *19*, 449–461.

Weinstein, D.C., Ruiz i Altaba, A., Chen, W.S., Hoodless, P., Prezioso, V.R., Jessell, T.M., and Darnell, J.E. (1994). The winged-helix transcription factor HNF-3b is required for notochord development in the mouse embryo. Cell *78*, 575–588.

Xiang, Y., Zhu, Z., Han, G., Lin, H., Xu, L., and Chen, C.D. (2007). JMJD3 is a histone H3K27 demethylase. Cell Res. *17*, 850–857.

Xie, H., Ye, M., Feng, R., and Graf, T. (2004). Stepwise Reprogramming of B Cells into Macrophages. Cell *117*, 663–676.

Xie, X., Fu, Y., and Liu, J. (2017). Chemical reprogramming and transdifferentiation. Curr. Opin. Genet. Dev. *46*, 104–113.

Xu, J., Du, Y., and Deng, H. (2015). Review Direct Lineage Reprogramming : Strategies, Mechanisms, and Applications. Cell Stem Cell *16*, 119–134.

Yuan, X. (2011). Combined Chemical Treatment Enables Oct4 -Induced Reprogramming from Mouse Embryonic Fibroblasts. Stem Cells. 549–553.

Zakikhan, K., Pournasr, B., Nassiri-Asl, M., and Baharvand, H. (2016). Enhanced direct conversion of fibroblasts into hepatocyte-like cells by Kdm2b. Biochem. Biophys. Res. Commun. *474*, 97–103.

Zhao, Y., Zhao, T., Guan, J., Zhang, X., Fu, Y., Ye, J., Zhu, J., Meng, G., Ge, J., Yang, S., et al. (2015). A XEN-like State Bridges Somatic Cells to Pluripotency during Chemical Reprogramming. Cell *163*, 1678–1691.

Zhu, S., Li, W., Zhou, H., Wei, W., Ambasudhan, R., Lin, T., Kim, J., Zhang, K., and Ding, S. (2010). Reprogramming of human primary somatic cells by OCT4 and chemical compounds. Cell Stem Cell *7*, 651–655.

Vita

Eray Enustun was born in Istanbul, Turkey on June 30, 1993. He received his Bachelor of Science degrees with a double major in Chemical and Biological Engineering and Molecular Biology and Genetics from Koç University, Istanbul in 2016. He is working towards his Master of Science degree in Molecular Biology and Genetics from Koç University, Istanbul. He is accepted from University of California, San Diego for his Ph.D. studies.